COT REPRESENTATIONS OF 2D HAMILTONIAN FLOWS AND THEIR COMPUTABLE APPLICATIONS

TETSUO YOKOYAMA AND TOMOO YOKOYAMA

Abstract. Complete invariants of Hamiltonian surface flows, called *partially cyclically ordered rooted tree* (COT) representations, are introduced. The invariants can uniquely assign a generic Hamiltonian surface flow to a word. Moreover, all generic transition rules between generic Hamiltonian flows using the COT representations are listed. As an application, all generic transitions of the Reeb graphs of Morse functions on orientable closed surfaces are also listed.

1. Introduction

The topological properties of Hamiltonian flows on compact surfaces have been studied from the viewpoints of dynamical systems, integrable systems, and fluid mechanics. For instance, Hamiltonian flows with finitely many singular points have been topologically classified on a plane [2], sphere [8], and torus [11] from the viewpoint of fluid mechanics. From the perspective of integrable systems, such flows have also been topologically classified on closed surfaces [6]. Various fluid phenomena have been modeled based on incompressible fluids, and incompressible flows on spheres behave like Hamiltonian flows (cf. [9]). Structural stability is important in terms of the dynamical systems because the set of structurally stable Hamiltonian flows on compact surfaces or unbounded puctured planes is open dense [9, 16]. In other words, any Hamiltonian surface flow can be approximated by such Hamiltonian surface flows, and the topological equivalence classes of these flows are preserved under small perturbations. Structural stability is also crucial for applications because experimentally observed and numerically computed Hamiltonian flows are structurally stable almost constantly. Structurally stable Hamiltonian flows on compact surfaces and unbounded punctured planes have been classified topologically [9, 16], and there are some representations of their topologies [6, 12, 13, 16]. For instance, all topologies of generic embedded closed orientable surfaces in $\mathbb{R}^3$ can be bijectively represented by labelled graphs, called *molecules*; labels are called atoms [6]. Moreover, all topologies of structurally stable Hamiltonian flows on bounded/unbounded punctured disks can be represented by sequences of symbols, called *maximal words* [16]. The topologies of such flows are in one-to-one correspondence with labelled directed rooted trees [13]. It should be noted that molecules are non-rooted, whereas tree and word representations are rooted and can be encoded as sequences of symbols. Theoretically, one can list all generic transitions between the topologies of structurally stable Hamiltonian surface flows using tree representations. In other words, the generic transitions between topological equivalence classes of structurally stable Hamiltonian surface flows are numerable. On the other hand, word representations and the tree representations distinguish neither centers from boundaries nor circular arrangements from linear arrangements. Moreover, word representations are many-to-one correspondences and the tree representations are not intuitively related to the orbit structures. Contrarily, word representations are directly related to the orbit structures and need to be generalized to tree representations, called *partially cyclically ordered rooted tree* (*COT*) *representations*, to allow listing all generic transitions. Moreover, unlike word and tree representations (resp. circular and linear arrangements), COT representations distinguish centers from boundaries (resp. circular arrangements from linear arrangements). In other words, COT representations of structurally stable Hamiltonian surface flows correspond to the topological equivalence classes of such flows. In terms of computational efficiency, COT representations in topological data flow analysis are as efficiently processed as word representations.

The present paper consists of seven sections. In the following section, we introduce the notions of graph theory and dynamical systems. In §3, we introduce a complete invariant of structurally stable Hamiltonian surface flows, called a COT representation, using formal grammars. In §4, we describe the complete creation rules of genus elements incremented by one a structurally stable Hamiltonian flow. In §5, we detail the complete generic transition rules between structurally stable Hamiltonian surface flows. In §6, we apply the transition results of structurally stable Hamiltonian surface flows into Reeb graphs of Morse functions on a closed surface. In particular, we list all generic transitions of the Reeb graphs of Morse functions. In the final section, we remark the annihilations of boundaries, "higher codimensional transitions", and the point at infinity which is more degenerate than a 1-source–sink point of Hamiltonian surface flows.

2. Preliminary

2.1. **Notion of graphs.** An ordered pair $G := (V, D)$ is a directed graph if V is a set and $D \subseteq V \times V$. An ordered triplet $G := (V, E, r)$ is an abstract directed multi-graph if V and E are sets and $r : E \to \{(x, y) \mid x, y \in V\}$. A graph is a geometric realization of an abstract directed multi-graph (i.e., a cell complex whose dimension is at most one). A directed graph is a graph with the directed structure of the abstract directed multi-graph. Finite (directed) multi-graphs can be embedded on some surface, that is, they can be drawn so that no edges cross each other. Such a drawing is called a surface (directed) graph.

2.2. **Notion of surfaces.** In this paper, a *surface* is a two-dimensional manifold with or without boundary. A disk is homeomorphic to either a closed unit disk $\{(x, y) \in \mathbb{R}^2 \mid x^2 + y^2 \leq 1\}$ or an open unit disk $\{(x, y) \in \mathbb{R}^2 \mid x^2 + y^2 < 1\}$. A point in a surface S is a boundary point if and only if it has a neighborhood in S that is homeomorphic to a half disk $\{(x, y) \in \mathbb{R}^2 \mid x^2 + y^2 \leq 1, y \geq 0\}$. The boundary ∂S of a compact surface S is the set of boundary points. It should be noted that the boundary ∂S is the boundary of S as a manifold and not necessarily as a subset of the surface; it is also a finite disjoint union of circles. Such circle is called the *boundary component of S*. A *punctured sphere* is a connected surface with or without boundary contained in a two-dimensional sphere $\mathbb{S}^2$. To recall these basic concepts, the reader may refer to the books by S. Aranson, G. Belitsky, and E. Zhuzhoma [1] and by T. Ma and S. Wang [9].

2.3. **Notion of flows.** Roughly speaking, a flow is a continuous family $\{v(t,\cdot) \mid t \in \mathbb{R}\}$ of homeomorphisms $v(t,\cdot) : S \to S$ on a compact surface S, and the point $v(t,x)$ is a position of a point x after time t. Precisely, a continuous mapping $v : \mathbb{R} \times S \to S$ on a compact surface S is a *flow* if it satisfies the following two conditions:

(1) $v(0,\cdot) : S \to S$ is an identity mapping on S, and
(2) $v(t, v(s,x)) = v(t+s, x)$.

The second condition implies that $v(t,\cdot) \colon S \to S$ is a homeomorphism. For a point x of S, *the orbit of* x can be defined as $O(x) := \{v(t,x) \mid t \in \mathbb{R}\}$. A subset is saturated if it is a union of orbits.

Hereafter, we assume that v is a flow on a compact surface S, unless otherwise stated.

2.3.1. *Topological equivalence.* A flow v on a compact surface S is topologically equivalent to a flow v' on a compact surface S' if there is a homeomorphism $h \colon S \to S'$ which maps orbits of v to orbits of v' and preserves the direction of orbits. For a flow v on on a compact surface S and a flow v' on a compact surface S', a point $x \in S$ is locally topologically equivalent to a point $y \in S'$ if there are neighborhoods U_x and U_y of x and y respectively, and a homeomorphism $h \colon U_x \to U_y$ capable of preserving the direction of the orbits such that the images of connected components of the intersection of an orbit of v and U_x correspond to those of the intersection of an orbit of v' and U_y (i.e., $h(C_p) = C_{h(p)}$ for any point $p \in U_x$, where C_p is the connected component of $O_v(p) \cap U_x$ containing p and $C_{h(p)}$ is the connected component of $O_{v'}(h(p)) \cap U_y$ containing $h(p)$). Similarly, a vector field X on a compact surface S is topologically equivalent to a vector field X' on a compact surface S' if there is a homeomorphism $h \colon S \to S'$ that maps orbits of X to orbits of X' and preserves the direction of orbits.

2.3.2. *Types of points and orbits.* A point x is *singular* if its orbit consists of one point, i.e., $x = v(t,x)$ for any $t \in \mathbb{R}$. A point x is *periodic* if there is a positive number $T > 0$ such that $x = v(T,x)$ and $x \neq v(t,x)$ for any $t \in (0,T)$. Roughly speaking, periodic points are points with circular orbits. Singular and periodic points are *closed* points, but each point x cannot be both singular and periodic. The set of singular (resp. periodic, closed) points is denoted by $\mathrm{Sing}(v)$ (resp. $\mathrm{Per}(v)$, $\mathrm{Cl}(v)$). An orbit is *singular* (resp. *periodic*, *closed*) if it contains a singular (resp. periodic, closed) point. An orbit is *proper* if there is a neighborhood of it where the orbit becomes a closed set. The union of non-closed proper orbits is denoted by $\mathrm{P}(v)$. A point is wandering if there are its neighborhood U and a positive number N such that $v_t(U) \cap U = \emptyset$ for any $t > N$; then, U is called a wandering domain. Contrarily, a point is non-wandering if it is not wandering (i.e., for any its neighborhood U and for any positive number N, there is a number $t \in \mathbb{R}$ with $|t| > N$ such that $v_t(U) \cap U \neq \emptyset$). Because each orbit of the flows on a compact punctured sphere $S \subseteq \mathbb{S}^2$ is proper [10], the following decomposition can be derived.

Lemma 1. *Let v be a flow on a compact punctured sphere $S \subseteq \mathbb{S}^2$. Then $S = \mathrm{Sing}(v) \sqcup \mathrm{Per}(v) \sqcup \mathrm{P}(v)$, where $\sqcup$ denotes a disjoint union.*

2.3.3. *Non-degeneracy of singular points.* A singular point is *isolated* if there is a neighborhood that contains only one singular point. It should be noted that each

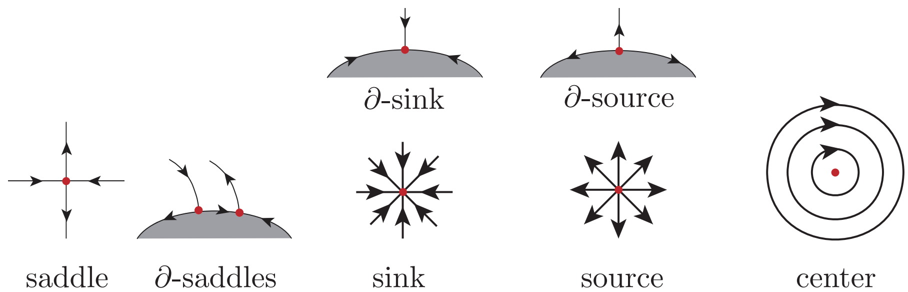

FIGURE 1. Non-degenerate singular points.

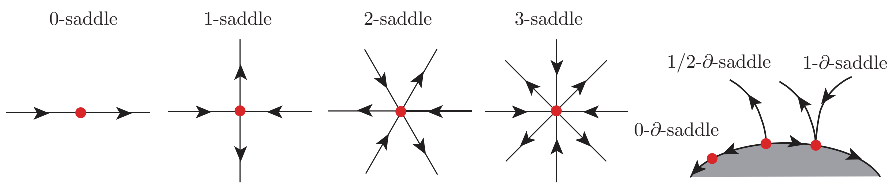

FIGURE 2. Examples of multi-saddles.

singular point of a flow with finitely many singular points is isolated. An isolated singular point p of a flow generated by a C^1-vector field X is non-degenerate if its determinant of the Hesse matrix $(\partial X_i/\partial x_j(p))_{i,j}$ is nonzero (i.e., $\partial X_1/\partial x_1(p) \cdot \partial X_2/\partial x_2(p) - \partial X_1/\partial x_2(p) \cdot \partial X_2/\partial x_1(p) \neq 0$) (see Figure 1). A non-degenerate singular point is a *center* if the Hesse matrix eigenvalues are purely imaginary. A non-degenerate singular point outside of the boundary is a *sink* or *source* if the Hesse matrix eigenvalues have a positive or negative real part, respectively. A non-degenerate singular point on the boundary is a *∂-sink* or *∂-source* if the Hesse matrix eigenvalues are positive or negative, respectively. A non-degenerate singular point outside of or on the boundary is a *saddle* or *∂-saddle*, respectively, if the Hesse matrix eigenvalues have both a positive and negative component. Therefore, a non-degenerate singular point is a saddle if and only if it has exactly four separatrices, whereas a non-degenerate singular point is a ∂-saddle if and only if it has exactly three separatrices, counted with multiplicity. By definition of types of singular points, a non-degenerate singular point is either a sink, a ∂-sink, a source, a ∂-source, a saddle, a ∂-saddle, or a center.

2.3.4. *Multi-saddle, (∂-)saddles, and (multi-)saddle connection diagram.* A *k-saddle* is an isolated singular point outside of the boundary of a compact surface with exactly $(2k + 2)$-separatrices, counted with multiplicity for a non-negative integer $k \in \mathbb{Z}_{\geq 0}$ as shown in Figure 2. A *∂-$k/2$-saddle* is an isolated singular point on the boundary of a compact surface with exactly $(k+2)$-separatrices, counted with multiplicity for a non-negative integer $k \in \mathbb{Z}_{\geq 0}$ as shown in Figure 2. A *multi-saddle* is either a k-saddle or ∂-$k/2$-saddle for a non-negative integer k. A 0-saddle is called a fake saddle; similarly, a ∂-0-saddle is called a fake ∂-saddle (see Figure 3). A fake multi-saddle is either a fake saddle or a fake ∂-saddle. A non-singular orbit is a *sep-*

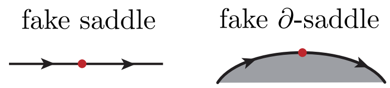

FIGURE 3. Fake saddle and fake ∂-saddle.

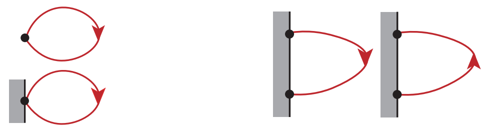

FIGURE 4. Homoclinic orbits (left) and self-connected heteroclinic but non-homoclinic orbits (right).

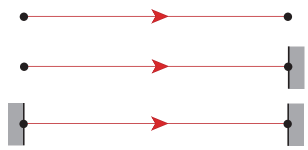

FIGURE 5. Heteroclinic orbits. Both ends are either distinct saddles in the uppermost diagram, a saddle and a ∂-saddle in the middle diagram, or distinct ∂-saddles in the lowermost diagram.

aratrix if it begins from or ends to a singular point. A separatrix is a *multi-saddle* separatrix if it begins from and ends to multi-saddles. It should be noted that a saddle (resp. ∂-saddle) is a 1-saddle (resp. ∂-1/2-saddle). The *saddle connection diagram* presents a union of saddles, ∂-saddles, and orbits beginning from or ending to them. A *saddle connection* is a connected component of the saddle connection diagram. Similarly, the *multi-saddle connection diagram* presents a union of multi-saddles and multi-saddle separatrices. A *multi-saddle connection* is a connected component of the multi-saddle connection diagram. It should be noted that the saddle connection diagram in the unbounded case is called the ss-saddle connection diagram in [16].

2.3.5. *Self-connectedness of separatrices.* A separatrix is *self-connected* if it connects either the same saddle or two ∂-saddles on the same boundary component of the compact surface. All possible scenarios for self-connected separatrices are shown in Figure 4. A (multi-)saddle connection is *self-connected* if each non-singular orbit in it is self-connected (upper case in Figure 4). A separatrix is *homoclinic* if it connects the same multi-saddle (left case in Figure 4). All possible scenarios are shown in the left case in Figure 4. A separatrix is *heteroclinic* if it connects distinct multi-saddles. All possible combinations are shown in Figure 5. Because those orbits in Figure 5 are heteroclinic, two singular points in the uppermost diagram and two boundaries in the lowermost diagram are not identical.

2.3.6. *Topological center, trivial flow box, and periodic annulus.* A singular point of a flow v is a topological center if there is a saturated open neighborhood U of it such that the restriction $v|_U$ is topologically equivalent to the restriction of a flow to an open neighborhood of a center. A disk is a center disk if it consists of a

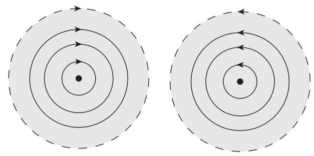

FIGURE 6. Center disks.

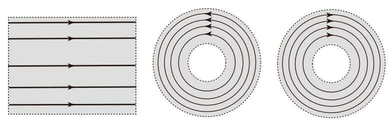

FIGURE 7. Trivial flow box (left) and periodic annuli (right).

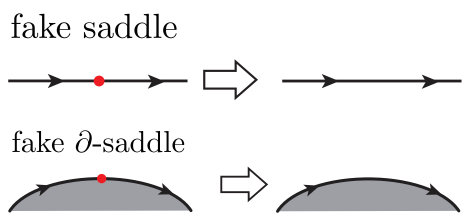

FIGURE 8. Vanishing of a fake saddle and a fake ∂-saddle.

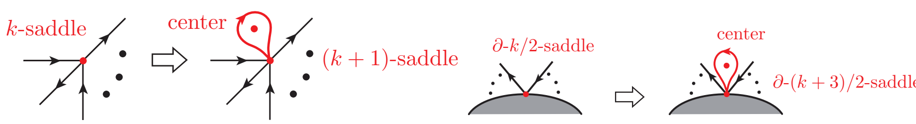

FIGURE 9. Creation of a center.

topological center and periodic orbits, as illustrated in Figure 6. A saturated disk is a trivial flow box if it consists of non-closed proper orbits, and a saturated annulus is a periodic annulus if it consists of periodic orbits, as shown in Figure 7.

2.3.7. *Creations and annihilations of topological centers and multi-saddles.* By the Poincaré-Hopf theorem, fake saddles and fake ∂-saddles can emerge (creation process) or vanish (annihilation process), as shown in Figure 8. Emerging is the inverse operation of vanishing. On the other hand, a center is created via the splitting a k-saddle (resp. ∂-$k/2$-saddle), and a $(k+1)$-saddle (resp. ∂-$(k+3)/2$-saddle), and an annihilation of a center is the inverse operation of the creation (see Figure 9).

2.3.8. *1-source–sink point, ss-orbits and ss-separatrices.* A degenerate singular point is a 1-source–sink point if it is locally topologically equivalent to the point at infinity by taking a one point compactification of $\mathbb{R}^2$ with a uniform flow. Intuitively, the dashed boundary of the left flow box in Figure 7 collapses into a point in Figure 10 (see [16] for a detailed definition of a 1-source–sink point). Here a uniform flow on a punctured sphere is a flow generated by a vector field $(1,0)$ on $\mathbb{R}^2$. It should be noted that a 1-source–sink point is also known as a bipole and that a 1-source–sink point can be obtained by merging a sink and a source or by merging two centers.

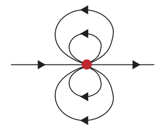

FIGURE 10. 1-source–sink point obtained by the one-point compactification of a uniform flow.

A separatrix is an ss-orbit if it connects from and to a 1-source–sink point. A separatrix is an ss-separatrix if it connects between a multi-saddle and a 1-source–sink point. The restriction of a flow with a 1-source–sink point ∞ on a compact surface S to the complement $S - \{\infty\}$ is called a *flow on a punctured surface* $S - \{\infty\}$.[1] A punctured surface is the complement $S - \{\infty\}$; punctured surfaces are unbounded. When the compact surface S is contained in a sphere, the punctured surface is also called a punctured plane.

2.3.9. *Divergence-free vector fields.* A C^r ($r \in \mathbb{Z}_{>0}$) vector field X on a surface S is divergence-free if $\mathrm{div}X = 0$, where $\mathrm{div}X$ is the divergence of X.[2] In other words, the divergence-free vector field X is locally defined by $\mathrm{div}X := \partial H/\partial x_1 + \partial H/\partial x_2 = 0$ in any local coordinate system (x_1, x_2) of a point $p \in S$. It is known that the flow generated by a divergence-free vector field on a compact surface is non-wandering. Indeed, Liouville's theorem states that the flow generated by a divergence-free vector field is volume-preserving. As the volume of any compact surface is finite, any volume-preserving vector field on a compact surface has no wandering domains and so is non-wandering. Herein, a non-wandering vector field possesses no non-wandering domains. This means that any divergence-free vector field on a compact surface is non-wandering.

2.4. **Hamiltonian dynamics.**

2.4.1. *Hamiltonian vector fields.* A vector field X on a compact surface S is a C^r-Hamiltonian vector field with a C^{r+1}-Hamiltonian $H\colon S \to \mathbb{R}$ ($r \geq 1$) if the Hamiltonian vector field X is locally defined by $X = (\partial H/\partial x_2, -\partial H/\partial x_1)$ in any local coordinate system (x_1, x_2) of a point $p \in S$.[3] It should be noted that any Hamiltonian vector field is divergence-free. Indeed, it stands that $\mathrm{div}X := \partial H/\partial x_1 + \partial H/\partial x_1 = \partial^2 H/\partial x_1 \partial x_3 + \partial^2 H/\partial x_2 \partial x_1 = 0$. A C^r Hamiltonian vector field X ($r \geq 1$) is *structurally stable* if the resulting vector field by any C^1 small perturbation in the set of C^r Hamiltonian vector fields is topologically equivalent to X. Let $\chi_{\mathrm{Ham,bd}}$ be the set of C^r Hamiltonian vector fields ($r \in \mathbb{Z}_{\geq 1}$) with finitely many singular points on connected compact surfaces. Equip $\chi_{\mathrm{Ham,bd}}$ with the C^1 topology. Denote by $\chi_{\mathrm{Ham,bd,str}}$ the set of Hamiltonian flows in $\chi_{\mathrm{Ham,bd}}$ which are structurally stable in $\chi_{\mathrm{Ham,bd}}$.

[1] The set difference is denoted as $X \setminus Y$. Especially, when $Y \subseteq X$, the set difference is denoted as $X - Y$.

[2] More precisely, $\mathrm{div}X := * d * g(X, \cdot)$, where $*$ is the Hodge star operator, d is the exterior derivative, and g is a Riemannian metric.

[3] Generally, the Hamiltonian vector field X is defined by $dH = \omega(X, \cdot)$ as a one-form, where ω is a volume form of S. It should be noted that a volume form on an orientable surface is a symplectic form.

2.4.2. *Hamiltonian vector fields with a 1-source–sink point.* A vector field with a 1-source–sink point ∞ on a connected compact surface S is a *Hamiltonian vector field with a 1-source–sink point* if the restriction of the vector field on $S - \{\infty\}$ is a Hamiltonian vector field.[4] In this paper, we call the restriction of a Hamiltonian vector field with a 1-source–sink point ∞ to the complement $S - \{\infty\}$ a *Hamiltonian vector field on an unbounded punctured surface.* In other words, a Hamiltonian vector field on a punctured surface is a vector field whose resulting vector field by a one-point compactification is a Hamiltonian vector field with a 1-source–sink point on a compact surface. Let $\chi_{\mathrm{Ham,ubd}}$ be the set of C^r Hamiltonian vector fields ($r \in \mathbb{Z}_{\geq 1}$) with a 1-source–sink point and with finitely many singular points on connected compact surfaces. Equip $\chi_{\mathrm{Ham,ubd}}$ with the C^1 topology. Denote by $\chi_{\mathrm{Ham,ubd,str}}$ the set of Hamiltonian flows in $\chi_{\mathrm{Ham,ubd}}$ which are structurally stable in $\chi_{\mathrm{Ham,ubd}}$.

2.4.3. *Hamiltonian flows.* We call that a flow on a surface S is a *Hamiltonian flow* if it is a flow generated by a Hamiltonian C^1-vector field. Moreover, we have a following properties.

Lemma 2. *The following statements hold for a Hamiltonian flow v on a compact surface S:*
(1) *The flow v is non-wandering.*
(2) $S = \mathrm{Sing}(v) \sqcup \mathrm{Per}(v) \sqcup \mathrm{P}(v)$.
(3) *A connected component of the union* $\mathrm{Sing}(v) \sqcup \mathrm{P}(v)$ *is a periodic annulus.*
(4) $\overline{O} - O \subseteq \mathrm{Sing}(v)$ *for any orbit O.*
Moreover, if v has at most finitely many singular points, then the following statements hold:
(5) *Each singular point is either a topological center or a multi-saddle.*
(6) *The multi-saddle connection diagram $D(v)$ is the union of multi-saddles and* $\mathrm{P}(v)$ *such that the complement $S - D(v)$ is the union of topological centers and* $\mathrm{Per}(v)$.

Proof. Let H be the Hamiltonian generating v. By definition, each orbit are contained in the inverse image $H^{-1}(c)$ for some $c \in \mathbb{R}$. We claim that any orbit is proper. Indeed, let x be a non-singular point. The flow box theorem (cf. [1, Theorem 1.1, p.45]) implies that there is an open flow box U_x containing x. Then an open flow box consists of open orbit arcs. Here an open orbit arc is an arc contained in an orbit. By definition of Hamiltonian flow, the orbit arcs have pairwise different values of the Hamiltonian H. This means that the intersection of $U_x \cap O(x)$ is an open orbit arc, and, subsequently, the orbit $O(x)$ is proper. Thus $S = \mathrm{Sing}(v) \sqcup \mathrm{Per}(v) \sqcup \mathrm{P}(v)$. As mentioned above, any Hamiltonian vector field is divergence-free, and the flow generated on a compact surface is non-wandering. This implies that all Hamiltonian flows are non-wandering. [14, Theorem 2.5] implies that the union $\mathrm{Per}(v)$ is open, and thus the complement $S - \mathrm{Per}(v) = \mathrm{Sing}(v) \sqcup \mathrm{P}(v)$ is closed. Following [14, Proposition 2.6], $\overline{O} - O \subseteq \mathrm{Sing}(v)$ for any orbit O.

---

[4]More precisely, the definition of “Hamiltonian vector field with a 1-source–sink point” requires that the 1-source–sink point ∞ has a neighborhood U of ∞ and a bounded disk D in $\mathbb{R}^2$ such that the restriction to the intersection $U \cap (S - \{\infty\})$ of the symplectic form on $S - \{\infty\}$ is a pull back of the restriction to the complement $\mathbb{R}^2 - D$ of the standard volume form $dx \wedge dy$ on the plane $\mathbb{R}^2$.

Suppose that v has at most finitely many singular points. By [4, Theorem 3], each singular point of a Hamiltonian flow with finitely many singular points on a compact surface is either a multi-saddle or a topological center. This implies that the difference $\overline{O} - O \subseteq \mathrm{Sing}(v)$ for any orbit O consists of multi-saddles. Let $\mathrm{Sing}_c(v)$ be the set of topological centers and $D(v)$ the multi-saddle connection diagram. Then $D(v) = (\mathrm{Sing}(v) - \mathrm{Sing}_c(v)) \sqcup \mathrm{P}(v)$ and $S - D(v) = \mathrm{Sing}_c(v) \sqcup \mathrm{Per}(v)$. $\square$

A *Hamiltonian flow with a 1-source–sink point* is the flow generated by a Hamiltonian vector fields with a 1-source–sink point. In this paper, we call the restriction of a Hamiltonian flow with a 1-source–sink point ∞ to the complement $S - \{\infty\}$ a *Hamiltonian flow on an unbounded punctured surface*. Moreover, a Hamiltonian flow on an unbounded punctured surface is called a *Hamiltonian flow on a punctured plane* if the compact surface S is a compact punctured sphere. In other words, a Hamiltonian flow on a punctured plane results in Hamiltonian flow on a compact punctured sphere with a 1-source–sink point via one-point compactification.

2.4.4. *Classes of Hamiltonian flows.* A *genus element* is either a topological center or a boundary component. The set of Hamiltonian flows on compact punctured spheres (resp. connected compact surfaces of genus g) is denote by $\mathcal{H}_{\mathrm{bd}}$ (resp. $\mathcal{H}_{g,\mathrm{bd}}$), and the set of Hamiltonian flows on the punctured planes (resp. unbounded punctured surfaces of genus g) is denoted by $\mathcal{H}_{\mathrm{ubd}}$ (resp. $\mathcal{H}_{g,\mathrm{ubd}}$). It should be noted that $\mathcal{H}_{\mathrm{bd}} = \mathcal{H}_{0,\mathrm{bd}}$ and $\mathcal{H}_{\mathrm{ubd}} = \mathcal{H}_{0,\mathrm{ubd}}$. We denote by $\mathcal{H}_{\mathrm{bd}}(n)$ (reps. $\mathcal{H}_{g,\mathrm{bd}}(n)$) the set of Hamiltonian flow with finitely many singular points in $\mathcal{H}_{\mathrm{bd}}$ (resp. $\mathcal{H}_{g,\mathrm{bd}}$) such that the number of genus elements (i.e., the sum of numbers of centers and boundary components) is n. Finally, we denote by $\mathcal{H}_{\mathrm{ubd}}(n)$ (resp. $\mathcal{H}_{g,\mathrm{ubd}}(n)$) the set of Hamiltonian flows with finitely many singular points in $\mathcal{H}_{\mathrm{ubd}}$ (resp. $\mathcal{H}_{g,\mathrm{ubd}}$) such that the number of genus elements is n. We have the following observations.

Lemma 3. *For a Hamiltonian flow v on an unbounded punctured surface S, there are a Hamiltonian flow w on a compact surface T, and a closed interval I in T and a homeomorphism $h\colon S \to T - I$ such that for any orbit O of v there is a unique orbit O' of w such that $h^{-1}(O' \setminus I) = O$, and that h preserves the direction of the orbits.*

Proof. Let v be a Hamiltonian flow with a 1-source–sink point on an unbounded punctured surface $S_\infty := S \sqcup \{\infty\}$, $D_r := \{(x, y) \in \mathbb{R}^2 \mid x^2 + y^2 \leq r\}$ the closed disk centered at the origin with radius $r > 0$, and u a uniform flow on $\mathbb{R}^2$ by $u(t, (x, y)) := (x+t, y)$. The existence of a 1-source–sink point implies that there are a compact surface D in S, a closed disk D_r for some $r > 0$, and a homeomorphism $h'\colon S - D \to \mathbb{R}^2 - D_r$ such that the restriction $v|_{S-D}$ corresponds to $u|_{\mathbb{R}^2 - D_r}$ (i.e. the image of any connected component of the intersection $O_v \cap (S - D)$ of $S - D$ and an orbit O_v of v is a connected component of the intersection $O_u \cap (\mathbb{R}^2 - D_r)$ of $\mathbb{R}^2 - D_r$ and an orbit O_u of u). Let u_1 be a flow on an open annulus $\mathbb{A} := \mathbb{R}/\mathbb{Z} \times \mathbb{R}$ by $u(t, [x, y]) := [x+t, y]$ and $k\colon \mathbb{R}^2 \to \mathbb{A}$ an embedding with $k(\mathbb{R}, y) = [(0, 1)] \times \{y\}$. Then, $S - D$ can be identified with a subset of $[(0, 1)] \times \mathbb{R} \subset \mathbb{A}$. Replacing D with D_r, we can construct a flow v_1 on the resulting surface S_1 such that the flow v_1 corresponds to v on D and to u_1 on $S_1 \setminus D$. Precisely, any connected component of the intersection $(S_1 \setminus D) \cap O_{u_1}$ of $(S_1 \setminus D)$ and an orbit O_{u_1} of u_1 is a connected component of the intersection $(S_1 \setminus D) \cap O_{v_1}$ for an orbit O_{v_1} of v_1. Further, any connected component of the intersection $D \cap O_v$ of D and an orbit O_v of v is a connected component of the intersection $D \cap O_{v_1}$ for an orbit O_{v_1} of v_1. Then for any orbit O of v there is a unique orbit O_1 of v_1 such that $O = O_1 \setminus ([0] \times \mathbb{R})$. Consequently, the two-point compactification S_2 of S_1 is a punctured sphere T, the resulting flow w from v_1 is desired, and the closed interval I is $T - S$. □

Lemma 4. *Each singular point of a Hamiltonian flow with finitely many singular points on either a compact surface or an unbounded punctured surface is either a multi-saddle or a topological center.*

Proof. Let v be a Hamiltonian flow with finitely many singular points on either a compact surface or an unbounded punctured surface S. If S is compact surface, then Lemma 2 implies that each singular point of v is either a multi-saddle or a topological center. Thus we may assume that S is an unbounded punctured surface. Lemma 3 implies that each singular point of v is either a multi-saddle or a topological center. □

It should be noted that the multi-saddle connection diagram $D(v)$ for a Hamiltonian flow with non-degenerate singular points on a surface corresponds to the saddle connection diagram. Moreover, Hamiltonian flows on a sphere correspond to incompressible flows (cf. [9]).

2.4.5. *Structurally stability of Hamiltonian flows.* A Hamiltonian flow is *structurally stable* if the generating Hamiltonian vector field is structurally stable. A flow is unstable if it is not structurally stable. The structural stability of Hamiltonian flows is generic and is topologically characterized as follows (see [9, 16] for details).

Lemma 5 (cf. [9, p. 74 Theorem 2.3.8] and [16, Theorem 3.2])**.** *Let $\mathcal{H}$ denote either $\mathcal{H}_{g,\mathrm{bd}}$ or $\mathcal{H}_{\mathrm{ubd}}$. The set of structurally stable Hamiltonian flows in $\mathcal{H}$ is open dense in $\mathcal{H}$. Moreover, the following statements are equivalent:*
(1) *A Hamiltonian flow in $\mathcal{H}$ is structurally stable in $\mathcal{H}$.*
(2) *Each singular point is non-degenerate and each saddle connection is self-connected* (i.e., *each separatrix either is self-connected or is an ss-separatrix*).

Proof. If $\mathcal{H} = \mathcal{H}_{g,\mathrm{bd}}$, then the above assertion holds from [9, p. 74 Theorem 2.3.8]. Therefore we may assume that $\mathcal{H} = \mathcal{H}_{g,\mathrm{ubd}}$. If $\mathcal{H} = \mathcal{H}_{\mathrm{ubd}}$, then the above assertion holds from [16, Theorem 3.2]. Replacing a punctured plane with an unbounded punctured surface, the same proof of [16, Theorem 3.2] implies the above assertion for $\mathcal{H}_{g,\mathrm{ubd}}$. □

2.4.6. *Complete invariance of the saddle connection diagrams of Hamiltonian flows.* Essentially, Morse theory states that any Hamiltonian flow with non-degenerate singular points is determined by the saddle connection diagram, up to topological equivalence. More precisely, the following statements hold.

Lemma 6 (cf. [9, p. 42 Theorem 1.4.6])**.** *Any Hamiltonian flow in $\mathcal{H}_{g,\mathrm{bd}}(n)$ for any non-negative integer n is determined by the multi-saddle connection diagram as a surface graph up to topological equivalence. Moreover, any connected component of the complement of the union of the saddle connection diagram and periodic orbits on the boundary of the compact surface is an open periodic annulus* (*see Figure 7*).

Proof. Let $v \in \mathcal{H}_{g,\mathrm{bd}}(n)$ be a Hamiltonian flow on a compact surface S for some non-negative integer n. Lemma 2 implies that the complement of the multi-saddle connection diagram is the union of topological centers and periodic annuli $\mathrm{Per}(v)$.

Therefore any connected component of the complement of the union $D(v) \cup (\partial S \cap \mathrm{Per}(v))$ of the saddle connection diagram and periodic orbits on the boundary ∂S is either an open periodic annulus or an open center disk. Since the saddle connection diagram $D(v)$ as a surface graph has the information of the boundary implicitly, it is a complete invariant of Hamiltonian flows in $\mathcal{H}_{\mathrm{bd}}(n)$. $\square$

Lemma 7 (cf. [16, p. 10 Remark after Theorem 3.2])**.** *Any Hamiltonian flow in $\mathcal{H}_{g,\mathrm{ubd}}(n)$ for any non-negative integer n is determined by the multi-saddle connection diagram as a surface graph up to topological equivalence. Moreover, any connected component of the union of the complement of the union of the saddle connection diagram and periodic orbits on the boundary of the punctured surface is either an open flow fox or open periodic annulus (see Figure 7).*

Proof. Let $v \in \mathcal{H}_{g,\mathrm{ubd}}(n)$ be a Hamiltonian flow on an unbounded punctured suface S for some non-negative integer n. Lemma 3 implies that there are a Hamiltonian flow w on a connected compact surface T, and a closed interval I in T and a homeomorphism $h \colon S \to T - I$ capable of preserving the direction of the orbits such that for any orbit O of v there is a unique orbit O' of w such that $h^{-1}(O' \setminus I) = O$. Lemma 6 implies that any connected component of the complement of the union $D(w) \cup (\partial T \cap \mathrm{Per}(w))$ of the saddle connection diagram and periodic orbits on the boundary ∂T is an open periodic annulus. This suggests that any connected component of the complement of the union $D(v) \cup (\partial S \cap \mathrm{Per}(v))$ of the saddle connection diagram and periodic orbits on the boundary ∂S corresponds to either an open center disk or the difference $A \setminus I$, where A is an open periodic annulus. Because the difference $A \setminus I$ is either an open flow fox or open periodic annulus, the above assertion holds. $\square$

It should be noted that a ∂-saddle is a non-degenerate ∂-1/2-saddle, and a pinching point, i.e., ∂-1-saddle, is degenerate and not included in structurally stable Hamiltonian flows.

2.4.7. *Typical transitions between Hamiltonian flows.* In real-world applications, the following four kinds of transitions between Hamiltonian flows with finitely many singular points are observed.

(i) Creations and annihilations of centers (see Figure 11)
  e.g., Creations and annihilations of vortices
(ii) Creations and annihilations of boundaries (see Figure 12)
  e.g., Appearances and disappearances of stones on the surface of a river
(iii) Non-self-connected separatrices
  e.g., Separatrices between saddles and ∂-saddles (see Figure 13)
(iv) Merging and splitting of multi-saddles
  e.g., Merging and splitting of ∂-saddles (see Figure 14)

In this paper, we deal with exactly four these transitions. It should be noted that the "creations and annihilations of boundaries" changes the whole compact surfaces, and that we fix a number of genus elements if we deal with transition without creations and annihilations of centers or creations and annihilations of boundaries.

2.4.8. *Transitions between structurally stable Hamiltonian flows.* A Hamiltonian flow with self-connected saddle connections is *f-unstable* if it has just one fake multi-saddle and all singular points excluding the fake multi-saddle are non-degenerate.

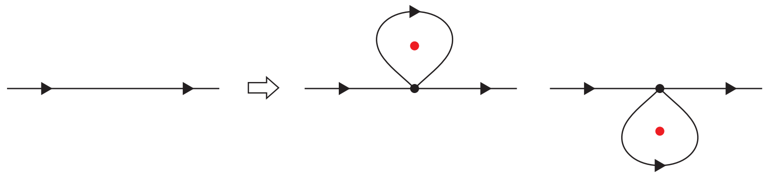

Figure 11. Creations of centers with counter-clockwise and clockwise flow directions.

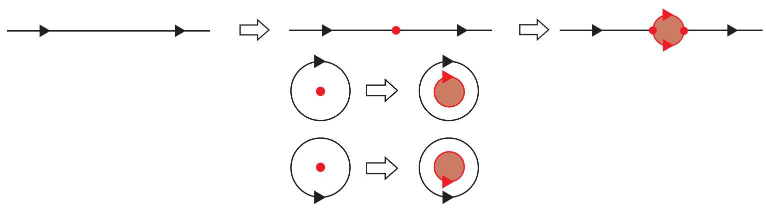

Figure 12. Creations of boundaries.

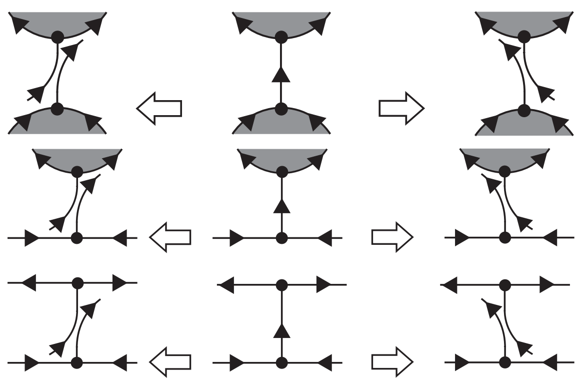

Figure 13. Separatrices between saddles and ∂-saddles.

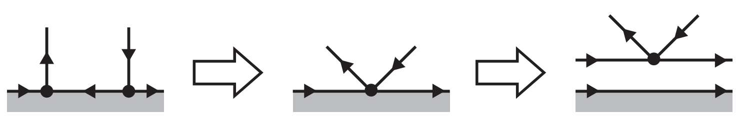

Figure 14. Merging of two ∂-saddles.

The "f" in "f-unstable" stands for "fake." A fake multi-saddle can be vanished under fixing the same number of genus elements (see Figure 8). Subsequently, any small perturbation of an f-unstable Hamiltonian flow on a compact surface or an unbounded punctured surface implies the emergence of the same structurally stable Hamiltonian flow up to topological equivalence. In other words, a transition whose intermediate flow is f-unstable is trivial under fixing of the same number of genus elements. In addition, a Hamiltonian flow with self-connected saddle connections is *t-unstable* if it has just one topological center, and all singular points excluding the topological center are non-degenerate. The "t" in "t-unstable" stands for "topological center". With the same fixed number of genus elements, any perturbation of a t-unstable Hamiltonian flow on a compact surface or an unbounded punctured surface implies the same structurally stable Hamiltonian flow up to topological equivalence. In other words, a transition whose intermediate flow is t-unstable is trivial under fixing of the same number of genus elements. Therefore, we consider the following condition for the non-existence of fake multi-saddles and topological centers to omit trivial transitions:

($A1$) Neither fake multi-saddles nor topological centers exist.

This condition means that any singular point of a Hamiltonian flow with finitely many singular points is either a center or non-fake multi-saddle under the above assumptions. A Hamiltonian flow with non-degenerate singular points is *h-unstable* if it has exactly one non-self-connected orbit in the saddle connection diagram. A Hamiltonian flow with self-connected saddle connections is *p-unstable* if it has just one pinching point and all singular points excluding the pinching point are non-degenerate. The "h" in "h-unstable" and the "p" in "p-unstable" stand for "heteroclinic" and "pinching", respectively. A generic transition between structurally stable Hamiltonian flows with the same number of genus elements is either p-unstable or h-unstable. More precisely, denote by χ_{Ham} the subset of vector fields without topological centers or fake multi-saddles in $\chi_{\mathrm{Ham,bd}}$ (resp. $\chi_{\mathrm{Ham,ubd}}$) and by $\chi_{\mathrm{Ham,str}}$ the set of structurally stable Hamiltonian vector fields without topological centers or fake multi-saddles in $\chi_{\mathrm{Ham,bd}}$ (resp. $\chi_{\mathrm{Ham,ubd}}$). Then the characterization of generic transitions of Hamiltonian flows is described as follows (see [12] for details).

Lemma 8 (cf. [12, Proposition 3.1])**.** *The set of p-unstable or h-unstable Hamiltonian vector fields in* χ_{Ham} *is an open dense subset of the difference* $\chi_{\mathrm{Ham}} - \chi_{\mathrm{Ham,str}}$.

Proof. Recall that the above assertion for $g = 0$ is [12, Proposition 3.1]. Fix a vector field $X \in \chi_{\mathrm{Ham}}$ on a compact surface S. It should be noted that any small perturbations of Hamiltonian vector fields can be correspond to adding the Hamiltonian vector fields generated by Hamiltonian functions whose values and derivatives are small. We claim that any small perturbations imply no merges of distinct multi-saddle connections. Indeed, the finite existence of multi-saddles implies that there is the maximal distance d_M of the distances of pairs of multi-saddles. Lemma 6 implies that the complement of the multi-saddle connection diagram $D(X)$ consists of open flow foxes and open periodic annuli. This implies that, for any multi-saddle connection C, there is an open neighborhood U of C with $U \cap D(X) = C$ such that the difference $U - C$ consists of open flow foxes and open periodic annuli and the boundary ∂U is contained in the multi-saddle connection diagram. In other words, any pairs of adjacent multi-saddle connections have different values of the Hamiltonian. Let V be the minimal value of differences of pairs of the values of distinct multi-saddle connections with respect to the Hamiltonian. Then the quotient V/d_M is a positive number. Fix the resulting vector field $\widetilde{X}$ from X by adding any Hamiltonian vector field whose max norm is less than V/d_M. The Hamiltonian H_Y which generates the adding Hamiltonian vector field Y, any pairs p and q of multi-saddles which belong to adjacent multi-saddle connections of X has still different values of the resulting Hamiltonian after the adding operation because the difference $|H_Y(p) - H_Y(q)|$ is more than $V - \int_\gamma |Y|dt > V - \int_\gamma V/d_M dt = 0$, where γ is a shortest arc-length curve from p to q. Therefore no merges of multi-saddle connections occur by any small perturbations. The claim means that any small perturbations deform multi-saddle connections individually. Therefore the proof of [12, Proposition 3.1] can be applied to the general case. $\square$

It should be noted that the difference $\chi_{\mathrm{Ham}} - \chi_{\mathrm{Ham,str}}$ in this lemma is the set of non-structurally–stable Hamiltonian vector fields, which are intermediate flows of non-trivial transitions. Thus a generic transition between structurally stable Hamiltonian vector fields in χ_{Ham} is either p-unstable or h-unstable. Let $\mathcal{H}$ be either the set of flow in $\mathcal{H}_{g,\mathrm{bd}}$ satisfying condition $(A1)$ or the set of flows in $\mathcal{H}_{g,\mathrm{ubd}}$ satisfying condition $(A1)$. Since a Hamiltonian flow is a flow generated by a Hamiltonian C^1-vector field, a generic transition between structurally stable Hamiltonian flows in $\mathcal{H}$ is either p-unstable or h-unstable. Consequently, the *transition graphs* of structurally stable Hamiltonian flows comprise vertices that are topologically equivalence classes of structurally stable Hamiltonian flows and edges that are topologically equivalence classes of p-unstable or h-unstable Hamiltonian flows. Then, the distance between structurally stable Hamiltonian flows can be defined as the path distance on the transition graph. The condition fixing a number of genus elements means that there occurs neither creation nor annihilation of genus elements.

2.4.9. *Elements of Hamiltonian Flows on compact surfaces and unbounded punctured surfaces.* From now on, we assume that each flow has at most finitely many singular points.

Our pictorially representation of a structurally stable Hamiltonian flow on either a compact surface or an unbounded punctured surface S is $D(v)$ which consists of saddles, ∂-saddle, and separatrices originating or ending to the saddles. Orbits and their directions are represented by curved lines and arrowheads, respectively . In fact, the orbits are classified so that the multi-saddle connection diagram $D(v)$ of a structurally stable Hamiltonian flow on a compact surface or an unbounded punctured surface consists of the orbits in (iii)–(iv) and (vi)–(vii):

(i) orbit in a periodic annulus on $S - \partial S$
   - periodic orbit outside of the boundary ∂S

(ii) non-singular orbit on $\partial S \setminus D(v)$
   - periodic orbit on the boundary ∂S

(iii) singular orbit on $D(v) \setminus \partial S$
   - **structurally stable**: saddle
   - **unstable**: k-saddle

(iv) singular orbit on $D(v) \cap \partial S$
   - **structurally stable**: ∂-saddle
   - **unstable**: ∂-$k/2$-saddle

(v) singular orbit outside of an unbounded punctured surface and compact surface
   - 1-source–sink

(vi) orbit in a trivial flow box in an unbounded punctured surface and outside of the multi-saddle connection diagram $D(v)$
   - ss-orbit

(vii) non-singular orbit on $D(v)$

- **structurally stable**: self-connected separatrix, ss-separatrix
- **unstable**: non-self-connected multi-saddle separatrix

(viii) singular orbit on $S - D(v)$
- topological center

We will show that analysis of Hamiltonian flows can be reduced into a symbolic processing.

Although this study does not deal with fake saddles and fake ∂-saddles, they are intermediate states in the creation and annihilation of topological centers. Indeed, the creation and annihilation of topological centers via a fake saddle and fake ∂-saddle can be analyzed via approximations of polynomial vector fields, like those illustrated in Figure 15 (cf. [3]).

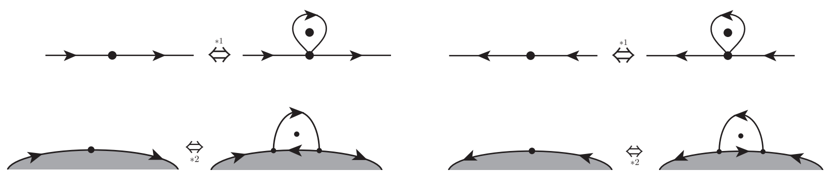

FIGURE 15. Creations and annihilations of self-connected orbits.

2.4.10. *Primitive local transformation rules.* The index of a topological center (resp. k-saddle, ∂-$k/2$-saddle) is one (resp. $-k$, $-k/2$). In this section, we demonstrate the absence of creation and annihilation of topological centers in $\mathcal{H}_{\mathrm{bd}}(n)$ or $\mathcal{H}_{\mathrm{ubd}}(n)$. In other words, there is no merge of non-fake multi-saddles and a positive number of topological centers into a multi-saddle in $\mathcal{H}(n)$.

Lemma 9. *Let $\mathcal{H}(n)$ be either $\mathcal{H}_{g,\mathrm{bd}}(n)$ or $\mathcal{H}_{g,\mathrm{ubd}}(n)$. The following statements hold:*
(1) *Neither creation nor annihilation of topological centers occurs in $\mathcal{H}(n)$.*
(2) *If a continuous path $p\colon (0,1) \to \mathcal{H}(n)$ does not contain creation and annihilation of fake multi-saddles, splitting and merging of multi-saddles, or merging and splitting of separatrices, then the Hamiltonian flows in the image of p are topologically equivalent to each other.*

Proof. Flows in $\mathcal{H}(n)$ have exactly n genus elements and finitely many singular points. Lemma 4 implies that any degenerate singular point is a multi-saddle or topological center, and that there are at most finitely many multi-saddles; therefore, the multi-saddle connection diagram is a finite union of orbits. Lemma 6 and Lemma 7 suggest that a Hamiltonian flow in $\mathcal{H}(n)$ can be determined by the multi-saddle connection diagram; hence any changes of topological equivalence classes of flows in $\mathcal{H}(n)$ owing to the creation or annihilation of topological centers and non-fake multi-saddles, splitting or merging of multi-saddles, and splitting or merging of separatrices. Because the Poincaré-Hopf theorem for continuous flows with finitely many singular points on compact surfaces holds using Gutierrez's smoothing theorem [7], annihilations of topological centers occur by merges of topological centers and multi-saddles. Since any topological centers are isolated, the existence of topological centers is an open condition. Finite existence of centers implies that any small perturbations implies no annihilations of topological centers in $\mathcal{H}(n)$. Hence each change of topological equivalence classes of flows in $\mathcal{H}(n)$ by a small

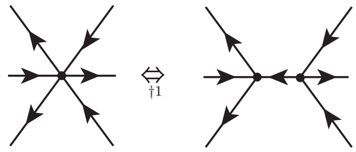

FIGURE 16. Primitive local transformation †1, which is not considered in this study. This changes the number of singular points but preserves the number of genus elements.

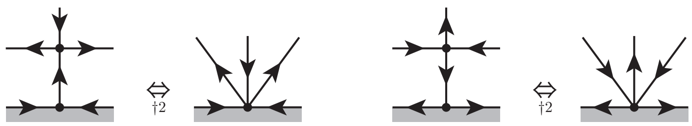

FIGURE 17. Primitive local transformation †2, which is not considered in this study. This changes the number of singular points but preserves the number of genus elements.

perturbation occurred by splitting or merging of separatrices, by splitting or merging of multi-saddles, by creating or annihilating a fake multi-saddle, or by splitting or merging of a non-fake multi-saddle and a topological center. Since any small perturbation of a non-fake multi-saddle moves the multi-saddle in a small open neighborhood, the above assertion holds. □

All local structures of transitions can be described by merging pairs of orbits.

Corollary 10. *Let $\mathcal{H}(n)$ be either the set of flow in $\mathcal{H}_{g,\mathrm{bd}}(n)$ satisfying condition $(A1)$ or the set of flows in $\mathcal{H}_{g,\mathrm{ubd}}(n)$ satisfying condition $(A1)$. Then any changes of topological equivalence classes of flows in $\mathcal{H}(n)$ occurred by splitting or merging of separatrices or by splitting or merging of multi-saddles.*

We describe all local structures of transitions by merging a pair of orbits.

Lemma 11. *Let $\mathcal{H}(n)$ be either $\mathcal{H}_{g,\mathrm{bd}}(n)$ or $\mathcal{H}_{g,\mathrm{ubd}}(n)$. All possible combinations of merging pairs of orbits and their inverse operations are listed in Table 1. Such operations are described as primitive local transformations in $\mathcal{H}(n)$, as shown in Figures 16–18.*

Proof. Flows in $\mathcal{H}(n)$ have exactly n genus elements, and degenerate singular points are multi-saddles or topological centers. There are finitely many multi-saddles; therefore, the saddle connection diagram is a finite union of orbits. Let v be a Hamiltonian flow in $\mathcal{H}(n)$. By Lemma 9, any small perturbation preserves the genus elements. It suffices to show that the inverse operations of orbit merging, as summarized in Table 1, reduce v into a structurally stable Hamiltonian flow in $\mathcal{H}_{g,\mathrm{bd}}$ or $\mathcal{H}_{g,\mathrm{ubd}}$ Lemma 6 and Lemma 7 imply that any connected component of the complement of the union $D(v) \sqcup (\partial S \cap \mathrm{Per}(v)) \sqcup \mathrm{Sing}_c(v)$ is either an open periodic annulus or a trivial flow box, where $\mathrm{Sing}_c(v)$ is the set of topological centers. Therefore v consists of one of the following orbits: (i) periodic orbits in an

		i	ii	iii	iv	v	vi	vii	viii
i	(orbit in $\operatorname{int}\operatorname{Per}(v)$)	1	3	2	4	—	—	1	9
ii	(orbit in $\partial\operatorname{Per}(v)$)		—	6	—	—	—	3	—
iii	(k-saddle)			†1	†2	—	2	2	*1
iv	(∂-$k/2$-saddle)				7	—	4	4	*2
v	(1-source–sink point)					—	5	—	—
vi	(ss-orbit)						8	1	—
vii	(separatrix)							1	—
viii	(topological center)								—

TABLE 1. Primitive local transformations by merging orbits of flows. Circled numbers correspond to primitive local transformations in Figure 18. "—" represents physically impossible combinations. †1 changes the number of singular points in the whitehead operation shown in Figure 16. ∂-3/2-saddles in †2 are non-generic unstable, as shown in Figure 17, because small perturbations can separate ∂-3/2-saddles into ∂-1/2-saddles and 1-saddles.

open periodic annulus; (ii) periodic orbits on the boundary; (iii) k-saddles; (iv) ∂-$k/2$-saddles; (v) the point at infinity (i.e., 1-source–sink point); (vi) ss-orbits; (vii) separatrices; (viii) topological centers. Because bounded and unbounded orbits cannot be merged, the pairs (i)-(vi), (ii)-(vi), and (vii)-(vi) cannot be realized. Since the point at infinity cannot be merged with bounded and unbounded orbits, the pairs (i)-(v), (ii)-(iii) and (v)-(vii) cannot be realized. Because the boundary components cannot be merged, the pairs (ii)-(ii) and (ii)-(iv) cannot be realized. Since a topological center and ∂S (resp. unbounded orbit, sepratrix, and topological center) cannot be merged in $\mathcal{H}(n)$, the pair (ii)-(viii) (resp. (vi)-(viii), (vii)-(viii), and (viii)-(viii)) cannot be realized. The point at infinity and another singular point cannot be merged in $\mathcal{H}(n)$, and so the pairs (iii)-(v), (iv)-(v), and (v)-(viii) cannot be realized. The uniqueness of the point at infinity implies the unfeasibility of the pair (v)-(v). All possible inverse operations of orbit merging are shown in Figures 16–18. □

Because p-unstable or h-unstable Hamiltonian flows can be obtained from structurally stable Hamiltonian flows through orbit merging, they can be described as primitive local transformations in $\mathcal{H}(n)$, as shown in Figure 18.

Corollary 12. *Let $\mathcal{H}(n)$ be either $\mathcal{H}_{g,\mathrm{bd}}(n)$ or $\mathcal{H}_{g,\mathrm{ubd}}(n)$. If $v \in \mathcal{H}(n)$ is either p-unstable or h-unstable, then there is a small open neighborhood $\mathcal{U}$ of v such that v can be obtained from a structurally stable Hamiltonian flow in $\mathcal{U}$ through orbit merging operations, which can be described as primitive local transformations in $\mathcal{H}(n)$, as shown in Figure 18.*

The global transformations of flows simultaneously replace the continuous tiles by the primitive local transformations as follows. When the local transformations are applied from left to right, unstable structures may appear on the merged orbits in which two saddle points are connected by two heteroclinic orbits. For example, the (global) transformation presented in Figure 19, which consists of three primitive local transformations, transforms a structurally stable Hamiltonian flow in $\mathcal{H}(n)$ to an unstable flow in $\mathcal{H}(n)$. Conversely, when the primitive local transformations are applied from right to left, structurally stable Hamiltonian flows are preserved and unstable structures may disappear. For example, the inverse transformation of Figure 19 transforms an unstable flow to a structurally stable Hamiltonian flow. Here, the primitive local transformation rules ① are ② are applied. An example global transformation from one structurally stable Hamiltonian flow to another via an unstable flow is shown in Figure 20. The thick and dashed lines on the left and right, respectively, are merged in the middle via the coupling of primitive local transformations shown in Figure 18. All the primitive local transformations in Figure 18 are applied from the left to the middle or from the right to the middle. Complete global transformations (hereafter, transformations, for simplicity) will be studied in later sections.

3. COT representations of Hamiltonian flows

To describe the topologies of Hamiltonian flows on punctured surfaces and global transformations among structurally stable Hamiltonian flows in a computable way, we refer to formal language theory.

3.1. **Notion of formal grammar.**

We follow the notations and terminologyies of [5].

3.1.1. *Regular tree grammar.*

The set of positive integers is denoted by $\mathbb{N}$. A *ranked alphabet* is the pair $(\mathcal{F}, \mathit{Arity})$ of a finite set $\mathcal{F}$ and a function $\mathit{Arity} : \mathcal{F} \to \mathbb{N}$. The *arity* of a symbol $f \in \mathcal{F}$ is $\mathit{Arity}(f)$, and the set of symbols of arity p is denoted by $\mathcal{F}_p$. Elements of arity $0, 1, \ldots, p$ are called constants, unary, binary, ..., and p-ary symbols, respectively. Herein, an abbreviated declaration of symbols with arity is employed. For example, $f(,)$ is a declaration for the binary symbol f. Let $\mathcal{X}$ be a set of constants called *variables* that is disjoint to $\mathcal{F}_0$. The set $T(\mathcal{F}, \mathcal{X})$ of *terms* over the ranked alphabet $\mathcal{F}$, and the set of variables $\mathcal{X}$ is the smallest set defined by:

- $\mathcal{F}_0 \subseteq T(\mathcal{F}, \mathcal{X})$,
- $\mathcal{X} \subseteq T(\mathcal{F}, \mathcal{X})$,
- if $p \geq 1$, $f \in \mathcal{F}_p$, and $t_1, \ldots, t_p \in T(\mathcal{F}, \mathcal{X})$, then $f(t_1, \ldots, t_p) \in T(\mathcal{F}, \mathcal{X})$.

If $\mathcal{X} = \emptyset$, $T(\mathcal{F}, \mathcal{X})$ is also written as $T(\mathcal{F})$.

A *regular tree grammar* $G = (S, N, \mathcal{F}, R)$ consists of

- a distinguished symbol S, which is called *axiom*,
- a finite set N of *non-terminal* symbols with $S \in N$,
- a finite set $\mathcal{F}$ of *terminal* symbols, and
- a finite set R of *production rules* in the form of $A \to \beta$, where A is a non-terminal of N, and β is a tree of $T(\mathcal{F} \cup N \cup \mathcal{X})$.

3.1.2. *Regular tree grammar with cyclic order.*

A *ranked alphabet with cyclic order* is a triplet $(\mathcal{F}, \mathit{Arity}, \mathit{Cyclic})$ of a finite set $\mathcal{F}$, function $\mathit{Arity} : \mathcal{F} \to \mathbb{N}$, and function $\mathit{Cyclic} : \mathcal{F} \to \{0, 1\}$. The alphabet f is called *cyclic* if $\mathit{Cyclic}(f) = 1$ and *acyclic* if $\mathit{Cyclic}(f) = 0$. Herein, an abbreviated declaration of ranked alphabets with cyclic order is employed. For example, $f(,)$ (resp. $f\{,\}$) is the declaration of a binary acyclic (resp. cyclic) symbol f. In a *regular tree grammar with cyclic order (COT)* $G = (S, N, \mathcal{F}, R)$, $\mathcal{F}$ is a finite set of a ranked alphabet with cyclic order.

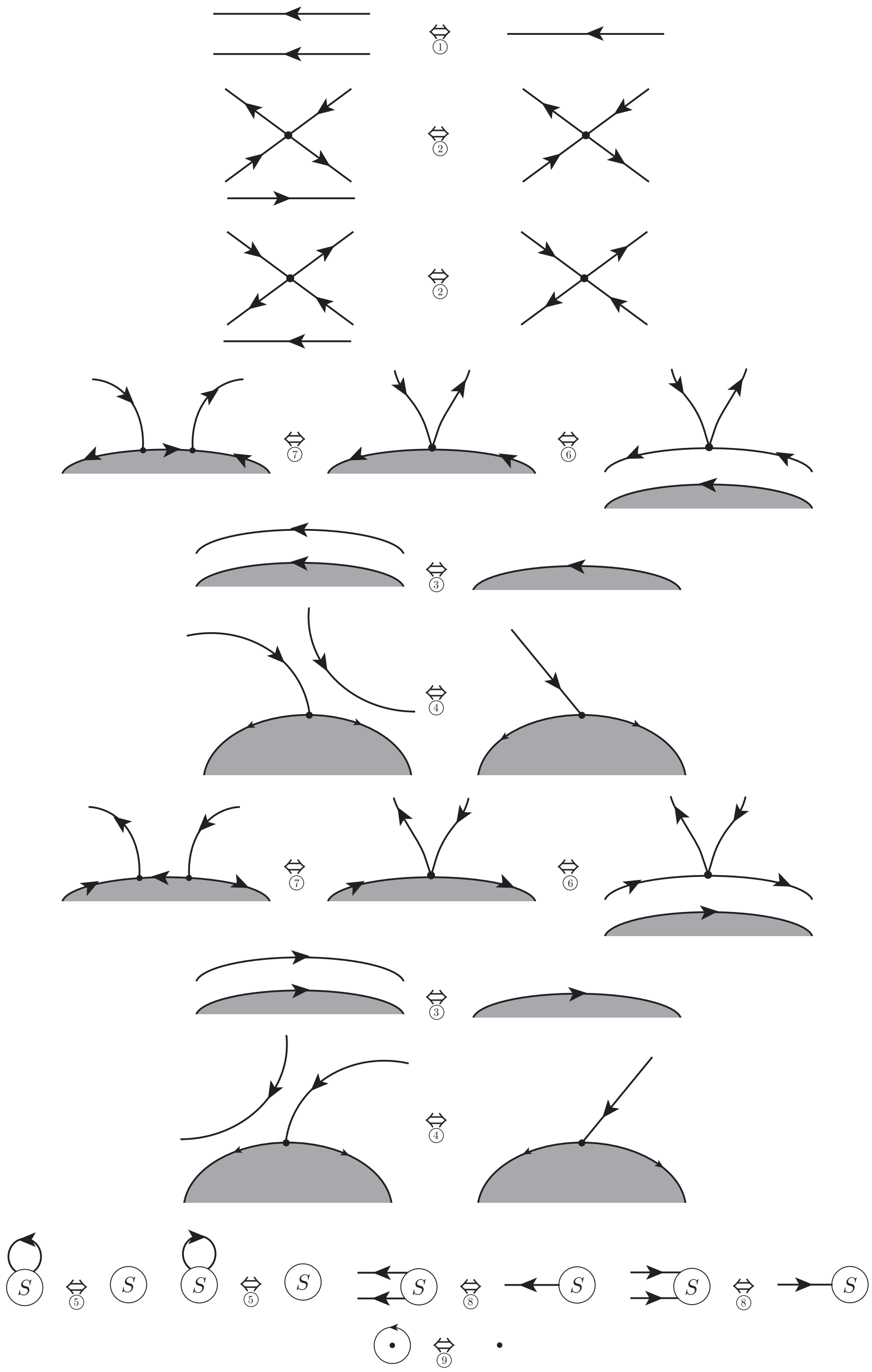

FIGURE 18. Primitive local transformations.

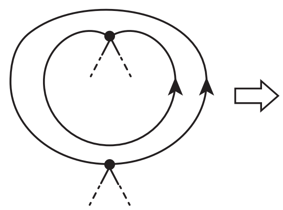

FIGURE 19. An example (global) transformation of a structurally stable Hamiltonian flow to an unstable flow.

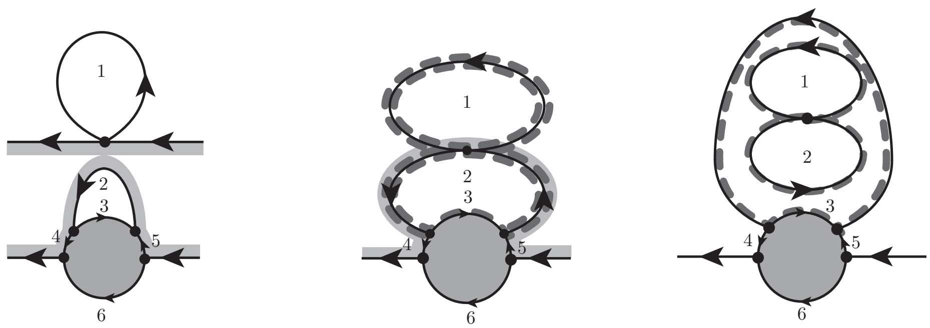

FIGURE 20. An example global transformation of a structurally stable Hamiltonian flow to another structurally stable Hamiltonian flow via an unstable flow.

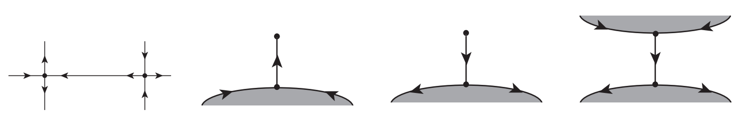

FIGURE 21. Heteroclinic orbits that induce the unstable flow structure in this study: heteroclinic saddle connection evolution.

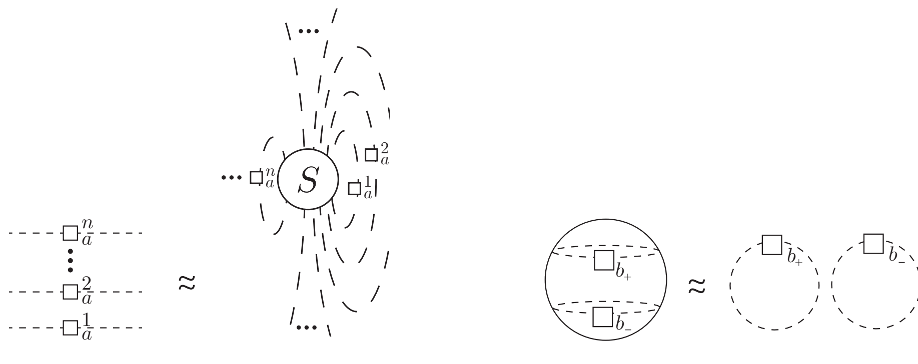

FIGURE 22. Basic patterns: left $a_\emptyset$, right $b_\emptyset$.

3.2. **Letters of COT representations of Hamiltonian surface flows.** From now on, we assume that each flow has neither fake saddles nor fake ∂-saddles.

Recall that the saddle connection diagram with the boundary information is a complete invariant of structurally stable Hamiltonian flows on compact punctured surfaces and unbounded punctured surfaces. To construct the saddle connection diagram inductively, we introduce replacements and insertions to the saddle connection diagram and identify them with the resulting orbit structures. Lemma 6 implies that any structurally stable Hamiltonian flows on a compact punctured sphere can be generated from a periodic annulus (see Figure 22) by iteratively applying ten operations, each of which replaces a saddle connection diagram: $b_{\pm\pm}$, $b_{\pm\mp}$, $\beta_\pm$, $c_\pm$, or $\sigma_\pm$ (see Figure 23). It should be noted that, in this paper, the double plus-minus sign corresponds to double plus and double minus, e.g., $b_{\pm\pm}$ means b_{++} and b_{--}. Similarly, Lemma 6 implies that any structurally stable Hamiltonian flows on a punctured plane can be generated from a uniform flow (see Figure 22) (i.e., a flow that is topologically equivalent to the flow generated by a vector field $(1,0)$) on the plane $\mathbb{R}^2$ by iteratively applying thirteen operations, each of which replaces a saddle connection diagram: $a_\pm$, a_2, $b_{\pm\pm}$, $b_{\pm\mp}$, $\beta_\pm$, $c_\pm$, or $\sigma_\pm$ (see Figure 23) [16].[5]

These suggest that the saddle connection diagram of any structurally stable Hamiltonian flows on a compact punctured sphere can be constructed from the saddle connection diagram of a uniform flow with two insertable places represented by $\square_{b-}$ and $\square_{b+}$ as shown in Figure 22. Additionally, the saddle connection diagram of any structurally stable Hamiltonian flows on a punctured plane can be constructed from the saddle connection diagram of a uniform flow with finitely many replaceable places represented by $\square_a^i$ as shown in Figure 22. A replaceable place in an unbounded region is represented by $\square_a$, and that replaceable place with a counter-clockwise (resp. clockwise) flow direction near the boundary is represented by $\square_{c+}$ (resp. $\square_{c-}$). An insertable place bounded by a saddle connection with a counter-clockwise (resp. clockwise) flow direction is represented by $\square_{b+}$ (resp. $\square_{b-}$). Insertable places need to be inserted into suitable orbit structures, whereas replaceable places need not. The thirteen operations $a_\pm$, a_2, $b_{\pm\pm}$, $b_{\pm\mp}$, $\beta_\pm$, $c_\pm$, and $\sigma_\pm$ are illustrated in Figure 23:

[5]Following the conventions of formal language theory, symbols are written in lower case. Moreover, for simplicity, I (resp. II) is replaced by a_2 (resp. $a_\pm$) because I and a_2 (resp. II and $a_\pm$) are equivalent as local structures.

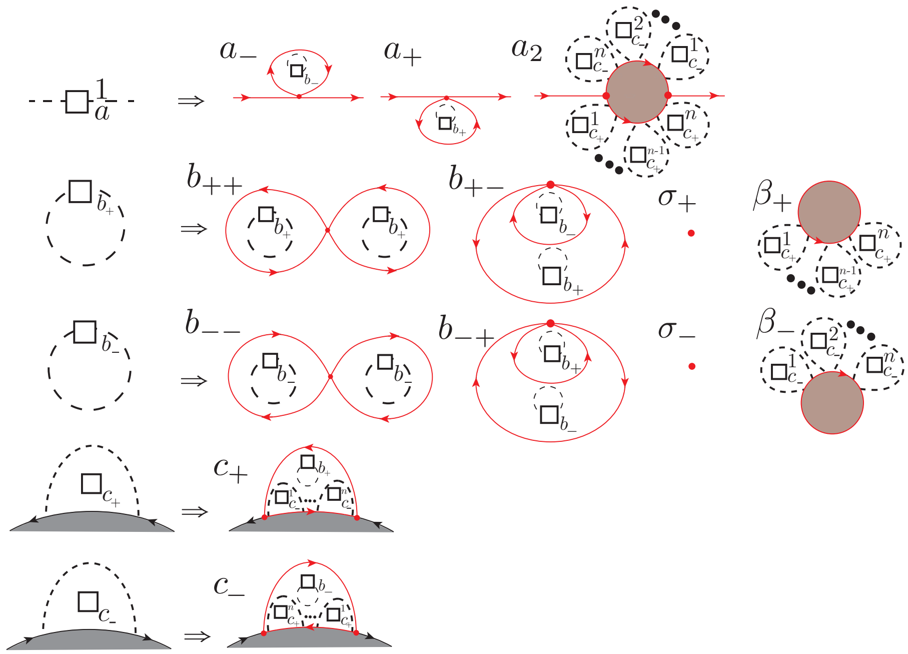

Figure 23. The thirteen fundamental operations $a_\pm$, a_2, $b_{\pm\pm}$, $b_{\pm\mp}$, $\beta_\pm$, $c_\pm$, and $\sigma_\pm$.

- ($a_\pm$) Operation $a_\pm$ replaces an ss-orbit with a saddle that consists of two ss-separatrices and one self-connected separatrix, which has one insertable region $\square_{b\pm}$.
- (a_2) Operation a_2 replaces an ss-orbit with a boundary component that consists of two ∂-saddles and two separatrices, which have finitely many replaceable regions $\square_{c-}$ and $\square_{c-}$.
- ($b_{-\pm}$) Operation $b_{-\pm}$ inserts a saddle with two self-connected separatrices into a region with a counter-clockwise flow direction, which has two insertable regions $\square_{b-}$ and $\square_{b\pm}$.
- ($b_{+\mp}$) Operation $b_{+\pm}$ inserts a saddle with two self-connected separatrices into a region with a counter-clockwise flow direction, which has two insertable regions $\square_{b+}$ and $\square_{b\pm}$.
- ($\sigma_\pm$) Operation σ_+ (resp. σ_-) inserts a center whose neighborhood rotates in the counter-clockwise (resp. clockwise) flow direction, which has neither insertable nor replaceable regions.
- ($\beta_\pm$) Operation β_+ (resp. β_-) inserts a periodic orbit with a counter-clockwise (resp. clockwise) flow direction (boundary component), which has finitely many replaceable regions $\square_{c\pm}$.
- ($c_\pm$) Operation c replaces a separatrix contained in the boundary by two ∂-saddles with four self-connected separatrices, which has one insertable region $\square_{b\pm}$ and finitely many replaceable regions $\square_{c\mp}$.

Each operation except for $\beta_\pm$ and $\sigma_\pm$ increments the number of genus elements by one. For example, a_2 adds a boundary component on the ss-orbit, and c adds a self-connected separatrix on the boundary component. Notice that operations are not always feasible; for instance, operation c_+ is not feasible if a_2 or β_+ have not been applied beforehand.

3.3. **Tree grammar for TFDA.** A regular tree grammar with cyclic order is defined as $G = (S, N, \mathcal{F}, R)$, where

- $N = \{S, A, A^*, B_+, B_-, C_+, C_-, C_+^*, C_-^*\}$;
- $\mathcal{F} = \mathcal{F}_\varepsilon \cup \mathcal{F}_A \cup \mathcal{F}_B \cup \mathcal{F}_C \cup \mathcal{F}_\sigma \cup \mathcal{F}_{list}$, where the set of non-terminal symbols $\mathcal{F}$ are divided into a set $\mathcal{F}_\varepsilon = \{a_\emptyset(), b_\emptyset(,)\}$ of the root symbols of flow, a set $\mathcal{F}_A = \{a_+(), a_-(), a_2(,)\}$ of A-type flow, a set $\mathcal{F}_B = \{b_{++}\{,\}, b_{+-}(,), b_{--}\{,\}, b_{-+}(,), \beta_+\{\}, \beta_-\{\}\}$ of B-type flow, a set $\mathcal{F}_C = \{c_+(,), c_-(,)\}$ of C-type flow, a set $\mathcal{F}_\sigma = \{\sigma_+, \sigma_-\}$ of singular points, and a set $\mathcal{F}_{list} = \{\lambda_a, \lambda_+, \lambda_-, \mathit{cons}_a(,), \mathit{cons}_+(,), \mathit{cons}_-(,)\}$ of alphabets for constructing lists;
- R is a set of production rules:

$$\begin{aligned}
S &\to a_\emptyset(A^*) \mid b_\emptyset(B_-, B_+)\\
A &\to a_+(B_+) \mid a_-(B_-) \mid a_2(C_+^*, C_-^*)\\
A^* &\to \lambda_a \mid \mathit{cons}_a(A, A^*)\\
B_+ &\to \sigma_+ \mid b_{++}\{B_+, B_+\} \mid b_{+-}(B_+, B_-) \mid \beta_+\{C_+^*\}\\
B_- &\to \sigma_- \mid b_{--}\{B_-, B_-\} \mid b_{-+}(B_-, B_+) \mid \beta_-\{C_-^*\}\\
C_+ &\to c_+(B_+, C_-^*)\\
C_- &\to c_-(B_-, C_+^*)\\
C_+^* &\to \lambda_+ \mid \mathit{cons}_+(C_+, C_+^*)\\
C_-^* &\to \lambda_- \mid \mathit{cons}_-(C_-, C_-^*)
\end{aligned}$$

X^* represents a list of zero or more elements of X. An empty list is represented by λ_a, λ_+, and λ_-, otherwise a list also includes *cons*, cons_+, and cons_-, respectively. A catenation $\cdot$ is used to represent two lists, and the terms are identified by the following rules.

$$\begin{aligned}
\lambda_a \cdot z &\approx z\\
\lambda_+ \cdot z &\approx z\\
\lambda_- \cdot z &\approx z\\
\mathit{cons}(x, y) \cdot z &\approx \mathit{cons}(x, y \cdot z)\\
\mathit{cons}_+(x, y) \cdot z &\approx \mathit{cons}_+(x, y \cdot z)\\
\mathit{cons}_-(x, y) \cdot z &\approx \mathit{cons}_-(x, y \cdot z)
\end{aligned}$$

for any regular tree x, y, z with cyclic order. For simplicity, a singleton list and its elements are identified when they appear in operands of catenation $\cdot$, and subscripts and arguments with parenthesis such as (σ), (σ, σ), (λ, λ), and (σ, λ) are omitted when clearly implied by the context. For example, $a_+ \cdot a_2$ is a shorthand notation for $\mathit{cons}(a_+(\sigma_+), \mathit{cons}(a_2(\lambda_+, \lambda_-), \lambda_a))$, and the term $a_\emptyset(a_+(b_{+-}(\beta_+\{c_+(\sigma, c_-)\cdot c_+\}, \sigma)))$ is derived from the grammar G.

For simplicity, the orbit structure of a term whose root is x is called *the orbit structure of* x. Each derived term of $T(\mathcal{F})$ represents an orbit topology. Given each derived term, the flow structure can be constructed recursively and uniquely. The flow structure of $\mathcal{F}_\epsilon$ is presented in Figure 22. Here, $\square_T^L$ is a hole for the term generated by the non-terminal symbol T, where label L is used for distinguishing holes. If $\square_{x\pm}$ is a hole for the term generated by the non-terminal symbol $X_\pm$, then $\square_{xs\pm}$ represents a hole for the term generated by the non-terminal symbol $X^*_\pm$ for any $x_\pm$ and $X_\pm$. For example, $\square_{b+}$ and $\square_{cs+}$ are holes for terms generated by the non-terminal symbols B_+ and and C^*_+, respectively. Hamiltonian flows in a punctured sphere are classified into either of the basic orbital patterns, i.e., $a_\emptyset$ or $b_\emptyset$. The orbit structure of $a_\emptyset$ represents a uniform flow, and can be regarded as a point dipole of flow, where the point is a 1-source–sink represented by Ⓢ. It has n orbit structures that are represented by $\square^1_a, \square^2_a, \dots, \square^n_a$. The orbit structure of $b_\emptyset$ is pictorially represented in two different ways. On the left, two holes of opposite flow directions are placed at the upper and lower hemispheres of a sphere, respectively. On the right, two holes of opposite flow directions are placed side-by-side. The two orbit structures of $b_\emptyset$ are represented by $\square_{b+}$ and $\square_{b-}$; because they can be distinguished by the type of structures B_+ and B_-, the labels are omitted.

The orbit structures of all elements in $\mathcal{F}_A$, $\mathcal{F}_B$, and $\mathcal{F}_C$ are shown in Figure 23. The orbit structures of the A family are unbounded, and the flow moves from right to left. The orbit structure of a_2 has a boundary represented by a shaded circle. The centers of the counter-clockwise flow σ_+ and clockwise flow σ_- are represented by dots. The orbit structures of the two arguments of b_{++} cannot be distinguishable. If we rotate the pictorial representation by π, the identical pictorial representation is obtained; the same applies to b_{--}. The orbit structures of the n arguments of β_+ and β_- are placed in a cyclic order and are indistinguishable. Brace brackets, "{" and "}", are used to represent that the structure does not change if its order changes cyclically. In other words, the trees iteratively transformed by the transformation rules

$$\beta_\pm\{\square^1_{cs\pm} \cdot \square^2_{cs\pm}\} \quad \approx_{\text{cyc}} \quad \beta_\pm\{\square^2_{cs\pm} \cdot \square^1_{cs\pm}\} \tag{1}$$
$$b_{\pm\pm}\{\square^1_{b\pm}, \square^2_{b\pm}\} \quad \approx_{\text{cyc}} \quad b_{\pm\pm}\{\square^2_{b\pm}, \square^1_{b\pm}\} \tag{2}$$

correspond to identical orbit structures.

Replacing holes with orbit structures with holes pictorially corresponds to replacing non-terminal symbols with trees of $T(\mathcal{F} \cup N)$ by productions. Iterative replacements eventually reconstruct the orbit, which is represented by a ground term of $T(\mathcal{F})$. An example of an orbit is shown in Figure 24. Generally, any topologies of Hamiltonian flows are generated by iteratively applying the operations shown in Figure 23 to the two basic patterns, $a_\emptyset$ and $b_\emptyset$, shown in Figure 22.

The tree of root $b_\emptyset$ changes its representation depending on the area that corresponds to the root (Figure 25). Concretely, the tree of root $b_\emptyset$ changes its representation based on the transformation rules presented in Figure 26.

Each tree derived from the tree grammar G modulo equivalence $\approx_{\text{cyc}}$ corresponds to a unique orbit structure in a punctured sphere.

Proposition 13. There is a bijection $f : L(G)/\approx_{\text{cyc}} \to \mathcal{H}_{\text{str}}/\approx_{\text{top}}$, where $\mathcal{H}_{\text{str}}$ is the union of the set of structurally stable Hamiltonian flows in $\mathcal{H}_{\text{bd}}$ and the set of those in $\mathcal{H}_{\text{ubd}}$; the relation $\approx_{\text{top}}$ is a topological equivalence; and the relation $\approx_{\text{cyc}}$ behaves as mentioned above.

Proof. The proof is based upon the structural induction on trees derived by the tree grammar G. $\square$

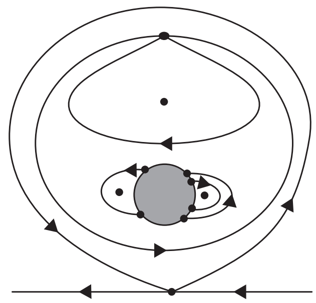

FIGURE 24. Orbit of tree representation $a_\emptyset(a_+(b_{+-}(\beta_+\{c_+(\sigma_+,c_-)\cdot c_+\},\sigma_-)))$.

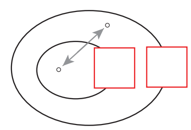

FIGURE 25. A family of transpositions of the root of COT trees.

The *flip* function is defined to flip all orbital directions:

$$
\begin{aligned}
\mathit{flip}(a_\emptyset(x_a)) &= a_\emptyset(\mathit{flip}(x_a))\\
\mathit{flip}(b_\emptyset(x_b^1,x_b^2)) &= b_\emptyset(\mathit{flip}(x_b^2),\mathit{flip}(x_b^1))\\
\mathit{flip}(x_a^1\cdot x_a^2) &= \mathit{flip}(x_a^1)\cdot \mathit{flip}(x_a^2)\\
\mathit{flip}(\lambda_a) &= \lambda_a\\
\mathit{flip}(b_\emptyset(x_{b-},x_{b+})) &= b_\emptyset(\mathit{flip}(x_{b+}),\mathit{flip}(x_{b-}))\\
\mathit{flip}(a_\pm(x_{b\pm})) &= a_\mp(\mathit{flip}(x_{b\pm}))\\
\mathit{flip}(a_2(x_{cs+},x_{cs-})) &= a_2(\mathit{flip}(x_{cs-}),\mathit{flip}(x_{cs+}))\\
\mathit{flip}(b_{\pm\pm}\{x_{b\pm}^1,x_{b\pm}^2\}) &= b_{\mp\mp}\{\mathit{flip}(x_{b\mp}^1),\mathit{flip}(x_{b\mp}^2)\}\\
\mathit{flip}(b_{\pm\mp}(x_{b\pm}^1,x_{b\mp}^2)) &= b_{\mp\pm}(\mathit{flip}(x_{b\pm}^1),\mathit{flip}(x_{b\mp}^2))\\
\mathit{flip}(x_{cs\pm}^1\cdot x_{cs\pm}^2) &= \mathit{flip}(x_{cs\pm}^1)\cdot \mathit{flip}(x_{cs\pm}^2)\\
\mathit{flip}(\lambda_\pm) &= \lambda_\mp\\
\mathit{flip}(c_\pm(x_{b\pm},x_{cs\mp})) &= c_\mp(\mathit{flip}(x_{b\pm}),\mathit{flip}(x_{cs\mp}))\\
\mathit{flip}(\sigma_\pm) &= \sigma_\mp
\end{aligned}
$$

The *flip* function basically flips the signature of the potential functions and preserves the cyclic order without changing the order of sequence of the A and C families.

Lemma 14. *The domain of the flip function over holes can be extended as follows:*

$$
\begin{aligned}
\mathit{flip}(\Box_a^i) &= \Box_a^i\\
\mathit{flip}(\Box_{b+}^i) &= \Box_{b-}^i\\
\mathit{flip}(\Box_{b-}^i) &= \Box_{b+}^i
\end{aligned}
$$

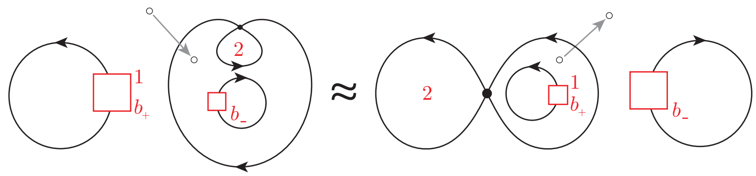

$$b_\emptyset(\square^1_{b+}, b_{-+}(\square_{b-}, \square^2_{b+})) \approx_{\text{cyc}} b_\emptyset(b_{++}\{\square^1_{b+}, \square^2_{b+})\}, \square_{b-})$$

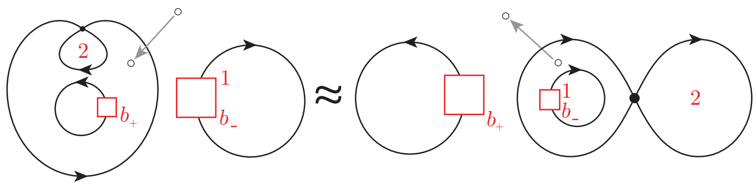

$$b_\emptyset(b_{+-}(\square_{b+}, \square^2_{b-}), \square^1_{b-}) \approx_{\text{cyc}} b_\emptyset(\square_{b+}, b_{--}\{\square^1_{b-}, \square^2_{b-})\})$$

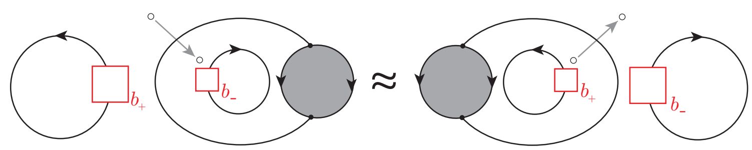

$$b_\emptyset(\square_{b+}, \beta_-\{c_-(\square_{b-}, \square_{cs+}) \cdot \square_{cs-}\}) \approx_{\text{cyc}} b_\emptyset(\beta_+\{c_+(\square_{b+}, \square_{cs-}) \cdot \square_{cs+}\}, \square_{b-})$$

FIGURE 26. Instances of transposition of the root of the COT trees shown in Figure 25 by χ_- for the inner box and by χ_2 for the outer box.

$$\mathit{flip}(\square^i_{cs+}) = \square^i_{cs-}$$
$$\mathit{flip}(\square^i_{cs-}) = \square^i_{cs+}$$

Let the flip_{name} function replace + and − with − and +, respectively. For any rule $name : context_1 \to context_2$, we have $\mathit{flip}_{name}(name) : \mathit{flip}(context_1) \to \mathit{flip}(context_2)$.

Applying *flip* twice reduces itself.

Lemma 15. *For any $x \in T(\mathcal{F})$, we deduce*

$$\mathit{flip}(\mathit{flip}(x)) \to^* x$$

The relation $\approx_{\text{cyc}}$ shown in Figure 26 can be implemented for reducing the given terms to a normal form.

$$nf_r(b_\emptyset(\sigma_-, x_{b-})) = b_\emptyset(\sigma_-, x_{b-})$$
$$nf_r(b_\emptyset(x^1_{b+}, b_{-+}(x_{b-}, x^2_{b+}))) = nf_r(b_\emptyset(b_{++}\{x^1_{b+}, x^2_{b+})\}, x_{b-}))$$
$$nf_r(b_\emptyset(b_{+-}(x_{b+}, x^2_{b-}), x^1_{b-})) = nf_r(b_\emptyset(x_{b+}, b_{--}\{x^1_{b-}, x^2_{b-})\}))$$
$$nf_r(b_\emptyset(x_{b+}, \beta_-\{c_-(x_{b-}, x_{cs+}) \cdot x_{cs-}\})) = nf_r(b_\emptyset(\beta_+\{c_+(x_{b+}, x_{cs-}) \cdot x_{cs+}\}, x_{b-}))$$

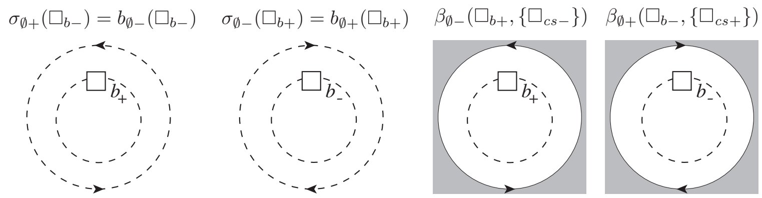

FIGURE 27. COT representations with outermost elements of Hamiltonian flows on punctured spheres.

For any $b_\emptyset(b_1, b_2) \in T(\mathcal{F})$, there exists b_3 such that $nf_r(b_\emptyset(b_1, b_2)) = b_\emptyset(\sigma_-, b_3))$. We can regard $b_\emptyset(\sigma_-, b_3))$ as a right normal form of $b_\emptyset(b_1, b_2)$. Similarly, we can define the function nf_l by adopting a left normal form.

3.4. **COT representations with outermost elements of Hamiltonian flows on punctured spheres.** We can consider a COT representation with an outermost element of a Hamiltonian flow on a punctured sphere. In fact, define $b_{\emptyset\pm}(\Box_{b\pm})$, $b_{\emptyset\pm}(\Box_{b\pm}, \{\Box_{cs\mp}\})$ as follows:
$\sigma_{\emptyset-}(\Box_{b+}) = b_+(\Box_{b+}) := b_\emptyset(\Box_{b+}, \sigma_-)$
$\beta_{\emptyset-}(\Box_{b+}, \{\Box_{cs-}\}) := b_\emptyset(\Box_{b+}, \beta_-\{\Box_{cs-}\})$
$\sigma_{\emptyset+}(\Box_{b-}) = b_-(\Box_{b-}) := b_\emptyset(\sigma_+, \Box_{b-})$
$\beta_{\emptyset+}(\Box_{b-}, \{\Box_{cs+}\}) := b_\emptyset(\beta_+\{\Box_{cs+}\}, \Box_{b-})$
Then the representation $b_{\emptyset+}(\Box_{b+})$ (resp. $b_{\emptyset-}(\Box_{b-})$) corresponds to a Hamiltonian flow on a punctured sphere whose root is a center with the clockwise (resp. counter-clockwise) flow direction, and the representation $\beta_{\emptyset-}(\Box_{b+}, \{\Box_{cs-}\})$ (resp. $\beta_{\emptyset+}(\Box_{b-}, \{\Box_{cs+}\})$) corresponds to a Hamiltonian flow on a punctured sphere whose root is a boundary component with the clockwise (resp. counter-clockwise) flow direction. This means that the outermost elements of the representations $b_{\emptyset\mp}(\Box_{b\pm})$ (resp. $\beta_{\emptyset\pm}(\Box_{b\pm}, \{\Box_{cs\mp}\})$) are centers (resp. boundary components) as shown in Figure 27. When COT representations clear from their context, we sometimes omit labels $a_\emptyset$, $b_\emptyset$, $b_{\emptyset\pm}$, $\sigma_\pm$, λ_a, and $\lambda_\pm$.

3.5. **Correspondence between COT representations of Hamiltonian flows and Reeb graphs of the Hamiltonians.** When we equip symbols with the critical values of the Hamiltonian at the corresponding singular points, COT representations become equivalent to labeled Reeb graphs. The labels correspond to saddle connections. Moreover, we can define a pseudo-distance between structurally stable Hamiltonian flows as an edit distance between the Reeb graphs using the values of the Hamiltonians.

TABLE 2. Correspondence between COT and molecule.

Terminal symbols of COT	Codes of molecule [6]
σ_+, σ_-	A
b_{++}, b_{--}	B
$b_{\pm\pm\pm}$	C (C_2)
$b_{(+-+)}, b_{(-+-)}$	D (D_1)
$b_{\pm\pm(\mp)}, b_{\pm\{\mp\mp\}}, b_{\pm(\mp(\pm))}, b_{\pm(\mp(\mp))}$	D (D_2)

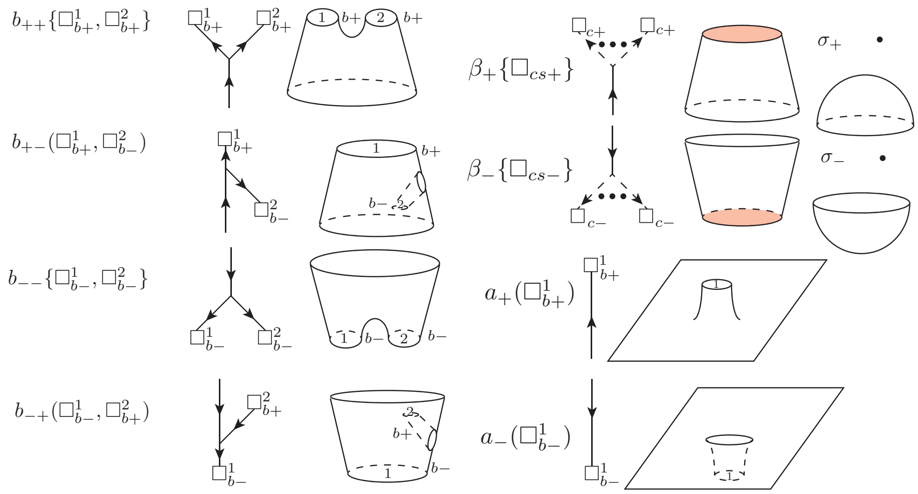

FIGURE 28. Correspondence between COT representations of Hamiltonian flows, and Reeb graphs and the graphs of the Hamiltonians.

Table 2 indicates that the correspondence between COT representations and molecules [6]. Because edges in molecules are not oriented, multiple COT representations correspond to a single molecule. Because we only consider 2D Hamiltonian flows, no COT representations correspond to the 3D structures such as molecule C_1.

Roughly speaking, the set of Hamiltonian flows with finitely many singular points can be naturally stratified in terms of stability. For instance, the structurally stable flows have "codimension" zero, generation transition has "codimension" one, and more unstable flows have hither "codimension". It should be noted that the codimension is not equal to the complexity; the complexity is the number of saddle points contained in saddle connection diagrams. In fact, the "codimension" is equal to the sum of $\Sigma_i(c_i - 1) + n_0 + \Sigma_{k\geq 1} 2(k-1)n_k + m_0 + \Sigma_{l\geq 1}(l-1)m_l$, where c_i are the complexities of atoms, n_k is the number of k-saddles, and m_l is the number of ∂-$(l/2)$-saddles. The COT representations of the flows of the higher codimension correspond to molecules E_3, F_2, G_1, G_2, G_3, H_1, H_2, etc.

3.6. **COT representations of Hamiltonian flows on compact surfaces and unbounded punctured surfaces.** Identifying the box $\square$, we can construct COT representations of Hamiltonian flows on compact surfaces and unbounded punctured surfaces. For instance, we can assign such Hamiltonian flows to COT representations by identifying boxes $\square$ using the breadth-first search as shown in Figure 29. A pair of filled boxes $\blacksquare^i_{b+}$ and $\blacksquare^i_{b-}$ corresponds to the operation identifying an open periodic annulus. Precisely, we define a regular tree grammar with cyclic order $G_0 = (S, N, \mathcal{F}, R)$ where

- $N = \{S, A, A^*, B_+, B_-, C_+, C_-, C^*_+, C^*_-\}$,
- $\mathcal{F} = \mathcal{F}_\varepsilon \cup \mathcal{F}_A \cup \mathcal{F}_B \cup \mathcal{F}_C \cup \mathcal{F}_\sigma \cup \mathcal{F}_{list}$ where the set of non-terminal symbols $\mathcal{F}$ are divided into the set $\mathcal{F}_\varepsilon = \{a_\emptyset(), b_\emptyset(,)\}$ of the root symbols of flow, the set $\mathcal{F}_A = \{a_+(), a_-(), a_2(,)\}$ of A-type flow, the set

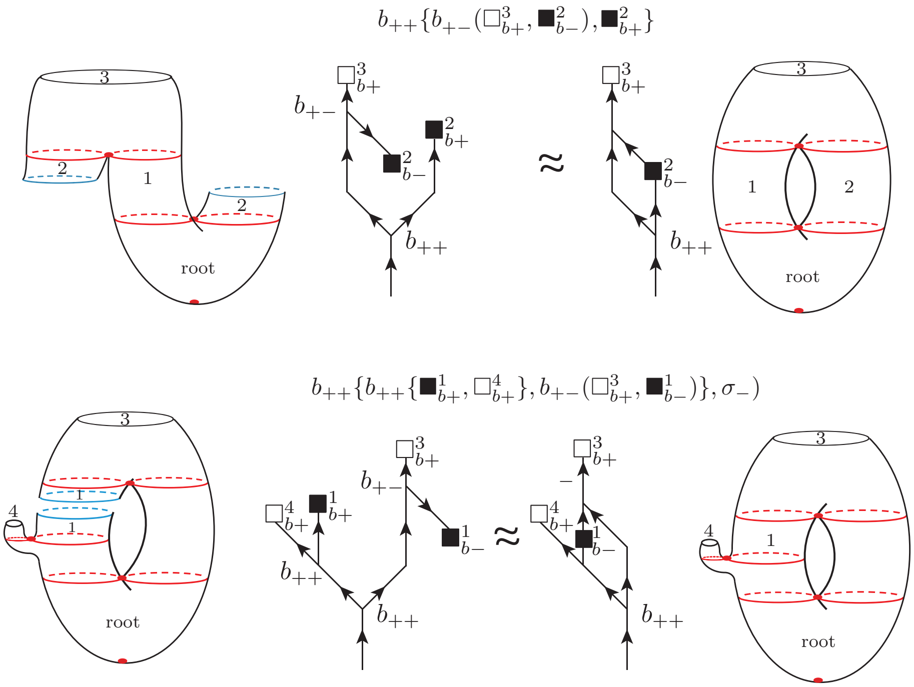

FIGURE 29. COT representations of Hamiltonian flows on compact surfaces.

$\mathcal{F}_B = \{b_{++}\{,\}, b_{+-}(,), b_{--}\{,\}, b_{-+}(,), \beta_+\{\}, \beta_-\{\}\}$ of B-type flow, the set $\mathcal{F}_C = \{c_+(,), c_-(,)\}$ of C-type flow, the set $\mathcal{F}_\sigma = \{\sigma_+, \sigma_-, b_{+,\delta}, b_{-,\delta}\}$ of singular points, and the set $\mathcal{F}_{list} = \{\lambda_a, \lambda_+, \lambda_-, cons_a(,), cons_+(,), cons_-(,)\}$ of alphabets for constructing lists, and

- R is a set of production rules:

$$
\begin{aligned}
S &\to a_\emptyset(A^*) \mid b_\emptyset(B_-, B_+)\\
A &\to a_+(B_+) \mid a_-(B_-) \mid a_2(C_+^*, C_-^*)\\
A^* &\to \lambda_a \mid cons_a(A, A^*)\\
B_+ &\to \sigma_+ \mid b_{+,\delta} \mid b_{++}\{B_+, B_+\} \mid b_{+-}(B_+, B_-) \mid \beta_+\{C_+^*\}\\
B_- &\to \sigma_- \mid b_{-,\delta} \mid b_{--}\{B_-, B_-\} \mid b_{-+}(B_-, B_+) \mid \beta_-\{C_-^*\}\\
C_+ &\to c_+(B_+, C_-^*)\\
C_- &\to c_-(B_-, C_+^*)\\
C_+^* &\to \lambda_+ \mid cons_+(C_+, C_+^*)\\
C_-^* &\to \lambda_- \mid cons_-(C_-, C_-^*)
\end{aligned}
$$

The symbols $b^L_{\pm,\delta}$ are also denoted by $\blacksquare^L_{\pm}$, where label L is used for distinguishing symbols. Each tree derived from the tree grammar G_0 modulo the equivalence $\approx_{\mathrm{cyc}}$ corresponds to a unique orbit structure in punctured surfaces.

Proposition 16. There is an injection $f : \mathcal{H}_{\mathrm{str}}/\approx_{\mathrm{top}} \to L(G_0)/\approx_{\mathrm{cyc}}$, where $\mathcal{H}_{\mathrm{str}}$ is the union of the set of structurally stable Hamiltonian flows in $\bigsqcup_{g\in\mathbb{Z}_{\geq 0}} \mathcal{H}_{g,\mathrm{bd}}$ and

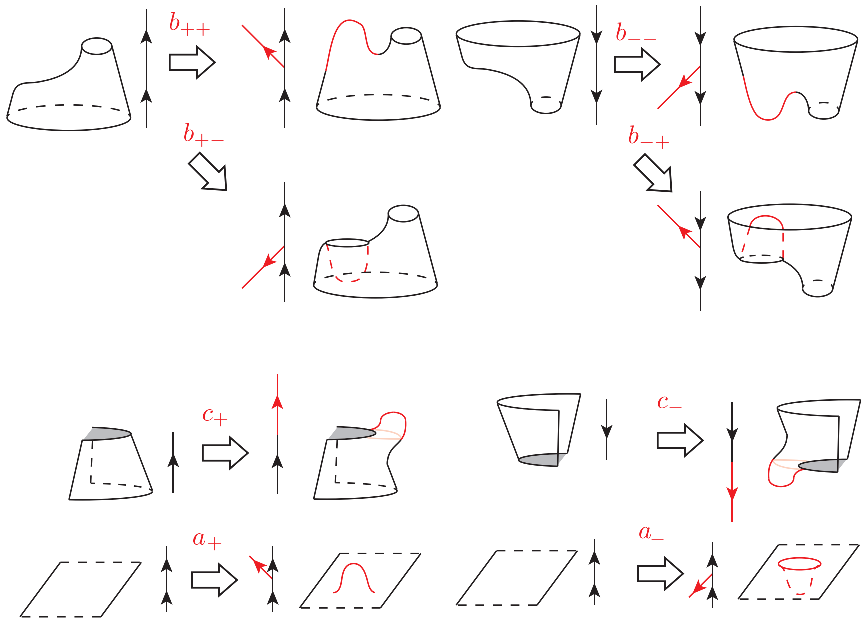

FIGURE 30. Creations of centers incremented by one of structurally stable Hamiltonian flows.

the set of those in $\bigsqcup_{g \in \mathbb{Z}_{\geq 0}} \mathcal{H}_{g,\mathrm{ubd}}$, the relation $\approx_{\mathrm{top}}$ is a topological equivalence, and the relation $\approx_{\mathrm{cyc}}$ is above-mentioned. Moreover, each acceptable word can be characterized as a word such that symbols $b_{+,\delta}$ and $b_{-,\delta}$ must appear in pairs.

4. Complete creation rules of genus elements incremented by one of structurally stable Hamiltonian flows

In this section, we list all creations of genus elements incremented by one of structurally stable Hamiltonian flows. Each subsection below is dedicated to a creation rule of genus elements incremented by one in structurally stable Hamiltonian flows.

4.1. Creations of centers incremented by one for structurally stable Hamiltonian flows.

The rules of creation of centers incremented by one for structurally stable Hamiltonian flows shown in Figure 30 are as follows:

$(b_{\pm\mp})$ $\square_{b\pm} \to b_{\pm\mp}(\square_{b\pm}, \sigma_{\mp})$
$(b_{\pm\pm})$ $\square_{b\pm} \to b_{\pm\pm}\{\square_{b\pm}, \sigma_{\pm}\}$
$(c_{\pm})$ $\square_{c\pm}^{\cdot k} \cdot \square_{c\pm}^{\cdot l} \to \square_{c\pm}^{\cdot k} \cdot c_{\pm} \cdot \square_{c\pm}^{\cdot l}$
$(a_{\pm})$ $a_{\emptyset}(\square_a^{\cdot k} \cdot \square_a^{\cdot l}) \to a_{\emptyset}(\square_a^{\cdot k} \cdot a_{\pm} \cdot \square_a^{\cdot l})$

Here, given an integer k, $\square_x^{\cdot k}$ represents a sequence of k $\square_x$:

$$\underbrace{\square_x \cdot \cdots \cdot \square_x}_{k \text{ times}}.$$

We have the following statements for generic creations of centers.

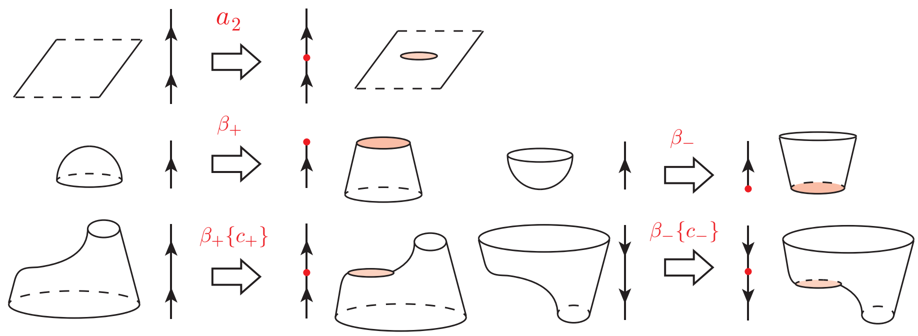

FIGURE 31. Creations of boundaries incremented by one of structurally stable Hamiltonian flows.

Lemma 17. *The complete generic creations of centers for structurally stable Hamiltonian flows on compact punctured spheres are described by the rules* $(b_{\pm\mp})$, $(b_{\pm\pm})$, *and* $(c_\pm)$, *as shown in Figure 30.*

Proof. Since all creations of centers for structurally stable Hamiltonian flows on punctured planes occur on either periodic annuli or the boundary, Figure 30 implies the above assertion. □

Lemma 18. *The complete generic creations of centers for structurally stable Hamiltonian flows on punctured planes are described by the rules* $(b_{\pm\mp})$, $(b_{\pm\pm})$, $(c_\pm)$, *and* $(a_\pm)$, *as shown in Figure 30.*

Proof. Since all creations of centers for structurally stable Hamiltonian flows on punctured planes occur on either flow boxes, periodic annuli, or the boundary, Figure 30 implies the above assertion. □

4.2. **Creations of boundaries incremented by one of structurally stable Hamiltonian flows.** The rules of creations of boundaries incremented by one of structurally stable Hamiltonian flows on compact punctured spheres and punctured planes shown in Figure 31 are as follows: for any $k, l \in \mathbb{Z}_{\geq 0}$

$$(a_2) \quad a_\emptyset(\square_a^{\cdot k} \cdot \square_a^{\cdot l}) \to a_\emptyset(\square_a^{\cdot k} \cdot a_2 \cdot \square_a^{\cdot l})$$
$$(\beta_\pm) \quad \sigma_\pm \to \beta_\pm$$
$$(\beta_\pm\{c_\pm\}) \quad \square_{b\pm} \to \beta_\pm\{c_\mp(\square_{b\pm}, \lambda_\mp)\}$$

It should be noted that creations of boundaries incremented by one for structurally stable Hamiltonian flows change the whole surfaces into the resulting surfaces by removing open disks. We have the following statements for generic creations of boundary components.

Lemma 19. *The complete generic creations of boundary components for structurally stable Hamiltonian flows on compact punctured spheres are described by the rules* $(\beta_\pm)$, *and* $(\beta_\pm\{c_\pm\})$, *as shown in Figure 31.*

Proof. Because the creations of boundary components for structurally stable Hamiltonian flows on punctured planes occur on either periodic annuli or centers, Figure 31 implies the above assertion. □

Lemma 20. *The complete generic creations of boundary components for structurally stable Hamiltonian flows on punctured plane are described by the rules* (a_2)*,* $(\beta_\pm)$*, and* $(\beta_\pm\{c_\pm\})$*, as shown in Figure 31.*

Proof. Since all creations of boundary components for structurally stable Hamiltonian flows on punctured planes occur on either flow boxes, periodic annuli, or centers, Figure 31 implies the above assertion. □

We can define a *transition graph* with creations incremented by one of structurally stable Hamiltonian flows as the graph whose vertices are topological equivalence classes of structurally stable Hamiltonian flows and whose edges are creations incremented by one genus element (i.e (a_2), $(\beta_\pm)$, and $(\beta_\pm\{c_\pm\})$) and topological equivalence classes of p-unstable or h-unstable Hamiltonian flows.

5. Complete generic transition rules

We state a complete generic transition rules of Hamiltonian flows.

Theorem 21. *The complete generic transition rules of Hamiltonian flows on compact punctured spheres and punctured planes are shown as follows:*

$$
\begin{aligned}
a_{\pm\pm}, a_{\pm\mp}, a_{22}, a_{\pm 2}, a_{2\pm} :& \square_a^1 \cdot \square_a^2 \to \square_a^2 \cdot \square_a^1 \\
a_{(+-)}, a_{(-+)} :& a_-(\square_{b-}^1) \cdot a_+(\square_{b+}^2) \to a_-(\square_{b-}^1) \cdot a_+(\square_{b+}^2) \\
a_{2(\mp\pm)} :& a_\mp(\square_{b\mp}^1) \cdot a_2(\square_{cs\pm}^2 \cdot c_\pm(\square_{b\pm}^3, \square_{cs\mp}^6) \cdot \square_{cs\pm}^5, \square_{cs\mp}^4) \to \\
& a_2(\square_{cs\pm}^2, \square_{cs\mp}^6 \cdot c_\mp(\square_{b\mp}^1, \square_{cs\pm}^5)) \cdot \square_{cs\mp}^4) \cdot a_\pm(\square_{b\pm}^3) \\
a_{\pm(\pm)} :& a_\pm(\square_{a\pm}^1) \cdot a_\pm(\square_{b\pm}^2) \ \to \ a_\pm(b_{\pm\pm}\{\square_{b\pm}^1, \square_{b\pm}^2\}) \\
a_{-(+)} :& a_-(\square_{b-}^1) \cdot a_+(\square_{b+}^2) \to a_-(b_{-+}(\square_{b-}^1, \square_{b+}^2)) \\
a_{+(-)} :& a_-(\square_{b-}^1) \cdot a_+(\square_{b+}^2) \to a_+(b_{+-}(\square_{b+}^2, \square_{b-}^1)) \\
a_{+(2)} :& a_2(\square_{cs+}^1, \square_{cs-}^2) \cdot a_+(\square_{b+}^3) \to a_+(\beta_+\{\square_{cs+}^1 \cdot c_+(\square_{b+}^3, \square_{cs-}^2)\}) \\
a_{-(2)} :& a_-(\square_{b-}^1) \cdot a_2(\square_{cs+}^2, \square_{cs-}^3) \to a_-(\beta_-\{c_-(\square_{b-}^1, \square_{cs+}^2) \cdot \square_{cs-}^3\}) \\
a_2(c_{+(+)}) :& a_+(\square_{b+}^1) \cdot a_2(\square_{cs+}^5 \cdot c_+(\square_{b+}^2, \square_{cs-}^3) \cdot \square_{cs+}^4, \square_{cs-}^6) \to \\
& a_2(\square_{cs+}^5 \cdot c_+(b_{++}\{\square_{b+}^1, \square_{b+}^2\}, \square_{cs-}^3) \cdot \square_{cs+}^4, \square_{cs-}^6) \\
a_2(c_{-(-)}) :& a_2(\square_{cs+}^1, \square_{cs-}^2 \cdot c_-(\square_{b-}^5, \square_{cs+}^4) \cdot \square_{cs-}^3) \cdot a_-(\square_{b-}^6) \to \\
& a_2(\square_{cs+}^1, \square_{cs-}^2 \cdot c_-(b_{--}\{\square_{b-}^5, \square_{b-}^6\}, \square_{cs+}^4) \cdot \square_{cs-}^3) \\
a_2(c_{+(-)}) :& a_-(\square_{b-}^1) \cdot a_2(\square_{cs+}^5 \cdot c_+(\square_{b+}^2, \square_{cs-}^3) \cdot \square_{cs+}^4, \square_{cs-}^6) \to \\
& a_2(\square_{cs+}^5 \cdot c_+(b_{+-}(\square_{b+}^2, \square_{b-}^1), \square_{cs-}^3) \cdot \square_{cs+}^4, \square_{cs-}^6) \\
a_2(c_{-(+)}) :& a_2(\square_{cs+}^1, \square_{cs-}^2 \cdot c_-(\square_{b-}^5, \square_{cs+}^4) \cdot \square_{cs-}^3) \cdot a_+(\square_{b+}^6) \to \\
& a_2(\square_{cs+}^1, \square_{cs-}^2 \cdot c_-(b_{-+}(\square_{b-}^5, \square_{b+}^6), \square_{cs+}^4) \cdot \square_{cs-}^3) \\
a_2(c_{+(2)}) :& a_2(\square_{cs+}^1, \square_{cs-}^2) \cdot a_2(\square_{cs+}^6 \cdot c_+(\square_{b+}^3, \square_{cs-}^4) \cdot \square_{cs+}^5, \square_{cs-}^7) \to \\
& a_2(\square_{cs+}^6 \cdot c_+(\beta_+\{\square_{cs+}^1 \cdot c_+(\square_{b+}^3, \square_{cs-}^2)\}, \square_{cs-}^4) \cdot \square_{cs-}^5, \square_{cs+}^7) \\
a_2(c_{-(2)}) :& a_2(\square_{cs+}^1, \square_{cs-}^2 \cdot c_-(\square_{b-}^5, \square_{cs+}^4) \cdot \square_{cs-}^3) \cdot a_2(\square_{cs+}^6, \square_{cs-}^7) \to \\
& a_2(\square_{cs+}^1, \square_{cs-}^2 \cdot c_-(\beta_-\{c_-(\square_{b-}^5, \square_{cs+}^6) \cdot \square_{cs-}^7\}, \square_{cs+}^4) \cdot \square_{cs-}^3)
\end{aligned}
$$

$$
\begin{aligned}
b_{\pm\pm\pm} :& b_{\pm\pm}\{\square^1_{b\pm}, b_{\pm\pm}\{\square^2_{b\pm}, \square^3_{b\pm}\}\} \to b_{\pm\pm}\{b_{\pm\pm}\{\square^1_{b\pm}, \square^2_{b\pm}\}, \square^3_{b\pm}\} \\
b_{\pm\pm(\mp)} :& b_{\pm\pm}\{\square^1_{b\pm}, b_{\pm\mp}(\square^2_{b\pm}, \square^3_{b\mp})\} \to b_{\pm\mp}(b_{\pm\pm}\{\square^1_{b\pm}, \square^2_{b\pm}\}, \square^3_{b\mp}) \\
b_{\pm\{\mp\mp\}} :& b_{\pm\mp}(b_{\pm\mp}(\square^2_{b\pm}, \square^3_{b\mp}), \square^1_{b\mp}) \ \to b_{\pm\mp}(b_{\pm\mp}(\square^2_{b\pm}, \square^1_{b\mp}), \square^3_{b\mp}) \\
b_{\pm(\mp(\mp))} :& b_{\pm\mp}(b_{\pm\mp}(\square^3_{b\pm}, \square^2_{b\mp}), \square^1_{b\mp}) \ \to b_{\pm\mp}(\square^3_{b\pm}, b_{\mp\mp}\{\square^1_{b\mp}, \square^2_{b\mp}\}) \\
b_{\pm(\mp(\pm))} :& b_{\pm\mp}(\square^3_{b\pm}, b_{\mp\pm}(\square^2_{b\mp}, \square^1_{b\pm})) \to b_{\pm\mp}(b_{\pm\pm}\{\square^1_{b\pm}, \square^3_{b\pm}\}, \square^2_{b\mp}) \\
b_{\pm\pm(2)} :& b_{\pm\pm}\{\beta_\pm\{\square^1_{cs\pm} \cdot c_\pm(\square^3_{b\pm}, \square^2_{cs\mp})\}, \square^4_{b\pm}\} \to \\
& \beta_\pm\{\square^1_{cs\pm} \cdot c_\pm(b_{\pm\pm}\{\square^3_{b\pm}, \square^4_{b\pm}\}, \square^2_{cs\mp})\} \\
b_{\pm\{\mp,2\}} :& b_{\pm\mp}(\beta_\pm\{c_\pm(\square^2_{b\pm}, \square^3_{cs\mp}) \cdot \square^4_{cs\pm}\}, \square^1_{b_{-+}}) \to \\
& \beta_\pm\{c_\pm(b_{\pm\mp}(\square^2_{b\pm}, \square^1_{b_{-+}}), \square^3_{cs\mp}) \cdot \square^4_{cs\pm}\} \\
b_{\pm(\mp(2))} :& b_{\pm\mp}(\square^4_{b\pm}, \beta_\mp\{c_\mp(\square^1_{b\mp}, \square^2_{cs\pm}) \cdot \square^3_{cs\mp}\}) \to \\
& b_{\pm\mp}(\beta_\pm\{c_\pm(\square^4_{b\pm}, \square^3_{cs\mp}) \cdot \square^2_{cs\pm}\}, \square^1_{b\mp}) \\
b_{\pm\{22\}} :& \beta_\pm\{\square^1_{cs\pm} \cdot c_\pm(\beta_\pm\{\square^3_{cs\pm} \cdot c_\pm(\square^5_{b\pm}, \square^4_{cs\mp})\}, \square^2_{cs\mp})\} \to \\
& \beta_\pm\{\square^3_{cs\pm} \cdot c_\pm(\beta_\pm\{\square^1_{cs\pm} \cdot c_\pm(\square^5_{b\pm}, \square^2_{cs\mp})\}, \square^4_{cs\mp})\} \\
c_\pm(c_{\mp(\mp)}) :& c_\pm(b_{\pm\mp}(\square^1_{b\pm}, \square^2_{b\mp}), \square^6_{cs\mp} \cdot c_\mp(\square^4_{b\mp}, \square^5_{cs\pm}) \cdot \square^3_{cs\mp}) \to \\
& c_+(\square^1_{b\pm}, \square^6_{cs\mp} \cdot c_\mp(b_{\mp\mp}\{\square^2_{b\mp}, \square^4_{b\mp}\}, \square^5_{cs\pm}) \cdot \square^3_{cs\mp}) \\
c_\pm(c_{\mp(\pm)}) :& c_\pm(b_{\pm\pm}\{\square^1_{b\pm}, \square^2_{b\pm}\}, \square^6_{cs\mp} \cdot c_\mp(\square^4_{b\mp}, \square^5_{cs\pm}) \cdot \square^3_{cs\mp}) \to \\
& c_\pm(\square^1_{b\pm}, \square^6_{cs\mp} \cdot c_\mp(b_{\mp\pm}(\square^4_{b\mp}, \square^2_{b\pm}), \square^5_{cs\pm}) \cdot \square^3_{cs\mp}) \\
c_\pm(c_{\mp(2)}) :& c_\pm(\square^1_{b\pm}, \square^7_{cs\mp} \cdot c_\mp(\beta_\mp\{\square^2_{cs\mp} \cdot c_\mp(\square^5_{b\mp}, \square^3_{cs\pm})\}, \square^6_{cs\pm}) \cdot \square^4_{cs\mp}) \to \\
& c_\pm(\beta_\pm\{c_\pm(\square^1_{b\pm}, \square^2_{cs\mp}) \cdot \square^3_{cs\pm}\}, \square^7_{cs\mp} \cdot c_\mp(\square^5_{b\mp}, \square^6_{cs\pm}) \cdot \square^4_{cs\mp}) \\
b_{(\pm\mp\pm)} :& b_{\pm\mp}(b_{\pm\pm}\{\square^1_{\pm}, \square^3_{\pm}\}, \square^2_{\mp}) \to b_{\pm\mp}(b_{\pm\pm}\{\square^1_{\pm}, \square^3_{\pm}\}, \square^2_{\mp}) \\
a_2(c_{(+--+)}) :& a_-(\square^1_{b-}) \cdot a_2(\square^8_{cs+} \cdot c_+(\square^5_{b+}, \square^6_{cs-}) \cdot \square^2_{cs+} \cdot c_+(\square^3_{b+}, \square^4_{cs-}) \cdot \square^7_{cs+}, \square^9_{cs-}) \to \\
& a_2(\square^8_{cs+} \cdot c_+(b_{++}\{\square^3_{b+}, \square^5_{b+}\}, \square^6_{cs-} \cdot c_-(\square^1_{b-}, \square^2_{cs+}) \cdot \square^4_{cs-}) \cdot \square^7_{cs+}, \square^9_{cs-}) \\
a_2(c_{(-+-)}) :& a_2(\square^9_{cs+}, \square^7_{cs-} \cdot c_-(\square^3_{b-}, \square^4_{cs+}) \cdot \square^2_{cs-} \cdot c_-(\square^5_{b-}, \square^6_{cs+}) \cdot \square^8_{cs-}) \cdot a_+(\square^1_{b+}) \to \\
& a_2(\square^9_{cs+}, \square^7_{cs-} \cdot c_-(b_{--}\{\square^3_{b-}, \square^5_{b-}\}, \square^4_{cs+} \cdot c_+(\square^1_{b+}, \square^2_{cs-}) \cdot \square^6_{cs+}) \cdot \square^8_{cs-}) \\
\beta_\pm(c_{(\pm\mp\pm)}) :& b_{\pm\mp}(\beta_\pm\{c_\pm(\square^1_{b\pm}, \square^2_{cs\mp}) \cdot \square^3_{cs\mp} \cdot c_\pm(\square^4_{b\pm}, \square^5_{cs\mp}) \cdot \square^6_{cs\pm}\}, \square^7_{b\mp}) \to \\
& \beta_\pm\{c_\pm(b_{\pm\pm}\{\square^1_{b\pm}, \square^4_{b\pm}\}, \square^2_{cs\mp} \cdot c_\mp(\square^7_{b\mp}, \square^3_{cs\pm}) \cdot \square^5_{cs\mp}) \cdot \square^6_{cs\pm}\} \\
c_\mp(c_{(\mp\pm\mp)}) :& c_\pm(b_{\pm\pm}\{\square^1_{b\pm}, \square^2_{b\pm}\}, \square^9_{cs\mp} \cdot c_\mp(\square^7_{b\mp}, \square^8_{cs\pm}) \cdot \square^6_{cs\mp} \cdot c_\mp(\square^4_{b\mp}, \square^5_{cs\pm}) \cdot \square^3_{cs\mp}) \to \\
& c_+(\square^1_{b\pm}, \square^9_{cs\mp} \cdot c_\mp(b_{\mp\mp}\{\square^4_{b\mp}, \square^7_{b\mp}\}, \square^8_{cs\mp} \cdot c_\pm(\square^2_{b\pm}, \square^6_{cs\mp}) \cdot \square^5_{cs\pm}) \cdot \square^3_{cs\mp}) \\
a_{2n2} :& a_2(\square^0_{cs+}, \square^{2n+1}_{cs-} \cdot c_-(\square^{2n'}_{b-}, \square^{2n}_{cs+}) \cdot \cdots \cdot c_-(\square^{4'}_{b-}, \square^4_{cs+}) \cdot \square^3_{cs-} \\
& \cdot c_-(\square^{2'}_{b-}, \square^2_{cs+}) \cdot \square^1_{cs-}) \cdot a_2(\square^{0'}_{cs+} \cdot c_+(\square^{1'}_{b+}, \square^{1''}_{cs-}) \cdot \square^{2''}_{cs+} \\
& \cdot c_+(\square^{3'}_{b+}, \square^{3''}_{cs-}) \cdot \cdots \cdot c_+(\square^{2n-1'}_{b+}, \square^{2n-1''}_{cs-}) \cdot \square^{2n''}_{cs+}, \square^{2n+1''}_{cs-}) \to \\
& a_2(\square^{0'}_{cs+}, \square^{1''}_{cs-} \cdot c_-(\square^{2'}_{b-}, \square^{2''}_{cs+}) \cdot \square^{3''}_{cs-} \cdot c_-(\square^{4'}_{b-}, \square^{4''}_{cs+}) \cdot \cdots
\end{aligned}
$$

$$
\begin{aligned}
&\cdot c_-(\square^{2n'}_{b-}, \square^{2n''}_{cs+}) \cdot \square^{2n+1''}_{cs-}) \cdot a_2(\square^{2n}_{cs+} \cdot c_+(\square^{2n-1'}_{b+}, \square^{2n-1}_{cs-}) \cdot \\
&\cdots \cdot c_+(\square^{3'}_{b+}, \square^{3}_{cs-}) \cdot \square^{2}_{cs+} \cdot c_+(\square^{1'}_{b+}, \square^{1}_{cs-}) \cdot \square^{0}_{cs+}, \square^{2n+1}_{cs-}) \\
\beta_\pm(c_{\pm(2n)}) :&\beta_\pm\{\square^{0}_{cs\pm} \cdot c_\pm(\beta_\pm\{\square^{0'}_{cs\pm} \cdot c_\pm(\square^{1'}_{b\pm}, \square^{1''}_{cs-}) \cdot \square^{2}_{cs\pm} \cdot c_\pm(\square^{3'}_{b\pm}, \square^{3''}_{cs-}) \cdot \\
&\cdots \cdot c_\pm(\square^{2n-1'}_{b\pm}, \square^{2n-1''}_{cs-})\}, \square^{2n-1}_{cs-} \cdot c_\mp(\square^{2n-2'}_{b\mp}, \square^{2}_{cs\pm}) \cdot \cdots \cdot \square^{3}_{cs-} \\
&\cdot c_\mp(\square^{2'}_{b\mp}, \square^{2}_{cs\pm}) \cdot \square^{1}_{cs-})\} \to \\
&\beta_\mp\{\square^{2n-1'}_{cs-} \cdot c_\mp(\beta_\mp\{\square^{0}_{cs-} \cdot c_\mp(\square^{2n-2'}_{b\mp}, \square^{2n-2}_{cs\pm}) \cdot \cdots \cdot c_\mp(\square^{3'}_{b\mp}, \square^{3}_{cs\pm}) \\
&\cdot \square^{2}_{cs-} \cdot c_\mp(\square^{1'}_{b\mp}, \square^{1}_{cs\pm})\}, \square^{1''}_{cs\pm} \cdot c_\pm(\square^{2'}_{b\pm}, \square^{2''}_{cs-}) \cdot \square^{3''}_{cs\pm} \cdot \cdots \\
&\cdot c_\pm(\square^{2n-2'}_{b\pm}, \square^{2n-2''}_{cs-}) \cdot \square^{2n-1''}_{cs\pm})\} \\
c_\pm(c_{\mp(2n)}) :&c_\pm(\square^{0'}_{b\pm}, \square^{0}_{cs\mp} \cdot c_\mp(\beta_\mp\{c_\mp(\square^{2n-1'}_{b\mp}, \square^{2n-1''}_{cs\pm}) \cdot \square^{2n-2''}_{cs\mp} \cdot \cdots \cdot \square^{2''}_{cs\mp} \cdot \\
&c_\mp(\square^{1'}_{b\mp}, \square^{1''}_{cs\pm}) \cdot \square^{0''}_{cs\mp}\}, \square^{1}_{cs\pm} \cdot c_\pm(\square^{2'}_{b\pm}, \square^{2}_{cs\mp}) \cdot \cdots \\
&\cdot c_\pm(\square^{2n-2'}_{b\pm}, \square^{2n-2}_{cs\mp}) \cdot \square^{2n-1}_{cs\pm}) \cdot \square^{2n}_{cs\mp}) \to \\
&c_\pm(\beta_\pm\{c_\pm(\square^{0'}_{b\pm}, \square^{0''}_{cs\mp}) \cdot \square^{2n-1''}_{cs\pm} \cdot c_\pm(\square^{2n-2'}_{b\pm}, \square^{2n-2''}_{cs\mp}) \cdot \cdots \\
&\cdot c_\pm(\square^{2'}_{b\pm}, \square^{2''}_{cs\mp}) \cdot \square^{1''}_{cs\pm}\}, \square^{0}_{cs\mp} \cdot c_\mp(\square^{1'}_{b\mp}, \square^{1}_{cs\pm}) \cdot \square^{2}_{cs\mp} \cdot \cdots \\
&\cdot \square^{2n-2}_{cs\mp} \cdot c_\mp(\square^{2n-1'}_{b\mp}, \square^{2n-1}_{cs\pm}) \cdot \square^{2n}_{cs\mp}) \\
a_2(c_{-(2n)}) :&a_2(\square^{2n+1}_{cs+}, \square^{2n}_{cs-} \cdot c_-(\beta_-\{\square^{0'}_{cs-} \cdot c_-(\square^{1'}_{b-}, \square^{1''}_{cs+}) \cdot \square^{2''}_{cs-} \\
&\cdot c_-(\square^{3'}_{b-}, \square^{3''}_{cs+}) \cdot \cdots \cdot c_-(\square^{2n-1'}_{b-}, \square^{2n-1''}_{cs+})\}, \square^{2n-1}_{cs+} \\
&\cdot c_+(\square^{2n-2'}_{b+}, \square^{2n-2}_{cs-}) \cdot \cdots \cdot c_+(\square^{2'}_{b+}, \square^{2}_{cs-}) \cdot \square^{1}_{cs+}) \cdot \square^{0}_{cs-}) \to \\
&a_2(\square^{2n+1}_{cs+}, \square^{2n}_{cs-} \cdot c_-(\square^{2n-1'}_{b-}, \square^{2n-1}_{cs+}) \cdot \cdots \cdot c_-(\square^{3'}_{b-}, \square^{3}_{cs+}) \\
&\cdot \square^{2}_{cs-} \cdot c_-(\square^{1'}_{b-}, \square^{1}_{cs+}) \cdot \square^{0}_{cs-}) \cdot a_2(\square^{1''}_{cs+} \cdot c_+(\square^{2'}_{b+}, \square^{2''}_{cs-}) \\
&\cdot \square^{3''}_{cs+} \cdot \cdots \cdot c_+(\square^{2n-2'}_{b+}, \square^{2n-2''}_{cs-}) \cdot \square^{2n-1''}_{cs+}, \square^{0'}_{cs-}) \\
a_2(c_{+(2n)}) :&a_2(\square^{0}_{cs+} \cdot c_+(\beta_+\{\square^{2n+1}_{cs+} \cdot c_+(\square^{2n-1'}_{b+}, \square^{2n-1}_{cs-}) \cdot \cdots \\
&\cdot c_+(\square^{3'}_{b+}, \square^{3}_{cs-}) \cdot \square^{2}_{cs+} \cdot c_+(\square^{1'}_{b+}, \square^{1}_{cs-})\}, \square^{1''}_{cs-} \cdot c_-(\square^{2'}_{b-}, \square^{2''}_{cs+}) \cdot \\
&\cdots \cdot c_-(\square^{2n-2'}_{b-}, \square^{2n-2''}_{cs+}) \cdot \square^{2n-1''}_{cs-}) \cdot \square^{2n}_{cs+}, \square^{0'}_{cs-}) \to \\
&a_2(\square^{2n+1}_{cs+}, \square^{2n-1}_{cs-} \cdot c_-(\square^{2n-2'}_{b-}, \square^{2n-2}_{cs+}) \cdot \cdots \cdot \square^{3}_{cs-} \\
&\cdot c_-(\square^{2'}_{b-}, \square^{2}_{cs+}) \cdot \square^{1}_{cs-}) \cdot a_2(\square^{0}_{cs+} \cdot c_+(\square^{1'}_{b+}, \square^{1''}_{cs-}) \cdot \square^{2''}_{cs+} \\
&\cdot c_+(\square^{3'}_{b+}, \square^{3''}_{cs-}) \cdot \cdots \cdot \square^{2n-2''}_{cs+} \cdot c_+(\square^{2n-1'}_{b+}, \square^{2n-1''}_{cs-}) \cdot \square^{2n''}_{cs+}, \square^{0'}_{cs-}) \\
a_\emptyset(\Lambda_\pm) :&a_2(\square^{1}_{cs\pm}, \lambda) \to a_\pm(\beta_+\{\square^{1}_{cs\pm}\}) \\
a_2(\Lambda_+) :&a_2(\square^{3}_{cs+} \cdot c_+(\square^{1}_{b+}, \lambda) \cdot \square^{2}_{cs+}, \square^{4}_{cs-}) \to a_+(\square^{1}_{b+}) \cdot a_2(\square^{3}_{cs+} \cdot \square^{2}_{cs+}, \square^{4}_{cs-}) \\
a_2(\Lambda_-) :&a_2(\square^{1}_{cs+}, \square^{2}_{cs-} \cdot c_-(\square^{4}_{b-}, \lambda) \cdot \square^{3}_{cs-}) \to a_2(\square^{1}_{cs+}, \square^{2}_{cs-} \cdot \square^{3}_{cs-}) \cdot a_-(\square^{4}_{b-}) \\
\beta_\pm(\Lambda_\pm) :&\beta_\pm\{\square^{1}_{cs+} \cdot c_\pm(\square^{2}_{b\pm}, \lambda)\} \to b_{\pm\pm}\{\beta_\pm\{\square^{1}_{cs\pm}\}, \square^{2}_{b\pm}\} \\
\beta_\pm(\Lambda_\mp) :&\ \beta_\pm\{c_\pm(\square^{2}_{b\pm}, \square^{1}_{cs\mp})\} \to b_{\pm\mp}(\square^{2}_{b\pm}, \square^{1}_{cs\mp}) \\
c_\pm(\Lambda_\pm) :&c_\pm(\square^{1}_{b\pm}, \square^{4}_{cs\mp} \cdot c_\mp(\square^{2}_{b\mp}, \lambda) \cdot \square^{3}_{cs\mp}) \to c_\pm(b_{\pm\mp}(\square^{1}_{b\pm}, \square^{2}_{b\mp}), \square^{4}_{cs\mp} \cdot \square^{3}_{cs\mp}) \\
c_{\pm\pm} :&c_\pm(b_{\pm\pm}\{\square^{2}_{b\pm}, \square^{1}_{b\pm}\}, \square^{4}_{cs\mp} \cdot \square^{3}_{cs\mp}) \to c_\pm(\square^{2}_{b\pm}, \square^{4}_{cs\mp}) \cdot c_\pm(\square^{1}_{b\pm}, \square^{3}_{cs\mp})
\end{aligned}
$$

$$
\begin{aligned}
a_2(c_+(c_-^R)) :& a_2(\square^6_{cs+} \cdot c_+(\square^1_{b+}, c_-(\square^2_{b-}, \square^3_{cs+}) \cdot \square^4_{cs-}) \cdot \square^5_{cs+}, \square^7_{cs-}) \to \\
& a_-(\square^2_{b-}) \cdot a_2(\square^6_{cs+} \cdot \square^3_{cs+} \cdot c_+(\square^1_{b+}, \square^4_{cs-}) \cdot \square^5_{cs+}, \square^7_{cs-}) \\
a_2(c_+(c_-^L)) :& a_2(\square^5_{cs+} \cdot c_+(\square^1_{b+}, \square^4_{cs-} \cdot c_-(\square^2_{b-}, \square^3_{cs+})) \cdot \square^6_{cs+}, \square^7_{cs-}) \to \\
& a_-(\square^2_{b-}) \cdot a_2(\square^5_{cs+} \cdot c_+(\square^1_{b+}, \square^4_{cs-}) \cdot \square^3_{cs+} \cdot \square^6_{cs+}, \square^7_{cs-}) \\
a_2(c_-(c_+^R)) :& a_2(\square^7_{cs+}, \square^6_{cs-} \cdot c_-(\square^2_{b-}, \square^5_{cs+} \cdot c_+(\square^3_{b+}, \square^4_{cs-})) \cdot \square^1_{cs-}) \to \\
& a_2(\square^7_{cs+}, \square^6_{cs-} \cdot c_-(\square^2_{b-}, \square^5_{cs+}) \cdot \square^4_{cs-} \cdot \square^1_{cs-}) \cdot a_+(\square^3_{b+}) \\
a_2(c_-(c_+^L)) :& a_2(\square^1_{cs+}, \square^2_{cs-} \cdot c_-(\square^7_{b-}, c_+(\square^6_{b+}, \square^5_{cs-}) \cdot \square^4_{cs+}) \cdot \square^3_{cs-}) \to \\
& a_2(\square^1_{cs+}, \square^2_{cs-} \cdot \square^5_{cs-} \cdot c_-(\square^7_{b-}, \square^4_{cs+}) \cdot \square^3_{cs-}) \cdot a_+(\square^6_{b+}) \\
\beta_\pm(c_\pm(c_\mp^L)) :& \beta_\pm\{\square^1_{cs\pm} \cdot c_\pm(\square^5_{b\pm}, \square^2_{cs\mp} \cdot c_\mp(\square^4_{b\mp}, \square^3_{cs\pm}))\} \to \\
& b_{\pm\mp}(\beta_\pm\{\square^1_{cs\pm} \cdot c_\pm(\square^5_{b\pm}, \square^2_{cs\mp}) \cdot \square^3_{cs\pm}\}, \square^4_{b\mp}) \\
\beta_\pm(c_\pm(c_\mp^R)) :& \beta_\pm\{\square^1_{cs\pm} \cdot c_\pm(\square^5_{b\pm}, c_\mp(\square^4_{b\mp}, \square^3_{cs\pm}) \cdot \square^2_{cs\mp})\} \to \\
& b_{\pm\mp}(\beta_\pm\{\square^1_{cs\pm} \cdot \square^3_{cs\pm} \cdot c_\pm(\square^5_{b\pm}, \square^2_{cs\mp})\}, \square^4_{b\mp}) \\
c_\pm(c_\mp(c_\pm^R)) :& c_\pm(\square^1_{b\pm}, \square^7_{cs\mp} \cdot c_\mp(\square^3_{cs\mp}, c_\pm(\square^4_{b\pm}, \square^5_{cs\mp}) \cdot \square^6_{cs\pm}) \cdot \square^2_{cs\mp}) \to \\
& c_\pm(b_{\pm\pm}\{\square^1_{b\pm}, \square^4_{b\pm}\}, \square^7_{cs\mp} \cdot \square^5_{cs\mp} \cdot c_\mp(\square^3_{b\mp}, \square^6_{cs\pm}) \cdot \square^2_{cs\mp}) \\
c_\pm(c_\mp(c_\pm^L)) :& c_\pm(\square^1_{b\pm}, \square^7_{cs\mp} \cdot c_\mp(\square^3_{cs\mp}, \square^6_{cs\pm} \cdot c_\pm(\square^4_{b\pm}, \square^5_{cs\mp})) \cdot \square^2_{cs\mp}) \to \\
& c_\pm(b_{\pm\pm}\{\square^4_{b\pm}, \square^1_{b\pm}\}, \square^7_{cs\mp} \cdot c_\mp(\square^3_{b\mp}, \square^6_{cs\pm}) \cdot \square^5_{cs\mp} \cdot \square^2_{cs\mp}) \\
a_2(c_+^L) :& a_2(\square^3_{cs+} \cdot c_+(\square^1_{b+}, \square^2_{cs-}), \square^4_{cs-}) \to a_2(\square^3_{cs+}, \square^2_{cs-} \cdot \square^4_{cs-}) \cdot a_+(\square^1_{b+}) \\
a_2(c_+^R) :& a_2(c_+(\square^1_{b+}, \square^2_{cs-}) \cdot \square^3_{cs+}, \square^4_{cs-}) \to a_2(\square^3_{cs+}, \square^4_{cs-} \cdot \square^2_{cs-}) \cdot a_+(\square^1_{b+}) \\
a_2(c_-^R) :& a_2(\square^1_{cs+}, c_-(\square^4_{b-}, \square^3_{cs+}) \cdot \square^2_{cs-}) \to a_-(\square^4_{b-}) \cdot a_2(\square^1_{cs+} \cdot \square^3_{cs+}, \square^2_{cs-}) \\
a_2(c_-^L) :& a_2(\square^1_{cs+}, \square^2_{cs-} \cdot c_-(\square^4_{b-}, \square^3_{cs+})) \to a_-(\square^4_{b-}) \cdot a_2(\square^3_{cs+} \cdot \square^1_{cs+}, \square^2_{cs-})
\end{aligned}
$$

It should be noted that rules $b_{(+-+)}$, $b_{(-+-)}$, and $a_{(+-)} = a_{(-+)}$ are identical. We will prove the previous theorem by cases in this section.

5.1. **H-unstable transitions on an open disk.**

5.1.1. *Tree grammar G_1.* We impose restrictions on tree grammar G to obtain tree grammar G_1 on open disks (i.e., one punctured spheres), which is defined as $G_1 = (S, N_1, \mathcal{F}_1, R_1)$. Here, S is an axiom, $N_1 = \{S, B_+, B_-\}$ is a set of non-terminal symbols, $\mathcal{F}_1 = \{b_\emptyset(,), b_{++}\{,\}, b_{+-}(,), b_{--}\{,\}, b_{-+}(,), \sigma_+, \sigma_-\}$ is a set of terminal symbols, and R_1 is a set of production rules:

$$
\begin{aligned}
S &\to b_\emptyset(B_-, B_+) \\
B_+ &\to \sigma_+ \mid b_{++}\{B_+, B_+\} \mid b_{+-}(B_+, B_-) \\
B_- &\to \sigma_- \mid b_{--}\{B_-, B_-\} \mid b_{-+}(B_-, B_+)
\end{aligned}
$$

For example, the orbit structure of the term $b_\emptyset(\sigma_-, b_{++}\{b_{+-}(b_{++}, \sigma_-), \sigma_+\})$, derived by G_1, is shown in Figure 32.

Because of the construction of G_1, we have that $L(G_1)$ is a subset of $L(G)$ and $L(G_1)/\approx_{\text{cyc}}$ is a subset of $L(G)/\approx_{\text{cyc}}$. Here, the language $L(X)/\approx_{\text{cyc}}$ is a set of terms which are derived by a grammar X. There is a one-to-one correspondence

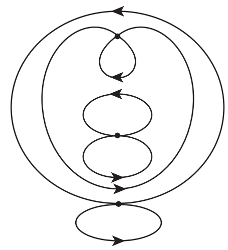

FIGURE 32. Streamline of the tree representation: $b_\emptyset(\sigma_-, b_{++}\{b_{+-}(b_{++}, \sigma_-), \sigma_+\})$ or $b_{++}\{b_{+-}(b_{++})\}$.

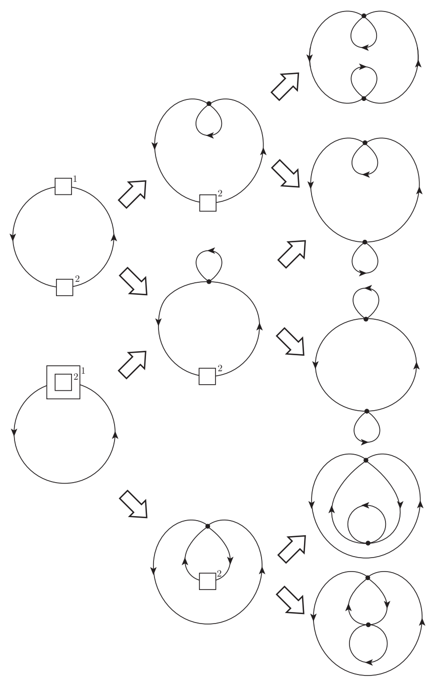

FIGURE 33. Complete list of five structurally unstable structures with heteroclinic counter-clockwise orbits on a bounded open disk.

between $L(G_1)/\approx_{\mathrm{cyc}}$ and the set of topological equivalence classes of structurally stable Hamiltonian flows on an open disk. We specify the complete transformation rules via a non-self-connected saddle connection for flows on an open disk.

Lemma 22. *The complete generic transitions of structurally stable Hamiltonian flows with non-degenerate singular points on an open disk are described by the rules* $(b_{\pm\pm\pm})$, $(b_{\pm\pm(\mp)})$, $(b_{\pm\{\mp\mp\}})$, $(b_{\pm(\mp(\mp))})$, $(b_{\pm(\mp(\pm))})$, *and* $(b_{(\pm\mp\pm)})$, *as shown in Figures 35–37.*

Proof. For structurally unstable structures with self-connected separatrices, we exhaustively check all possible orbit structures that can be obtained by applying the

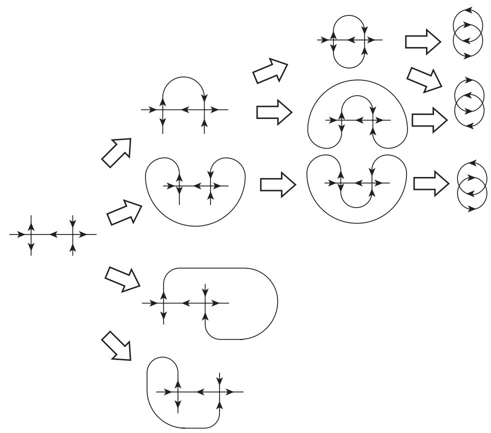

FIGURE 34. Complete list of one structurally unstable structure without self-connected separatrices in a bounded open disk.

primitive local transformations, as shown in Figure 33. All possible transformations with self-connected separatrices are listed in Figure 35 and Figure 36. For structurally unstable structures without self-connected separatrices, we exhaustively check all possible orbit structures that can be obtained by applying the primitive local transformations, as shown in Figure 34. All possible transformations without self-connected separatrices are listed in Figure 37. Under each pair of clockwise and counter-clockwise transformations, the corresponding transformation rules of terms are generated by grammar G_1. □

5.2. **H-unstable transitions on compact punctured spheres.**

5.2.1. *Tree grammar G_2.* We impose restrictions on tree grammar G to obtain tree grammar G_2 on punctured spheres, which is defined as $G_2 = (S, N_2, \mathcal{F}_2, R_2)$. Here, S is an axiom, $N_2 = \{S, B_+, B_-, C_+, C_-, C_+^*, C_-^*\}$ is a set of non-terminal symbols, $\mathcal{F}_2 = \{b_\emptyset(,)\} \cup \mathcal{F}_B \cup \mathcal{F}_C \cup \mathcal{F}_\sigma$ is a set of terminal symbols, and R_2 is a set of production rules:

$$
\begin{array}{rcl}
S & \to & b_\emptyset(B_-, B_+) \\
B_+ & \to & \sigma_+ \mid b_{++}\{B_+, B_+\} \mid b_{+-}(B_+, B_-) \mid \beta_+\{C_+^*\} \\
B_- & \to & \sigma_- \mid b_{--}\{B_-, B_-\} \mid b_{-+}(B_-, B_+) \mid \beta_-\{C_-^*\} \\
C_+ & \to & c_+(B_+, C_-^*) \\
C_- & \to & c_-(B_-, C_+^*) \\
C_+^* & \to & \lambda_+ \mid \mathit{cons}_+(C_+, C_+^*) \\
C_-^* & \to & \lambda_- \mid \mathit{cons}_-(C_-, C_-^*)
\end{array}
$$

5.2.2. *Transformation rules.* We specify the complete transformation rules via a non-self-connected saddle connection for flows on a compact punctured sphere. Because all transitions discussed in Subsection 5.1 are unrelated to boundaries, all generic transitions with two non-self-connected separatrices from/to boundaries are described. There are exactly four structurally unstable orbit structures in the center, as we counted above. Indeed, the picture shows this assertion. Three orbit

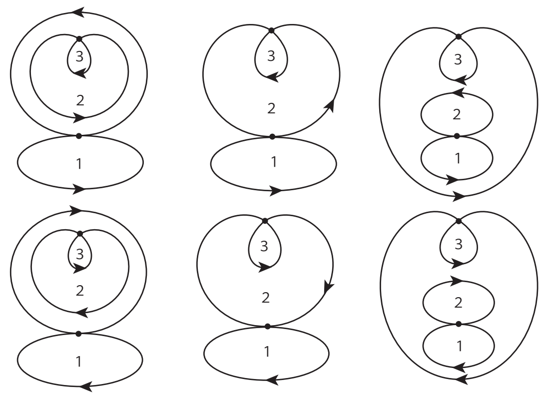

$$b_{\pm\pm(\mp)}:\ b_{\pm\pm}\{\square^1_{b\pm}, b_{\pm\mp}(\square^2_{b\pm}, \square^3_{b\mp})\} \ \to b_{\pm\mp}(b_{\pm\pm}\{\square^1_{b\pm}, \square^2_{b\pm}\}, \square^3_{b\mp})$$

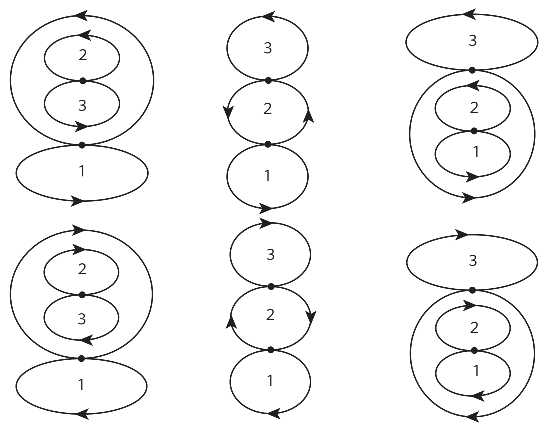

$$b_{\pm\pm\pm}:\ b_{\pm\pm}\{\square^1_{b\pm}, b_{\pm\pm}\{\square^2_{b\pm}, \square^3_{b\pm}\}\} \ \to b_{\pm\pm}\{b_{\pm\pm}\{\square^1_{b\pm}, \square^2_{b\pm}\}, \square^3_{b\pm}\}$$

FIGURE 35. Transformation rules for the trees of the outermost $b_{\pm\pm}$ structure.

structures are shown in each row in Figures 40–42; the left and right structurally stable orbit structures are converted to each other via the central structurally unstable orbit structure. There are exactly 34 structurally unstable orbit structures in the center, as we counted above.

Lemma 23. *The complete generic transitions of structurally stable Hamiltonian flows with non-degenerate singular points on compact punctured spheres are described by the rules* $(b_{\pm\pm\pm})$, $(b_{\pm\pm(\mp)})$, $(b_{\pm\{\mp\mp\}})$, $(b_{\pm(\mp(\mp))})$, $(b_{\pm(\mp(\pm))})$, $(b_{(\pm\mp\pm)})$, $(b_{\pm\pm(2)})$, $(b_{\pm\{\mp,2\}})$, $(b_{\pm(\mp(2))})$, $(b_{\pm\{22\}})$, $(c_\pm(c_{\mp(\mp)}))$, $(c_\pm(c_{\mp(\pm)}))$, $(c_\pm(c_{\mp(2)}))$, $(\beta_\pm(c_{(\pm\mp\pm)}))$, $(c_\pm(c_{(\mp\pm\mp)}))$, $(\beta_\pm(c_{\pm(2n)}))$, *and* $(c_\pm(c_{\mp(2n)}))$ *in Figures 35–37, Figures 40–43, and Figure 46.*

Proof. Lemma 22 implies that the complete generic transitions without ∂-saddles of structurally stable Hamiltonian flows with non-degenerate singular points on an open disk are described by the rules $(b_{\pm\pm\pm})$, $(b_{\pm\pm(\mp)})$, $(b_{\pm\{\mp\mp\}})$, $(b_{\pm(\mp(\mp))})$, $(b_{\pm(\mp(\pm))})$, and $(b_{(\pm\mp\pm)})$, as shown in Figures 35–37. Figure 38 indicates that there

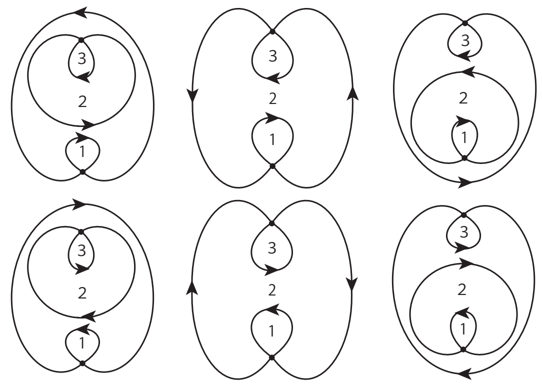

$$b_{\pm\{\mp\mp\}}:\ b_{\pm\mp}(b_{\pm\mp}(\square^2_{b\pm},\square^3_{b\mp}),\square^1_{b\mp}) \to b_{\pm\mp}(b_{\pm\mp}(\square^2_{b\pm},\square^1_{b\mp}),\square^3_{b\mp})$$

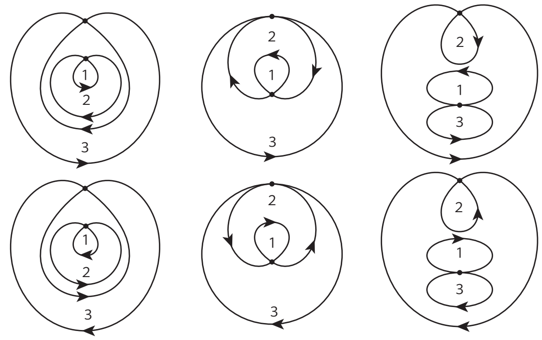

$$b_{\pm(\mp(\pm))}:\ b_{\pm\mp}(\square^3_{b\pm}, b_{\mp\pm}(\square^2_{b\mp},\square^1_{b\pm})) \to b_{\pm\mp}(b_{\pm\pm}\{\square^1_{b\pm},\square^3_{b\pm}\},\square^2_{b\mp})$$

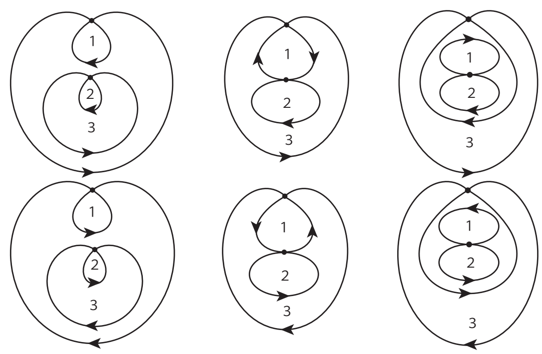

$$b_{\pm(\mp(\mp))}:\ b_{\pm\mp}(b_{\pm\mp}(\square^3_{b\pm},\square^2_{b\mp}),\square^1_{b\mp}) \to b_{\pm\mp}(\square^3_{b\pm}, b_{\mp\mp}\{\square^1_{b\mp},\square^2_{b\mp}\})$$

FIGURE 36. Transformation rules for the trees of the outermost $b_{\pm\mp}$ structure.

are precisely six structurally unstable local structures with self-connected separatrices and heteroclinic counter-clockwise orbits. Figure 39 indicates that there are precisely two structurally unstable local structures on bounded disks without

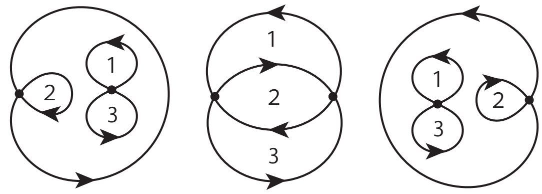

$$b_{(+-+)}:\; b_{+-}(b_{++}\{\square^1_+, \square^3_+\}, \square^2_-) \to b_{+-}(b_{++}\{\square^1_+, \square^3_+\}, \square^2_-)$$

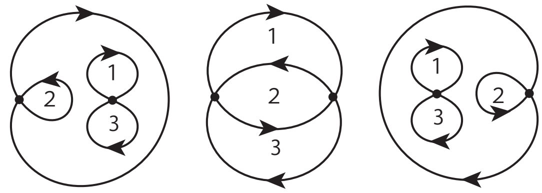

$$b_{(-+-)}:\; b_{-+}(b_{--}\{\square^1_-, \square^3_-\}, \square^2_+) \to b_{-+}(b_{--}\{\square^1_-, \square^3_-\}, \square^2_+)$$

FIGURE 37. Transformation rules for the trees of the bounded structures without self-connected separatrices in planes.

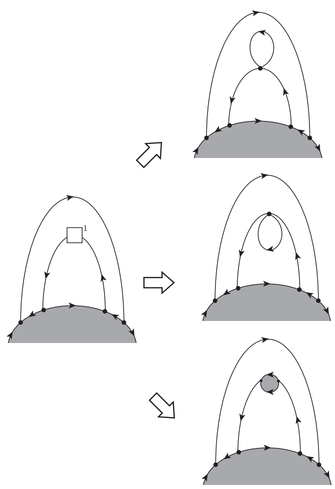

FIGURE 38. Complete list of three structurally unstable structures with heteroclinic counter-clockwise orbits on a boundary.

self-connected separatrices. Figure 44 indicates that there are precisely four structurally unstable local structures with heteroclinic counter-clockwise orbits. These local classifications imply that all possible transformations with ∂-saddles on compact punctured spheres are listed in Figures 40–43 and Figure 46. $\square$

5.3. **H-unstable transitions on planes.**

5.3.1. *Tree grammar G_3.* We impose restrictions on tree grammar G to obtain tree grammar G_3 on planes, which is defined as $G_3 = (S, N_3, \mathcal{F}_3, R_3)$. Here, S is an axiom, $N_3 = \{S, A, A^*, B_+, B_-\}$ is a set of non-terminal symbols, $\mathcal{F}_3 = \mathcal{F}_A \cup \mathcal{F}_\sigma \cup \{b_{++}\{,\}, b_{+-}(,), b_{--}\{,\}, b_{-+}(,), \lambda_a, cons_a\}$ is a set of terminal symbols,

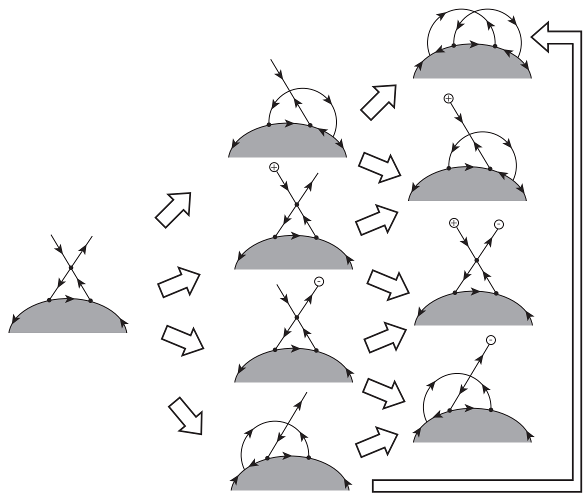

FIGURE 39. Complete list of four structurally unstable structures with a separatrix connecting a saddle and ∂-saddle but without self-connected separatrices in punctured spheres.

and R_3 is a set of production rules:

$$\begin{array}{rcl} S & \to & a_{\emptyset}(A^*) \\ A & \to & a_+(B_+) \mid a_-(B_-) \\ A^* & \to & \lambda_a \mid cons_a(A, A^*) \\ B_+ & \to & \sigma_+ \mid b_{++}\{B_+, B_+\} \mid b_{+-}(B_+, B_-) \\ B_- & \to & \sigma_- \mid b_{--}\{B_-, B_-\} \mid b_{-+}(B_-, B_+) \end{array}$$

5.3.2. *Transformation rules.* Here, all structurally unstable flows in planes are considered, except for those discussed in Subsections 5.1–5.2. All possible transformations with self-connected separatrices and with ss-separatrices in a plane are either instantiations of two non-overlapped holes on the same orbit structure in Figure 47 or instantiations of two nested holes on the orbit structure in Figure 50. All possible transformations without self-connected separatrices but with ss-separatrices in a plane are listed in Figure 48. Each hole is instantiated either into an upper or lower homoclinic orbit. Hence, there are exactly 21 unstable flows.

Lemma 24. *The complete generic transitions of structurally stable Hamiltonian flows with non-degenerate singular points on planes are described by the rules* $(b_{\pm\pm\pm})$, $(b_{\pm\pm(\mp)})$, $(b_{\pm\{\mp\mp\}})$, $(b_{\pm(\mp(\mp))})$, $(b_{\pm(\mp(\pm))})$, $(b_{(\pm\mp\pm)})$, $(a_{\pm\pm})$, $(a_{\mp\pm})$, $(a_{\pm(\pm)})$, $(a_{\mp(\pm)})$, *and* $(a_{(\mp\pm)})$, *as shown in Figures 35–37, Figure 49, and Figure 51.*

Proof. Lemma 22 implis that there are twelve unstable structures in Figure 33 and their inverses. Figure 47 indicates that there is precisely four unstable structures in planes. Figure 48 indicates that there is precisely one structurally unstable structures with a separatrix connecting saddles but without self-connected separatrices in punctured planes. Figure 50 indicates that there are precisely four structurally unstable structures with nested separatrices, as shown in Figure 51. □

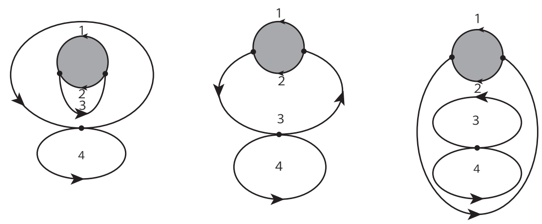

$$b_{++(2)} : b_{++}\{\beta_+\{\square^1_{cs+} \cdot c_+(\square^3_{b+}, \square^2_{cs-})\}, \square^4_{b+}\} \to \beta_+\{\square^1_{cs+} \cdot c_+(b_{++}\{\square^3_{b+}, \square^4_{b+}\}, \square^2_{cs-})\}$$

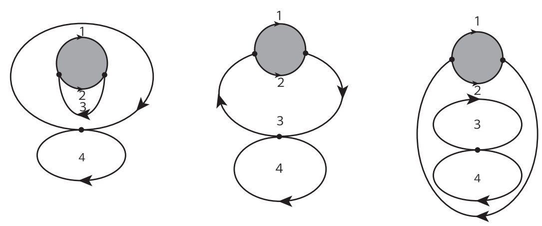

$$b_{--(2)} : b_{--}\{\beta_-\{\square^1_{cs-} \cdot c_-(\square^3_{b-}, \square^2_{cs+})\}, \square^4_{b-}\} \to \beta_-\{\square^1_{cs-} \cdot c_-(b_{--}\{\square^3_{b-} \cdot \square^4_{b-}\}, \square^2_{cs+})\}$$

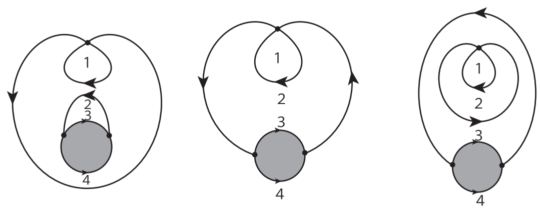

$$b_{+\{-,2\}} : b_{+-}(\beta_+\{c_+(\square^2_{b+}, \square^3_{cs-}) \cdot \square^4_{cs+}\}, \square^1_{b-}) \to \beta_+\{c_+(b_{+-}(\square^2_{b+}, \square^1_{b-}), \square^3_{cs-}) \cdot \square^4_{cs+}\}$$

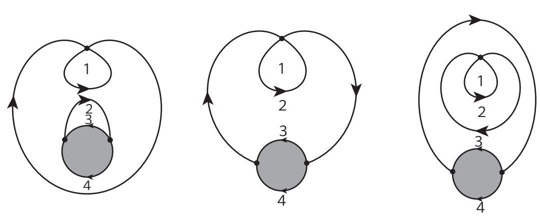

$$b_{-\{+,2\}} : b_{-+}(\beta_-\{c_-(\square^2_{b-}, \square^3_{cs+}) \cdot \square^4_{cs-}\}, \square^1_{b+}) \to \beta_-\{c_-(b_{-+}(\square^2_{b-}, \square^1_{b+}), \square^3_{cs+}) \cdot \square^4_{cs-}\}$$

It should be noted that the nested hole in a uniform flow precisely represents the flows shown in Figure 50. Box $\square$ represents one of the four flows (Figure 50(a), upper side). For example, the uppermost nested hole in Figure 50(a) is isomorphic to the lower right flow in Figure 50(b). Streamlines outside the boxes represent uniform flows from left to right, and only orbit structures inside the boxes are curved; as such, all orbit structures are continuous. The other three holes are similarly instantiated.

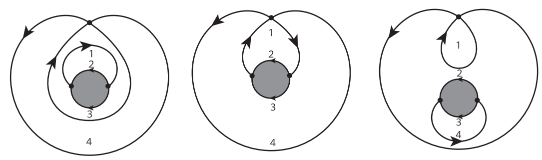

$$b_{+(-(2))} : b_{+-}(\square^4_{b+}, \beta_-\{c_-(\square^1_{b-}, \square^2_{cs+}) \cdot \square^3_{cs-}\}) \to$$
$$b_{+-}(\beta_+\{c_+(\square^4_{b+}, \square^3_{cs-}) \cdot \square^2_{cs+}\}, \square^1_{b-})$$

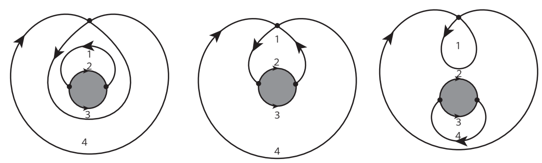

$$b_{-(+(2))} : b_{-+}(\square^4_{b-}, \beta_+\{c_+(\square^1_{b+}, \square^2_{cs-}) \cdot \square^3_{cs+}\}) \to$$
$$b_{-+}(\beta_-\{c_-(\square^4_{b-}, \square^3_{cs+}) \cdot \square^2_{cs-}\}, \square^1_{b+})$$

FIGURE 40. Transformation rules for the trees of the outermost $b_{\pm\pm}/b_{\pm\mp}$ structures containing a boundary component in punctured unbounded spheres.

5.4. H-unstable transitions on punctured planes.

5.4.1. *Tree grammar G.* We have tree grammar G on punctured planes.

5.4.2. *Transformation rules.* We specify the complete transformation rules via a non-self-connected saddle connection for flows on punctured planes. Because all transitions that are unrelated to boundaries in punctured disks are detailed in Subsections 5.2.1–5.3, we describe all generic transitions with ss-separatrices from/to boundaries.

Three orbit structures are displayed in each row in Figures 53–55 and Figure 57; the left and right structurally stable orbit structures are converted to each other via the central structurally unstable orbit structure. There are exactly 38 structurally unstable orbit structures in the center, as we counted above.

Lemma 25. *The complete generic transitions of Hamiltonian flow with non-degenerate singular points on punctured planes are described by the rules* $(b_{\pm\pm\pm})$, $(b_{\pm\pm(\mp)})$, $(b_{\pm\{\mp\mp\}})$, $(b_{\pm(\mp(\mp))})$, $(b_{\pm(\mp(\pm))})$, $(b_{(\pm\mp\pm)})$, $(b_{\pm\pm(2)})$, $(b_{\pm\{\mp,2\}})$, $(b_{\pm(\mp(2))})$, $(b_{\pm\{22\}})$, $(c_\pm(c_{\mp(\mp)}))$, $(c_\pm(c_{\mp(\pm)}))$, $(c_\pm(c_{\mp(2)}))$, $(\beta_\pm(c_{(\pm\mp\pm)}))$, $(c_\pm(c_{(\mp\pm\mp)}))$, $(\beta_\pm(c_{\pm(2n)}))$, $(c_\pm(c_{\mp(2n)}))$, $(a_{\pm\pm})$, $(a_{\pm\mp})$, $(a_{(\pm\mp)})$, $(a_{\pm(\pm)})$, $(a_{\mp(\pm)})$, $(a_{2(\mp\pm)})$, (a_{22}), $(a_{\pm2})$, $(a_{2\pm})$, $(a_{(\mp\pm)})$, $(a_{\pm(2)})$, $(a_2(c_{\pm(\pm)}))$, $(a_2(c_{\pm(\mp)}))$, $(a_2(c_{\pm(2)}))$, $a_2(c_{(\pm\mp\pm)})$, $a_2(c_{\pm(2n)})$, *and* (a_{2n2}), *as shown in Figures 35–37, Figures 40–43, Figures 45–46, Figure 49, Figure 51, Figures 53–55, and Figure 57.*

Proof. Lemma 23 implies that the complete generic transitions of Hamiltonian flows with non-degenerate singular points on closed disks in punctured planes are described by the rules $(b_{\pm\pm\pm})$, $(b_{\pm\pm(\mp)})$, $(b_{\pm\{\mp\mp\}})$, $(b_{\pm(\mp(\mp))})$, $(b_{\pm(\mp(\pm))})$, $(b_{(\pm\mp\pm)})$, $(b_{\pm\pm(2)})$, $(b_{\pm\{\mp,2\}})$, $(b_{\pm(\mp(2))})$, $(b_{\pm\{22\}})$, $(c_\pm(c_{\mp(\mp)}))$, $(c_\pm(c_{\mp(\pm)}))$, $(c_\pm(c_{\mp(2)}))$, $(\beta_\pm(c_{(\pm\mp\pm)}))$, $(c_\pm(c_{(\mp\pm\mp)}))$, $(\beta_\pm(c_{\pm(2n)}))$, and $(c_\pm(c_{\mp(2n)}))$ in Figures 35–37, Figures 40–43, and Figure 46. Lemma 24 implies that the complete generic transitions

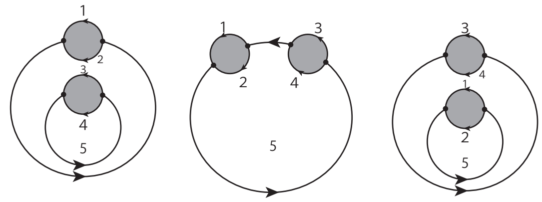

$$b_{+\{22\}} : \beta_+\{\square^1_{cs+} \cdot c_+(\beta_+\{\square^3_{cs+} \cdot c_+(\square^5_{b+}, \square^4_{cs-})\}, \square^2_{cs-})\} \to \beta_+\{\square^3_{cs+} \cdot c_+(\beta_+\{\square^1_{cs+} \cdot c_+(\square^5_{b+}, \square^2_{cs-})\}, \square^4_{cs-})\}$$

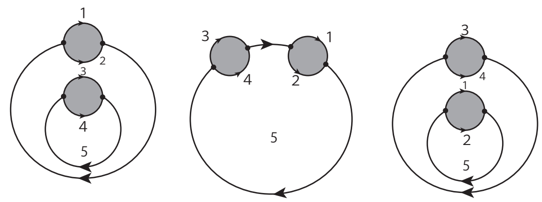

$$b_{-\{22\}} : \beta_-\{\square^1_{cs-} \cdot c_-(\beta_-\{\square^3_{cs-} \cdot c_-(\square^5_{b-}, \square^4_{cs+})\}, \square^2_{cs+})\} \to \beta_-\{\square^3_{cs-} \cdot c_-(\beta_-\{\square^1_{cs-} \cdot c_-(\square^5_{b-}, \square^2_{cs+})\}, \square^4_{cs+})\}$$

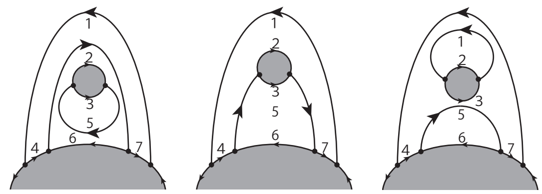

$$c_+(c_{-(2)}) : c_+(\square^1_{b+}, \square^7_{cs-} \cdot c_-(\beta_-\{\square^2_{cs-} \cdot c_-(\square^5_{b-}, \square^3_{cs+})\}, \square^6_{cs+}) \cdot \square^4_{cs-}) \to c_+(\beta_+\{c_+(\square^1_{b+}, \square^2_{cs-}) \cdot \square^3_{cs+}\}, \square^7_{cs-} \cdot c_-(\square^5_{b-}, \square^6_{cs+}) \cdot \square^4_{cs-})$$

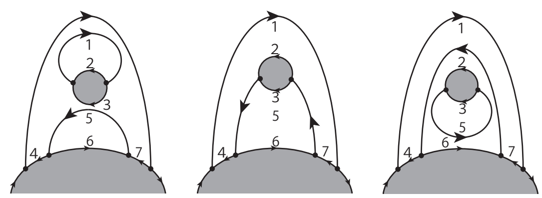

$$c_-(c_{+(2)}) : c_-(\square^1_{b-}, \square^7_{cs+} \cdot c_+(\beta_+\{\square^2_{cs+} \cdot c_+(\square^5_{b+}, \square^3_{cs-})\}, \square^6_{cs-}) \cdot \square^4_{cs+}) \to c_-(\beta_-\{c_-(\square^1_{b-}, \square^2_{cs+}) \cdot \square^3_{cs-}\}, \square^7_{cs+} \cdot c_+(\square^5_{b+}, \square^6_{cs-}) \cdot \square^4_{cs+})$$

FIGURE 41. Transformation rules for the trees of the outermost $\beta_\pm$ with a boundary component structure in bounded punctured disks.

with ss-separatrices in planes are described by the rules $(a_{\pm\pm})$, $(a_{\mp\pm})$, $(a_{\pm(\pm)})$, $(a_{\mp(\pm)})$, and $(a_{(\mp\pm)})$ as shown in Figure 49 and Figure 51. Figure 52 indicates that there are precisely thirteen structurally unstable structures with heteroclinic counter-clockwise orbits in punctured planes, as shown in Figure 53–55. Figure 39 indicates that there are precisely four structurally unstable local structures with a

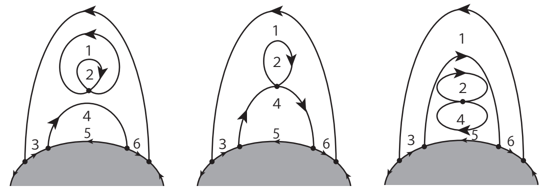

$$c_+(c_{-(-)}) : c_+(b_{+-}(\square^1_{b+}, \square^2_{b-}), \square^6_{cs-} \cdot c_-(\square^4_{b-}, \square^5_{cs+}) \cdot \square^3_{cs-}) \to c_+(\square^1_{b+}, \square^6_{cs-} \cdot c_-(b_{--}\{\square^2_{b-}, \square^4_{b-}\}, \square^5_{cs+}) \cdot \square^3_{cs-})$$

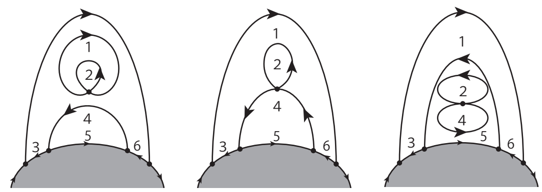

$$c_-(c_{+(+)}) : c_-(b_{-+}(\square^1_{b-}, \square^2_{b+}), \square^6_{cs+} \cdot c_+(\square^4_{b+}, \square^5_{cs-}) \cdot \square^3_{cs+}) \to c_-(\square^1_{b-}, \square^6_{cs+} \cdot c_-(b_{++}\{\square^2_{b+}, \square^4_{b+}\}, \square^5_{cs-}) \cdot \square^3_{cs+})$$

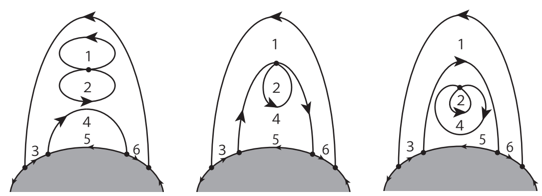

$$c_+ + (c_{-(+)}) : c_+(b_{++}\{\square^1_{b+}, \square^2_{b+}\}, \square^6_{cs-} \cdot c_-(\square^4_{b-}, \square^5_{cs+}) \cdot \square^3_{cs-}) \to c_+(\square^1_{b+}, \square^6_{cs-} \cdot c_-(b_{-+}(\square^4_{b-}, \square^2_{b+}), \square^5_{cs+}) \cdot \square^3_{cs-})$$

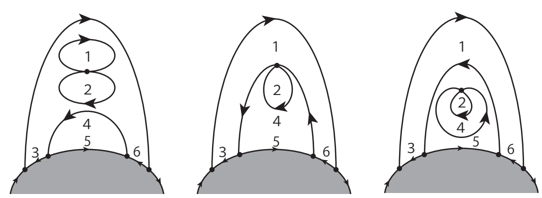

$$c_-(c_{+(-)}) : c_-(b_{--}\{\square^1_{b-}, \square^2_{b-}\}, \square^6_{cs+} \cdot c_+(\square^4_{b+}, \square^5_{cs-}) \cdot \square^3_{cs+}) \to c_-(\square^1_{b-}, \square^6_{cs+} \cdot c_+(b_{+-}(\square^4_{b+}, \square^2_{b-}), \square^5_{cs-}) \cdot \square^3_{cs+})$$

FIGURE 42. Transformation rules for the trees of the outermost $c_\pm$ with a $c_\mp$ structure in bounded punctured disks.

separatrix connecting a saddle and ∂-saddle but without self-connected separatrices in punctured planes, as shown in Figure 45 and Figure 54. Figure 56 indicates that three kinds of structurally unstable structures with heteroclinic counter-clockwise orbits in punctured planes, as shown in Figure 57. $\square$

5.5. **Pinching contained in a compact punctured sphere.**

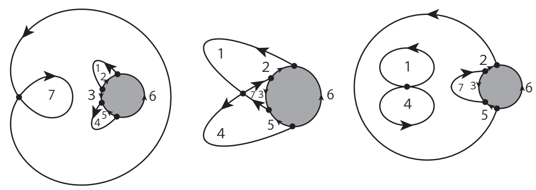

$$\beta_+(c_{(+-+)}):\quad b_{+-}(\beta_+\{c_+(\square^1_{b+},\square^2_{cs-})\cdot\square^3_{cs+}\cdot c_+(\square^4_{b+},\square^5_{cs-})\cdot\square^6_{cs+}\},\square^7_{b-})\to \beta_+\{c_+(b_{++}\{\square^1_{b+},\square^4_{b+}\},\square^2_{cs-}\cdot c_-(\square^7_{b-},\square^3_{cs+})\cdot\square^5_{cs-})\cdot\square^6_{cs+}\}$$

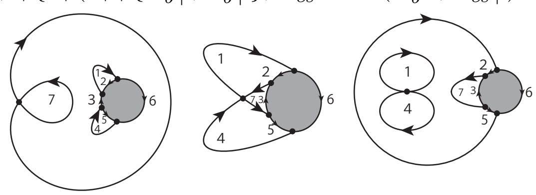

$$\beta_-(c_{(-+-)}):\quad b_{-+}(\beta_-\{c_-(\square^1_{b-},\square^2_{cs+})\cdot\square^3_{cs-}\cdot c_-(\square^4_{b-},\square^5_{cs+})\cdot\square^6_{cs-}\},\square^7_{b+})\to \beta_-\{c_-(b_{--}\{\square^1_{b-},\square^4_{b-}\},\square^2_{cs+}\cdot c_-(\square^7_{b+},\square^3_{cs-})\cdot\square^5_{cs+})\cdot\square^6_{cs-}\}$$

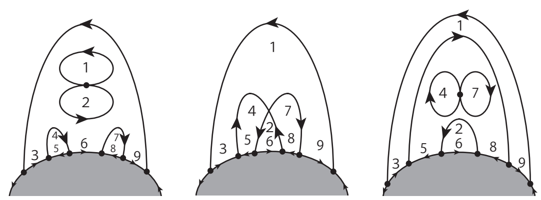

$$c_+(c_{(-+-)}):\quad c_+(b_{++}\{\square^1_{b+},\square^2_{b+}\},\square^9_{cs-}\cdot c_-(\square^7_{b-},\square^8_{cs+})\cdot\square^6_{cs-}\cdot c_-(\square^4_{b-},\square^5_{cs+})\cdot\square^3_{cs-})\to c_+(\square^1_{b+},\square^9_{cs-}\cdot c_-(b_{--}\{\square^4_{b-},\square^7_{b-}\},\square^8_{cs+}\cdot c_+(\square^2_{b+},\square^6_{cs-})\cdot\square^5_{cs+})\cdot\square^3_{cs-})$$

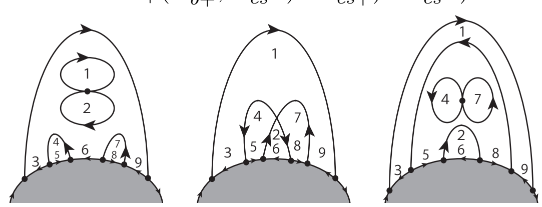

$$c_-(c_{(+-+)}):\quad c_-(b_{--}\{\square^1_{b-},\square^2_{b-}\},\square^9_{cs+}\cdot c_+(\square^7_{b+},\square^8_{cs-})\cdot\square^6_{cs+}\cdot c_+(\square^4_{b+},\square^5_{cs-})\cdot\square^3_{cs+})\to c_-(\square^1_{b-},\square^9_{cs+}\cdot c_+(b_{++}\{\square^4_{b+},\square^7_{b+}\},\square^8_{cs-}\cdot c_-(\square^2_{b-},\square^6_{cs+})\cdot\square^5_{cs-})\cdot\square^3_{cs+})$$

FIGURE 43. Transformation rules for the trees of the bounded structures without self-connected separatrices but with a separatrix connecting a saddle and ∂-saddle in bounded punctured spheres.

5.5.1. *Tree grammar G_2.* We have the tree grammar G_2 on punctured spheres.

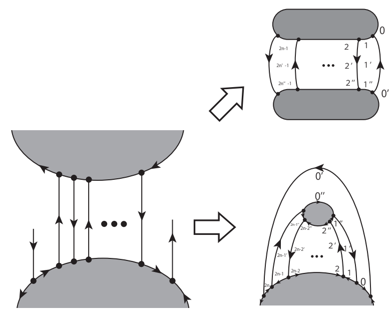

FIGURE 44. Complete list of two structurally unstable structures with heteroclinic counter-clockwise orbits.

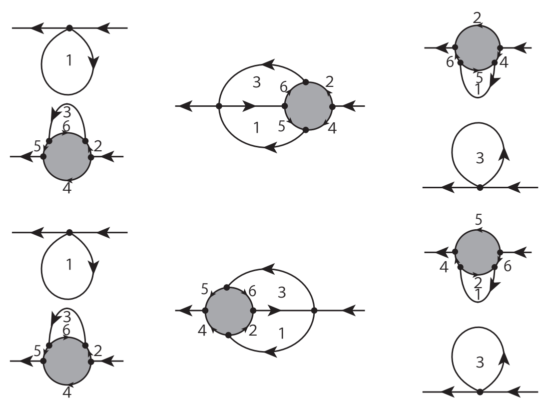

$$a_{2(\mp\pm)}: \quad a_\mp(\square^1_{b\mp}) \cdot a_2(\square^2_{cs\pm} \cdot c_\pm(\square^3_{b\pm}, \square^6_{cs\mp}) \cdot \square^5_{cs\pm}, \square^4_{cs\mp}) \to$$
$$a_2(\square^2_{cs\pm}, \square^6_{cs\mp} \cdot c_\mp(\square^1_{b\mp}, \square^5_{cs\pm})) \cdot \square^4_{cs\mp}) \cdot a_\pm(\square^3_{b\pm})$$

FIGURE 45. Transformation rules for the trees of the unbounded structures without self-connected separatrices but with exactly three separatrices each of which is between a saddle and ∂-saddle in punctured planes.

5.5.2. *Transformation rules.* We specify the complete transformation rules via pinching for flows on a compact punctured sphere. We describe all generic transitions via pinching on a compact punctured sphere. Three orbit structures are shown in each row in Figure 59; the left and right structurally stable orbit structures are converted to each other via the central structurally unstable orbit structure. There are structurally unstable orbit structures in the center, as we counted above. Indeed, the picture shows this assertion.

Lemma 26. *The complete generic transitions of Hamiltonian flows obtained via pinching on a compact punctured sphere are described by the rules* $(\beta_\pm(\Lambda_\pm))$, $(\beta_\pm(\Lambda_\mp))$, $(c_\pm(\Lambda_\pm))$, $(\beta_\pm(c_\pm(c^L_\mp)))$, $(\beta_\pm(c_\pm(c^R_\mp)))$, $(c_\pm(c_\mp(c^R_\pm)))$, $(c_\pm(c_\mp(c^L_\pm)))$, $(c_{\pm\pm})$ *as shown in Figure 59.*

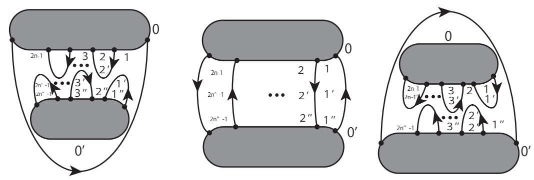

$$
\begin{array}{ll}
\beta_+(c_{+(2n)}): & \beta_+\{\square^0_{cs+} \cdot c_+(\beta_+\{\square^{0'}_{cs+} \cdot c_+(\square^{1'}_{b+}, \square^{1''}_{cs-}) \cdot \square^2_{cs+} \cdot c_+(\square^{3'}_{b+}, \square^{3''}_{cs-}) \cdots\cdot \\
& \cdot c_+(\square^{2n-1'}_{b+}, \square^{2n-1''}_{cs-})\}, \square^{2n-1}_{cs-} \cdot c_-(\square^{2n-2'}_{b-}, \square^2_{cs+}) \cdots\cdot\cdot \square^3_{cs-} \\
& \cdot c_-(\square^{2'}_{b-}, \square^2_{cs+}) \cdot \square^1_{cs-})\} \to \\
& \beta_-\{\square^{2n-1'}_{cs-} \cdot c_-(\beta_-\{\square^0_{cs-} \cdot c_-(\square^{2n-2'}_{b-}, \square^{2n-2}_{cs+}) \cdots\cdot\cdot c_-(\square^{3'}_{b-}, \square^3_{cs+}) \\
& \cdot \square^2_{cs-} \cdot c_-(\square^{1'}_{b-}, \square^1_{cs+})\}, \square^{1''}_{cs+} \cdot c_+(\square^{2'}_{b+}, \square^{2''}_{cs-}) \cdot \square^{3''}_{cs+} \cdots\cdot \\
& \cdot c_+(\square^{2n-2'}_{b+}, \square^{2n-2''}_{cs-}) \cdot \square^{2n-1''}_{cs+})\}
\end{array}
$$

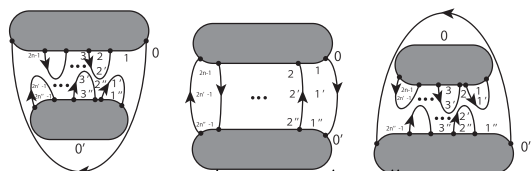

$$
\begin{array}{ll}
\beta_-(c_{-(2n)}): & \beta_-\{\square^0_{cs-} \cdot c_-(\beta_-\{\square^{0'}_{cs-} \cdot c_-(\square^{1'}_{b-}, \square^{1''}_{cs-}) \cdot \square^2_{cs-} \cdot c_-(\square^{3'}_{b-}, \square^{3''}_{cs-}) \cdots\cdot \\
& \cdot c_-(\square^{2n-1'}_{b-}, \square^{2n-1''}_{cs-})\}, \square^{2n-1}_{cs-} \cdot c_+(\square^{2n-2'}_{b+}, \square^2_{cs-}) \cdots\cdot\cdot \square^3_{cs-} \\
& \cdot c_+(\square^{2'}_{b+}, \square^2_{cs-}) \cdot \square^1_{cs-})\} \to \\
& \beta_+\{\square^{2n-1'}_{cs-} \cdot c_+(\beta_+\{\square^0_{cs-} \cdot c_+(\square^{2n-2'}_{b+}, \square^{2n-2}_{cs-}) \cdots\cdot\cdot c_+(\square^{3'}_{b+}, \square^3_{cs-}) \\
& \cdot \square^2_{cs-} \cdot c_+(\square^{1'}_{b+}, \square^1_{cs-})\}, \square^{1''}_{cs-} \cdot c_-(\square^{2'}_{b-}, \square^{2''}_{cs-}) \cdot \square^{3''}_{cs-} \cdots\cdot \\
& \cdot c_-(\square^{2n-2'}_{b-}, \square^{2n-2''}_{cs-}) \cdot \square^{2n-1''}_{cs-})\}
\end{array}
$$

Proof. Figure 58 indicates that there are precisely sixteen structurally unstable structures with heteroclinic counter-clockwise orbits in a compact punctured sphere. Therefore all possible generic transitions of Hamiltonian flows obtained via pinching on a compact punctured sphere are listed in Figure 59. □

5.6. **Pinching contained in punctured planes.**

5.6.1. *Tree grammar G.* We have the tree grammar G on punctured planes.

5.6.2. *Transformation rules.* We specify complete transformation rules via pinching for flows on punctured planes, and describe all corresponding generic transitions with two non-self-connected separatrices from/to boundaries on punctured planes.

Lemma 27. *The complete generic transitions of Hamiltonian flows obtained via pinching on punctured planes are described by the rules* $(\beta_\pm(\Lambda_\pm))$, $(\beta_\pm(\Lambda_\mp))$, $(c_\pm(\Lambda_\pm))$, $(c_{\pm\pm})$, $(\beta_\pm(c_\pm(c^L_\mp)))$, $(\beta_\pm(c_\pm(c^R_\mp)))$, $(c_\pm(c_\mp(c^R_\pm)))$, $(c_\pm(c_\mp(c^L_\pm)))$, $(a_\emptyset(\Lambda_\pm))$, $(a_2(\Lambda_\pm))$, $(a_2(c_\pm(c^R_\mp)))$, $(a_2(c_\pm(c^L_\mp)))$, *and* $(a_2(c^L_\pm))$, $(a_2(c^R_\pm))$, *as shown in Figure 59 and Figure 61.*

Proof. Lemma 26 implies that the complete generic transitions of Hamiltonian flow obtained via pinching on a bounded disk in the punctured plane are described by the rules $(\beta_\pm(\Lambda_\pm))$, $(\beta_\pm(\Lambda_\mp))$, $(c_\pm(\Lambda_\pm))$, $(c_{\pm\pm})$, $(\beta_\pm(c_\pm(c^L_\mp)))$, $(\beta_\pm(c_\pm(c^R_\mp)))$, $(c_\pm(c_\mp(c^R_\pm)))$, $(c_\pm(c_\mp(c^L_\pm)))$. Figure 60 indicates that there are exactly twelve transitions as shown in Figure 61. □

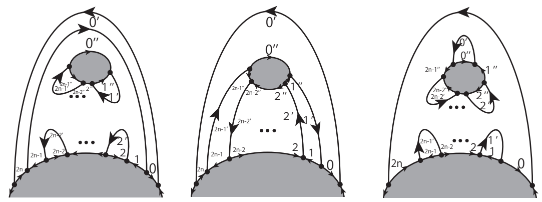

$$
\begin{aligned}
c_+(c_{-(2n)}) :\ & c_+(\square^{0'}_{b+}, \square^{0}_{cs-} \cdot c_-(\beta_-\{c_-(\square^{2n-1'}_{b-}, \square^{2n-1''}_{cs+}) \cdot \square^{2n-2''}_{cs-} \cdot \cdots \\
& \cdot \square^{2''}_{cs-} \cdot c_-(\square^{1'}_{b-}, \square^{1''}_{cs+}) \cdot \square^{0''}_{cs-}\}, \square^{1}_{cs+} \cdot c_+(\square^{2\prime}_{b+}, \square^{2}_{cs-}) \cdot \cdots \\
& \cdot c_+(\square^{2n-2'}_{b+}, \square^{2n-2}_{cs-}) \cdot \square^{2n-1}_{cs+}) \cdot \square^{2n}_{cs-}) \to \\
& c_+(\beta_+\{c_+(\square^{0\prime}_{b+}, \square^{0''}_{cs-}) \cdot \square^{2n-1''}_{cs+} \cdot c_+(\square^{2n-2'}_{b+}, \square^{2n-2''}_{cs-}) \cdot \cdots \\
& \cdot c_+(\square^{2'}_{b+}, \square^{2''}_{cs-}) \cdot \square^{1''}_{cs+}\}, \square^{0}_{cs-} \cdot c_-(\square^{1'}_{b-}, \square^{1}_{cs+}) \cdot \square^{2}_{cs-} \cdot \cdots \\
& \cdot \square^{2n-2}_{cs-} \cdot c_-(\square^{2n-1'}_{b-}, \square^{2n-1}_{cs+}) \cdot \square^{2n}_{cs-})
\end{aligned}
$$

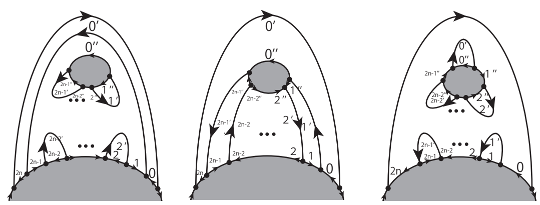

$$
\begin{aligned}
c_-(c_{+(2n)}) :\ & c_-(\square^{0'}_{b-}, \square^{0}_{cs+} \cdot c_+(\beta_+\{c_+(\square^{2n-1'}_{b+}, \square^{2n-1''}_{cs-}) \cdot \square^{2n-2''}_{cs+} \cdot \cdots \cdot \square^{2''}_{cs+} \\
& \cdot c_+(\square^{1'}_{b+}, \square^{1''}_{cs-}) \cdot \square^{0''}_{cs+}\}, \square^{1}_{cs-} \cdot c_-(\square^{2\prime}_{b-}, \square^{2}_{cs+}) \cdot \cdots \\
& \cdot c_-(\square^{2n-2'}_{b-}, \square^{2n-2}_{cs+}) \cdot \square^{2n-1}_{cs-}) \cdot \square^{2n}_{cs+}) \\
& \to c_-(\beta_-\{c_-(\square^{0\prime}_{b-}, \square^{0''}_{cs+}) \cdot \square^{2n-1''}_{cs-} \cdot c_-(\square^{2n-2'}_{b-}, \square^{2n-2''}_{cs+}) \cdot \cdots \\
& \cdot c_-(\square^{2'}_{b-}, \square^{2''}_{cs+}) \cdot \square^{1''}_{cs-}\}, \square^{0}_{cs+} \cdot c_+(\square^{1'}_{b+}, \square^{1}_{cs-}) \cdot \square^{2}_{cs+} \cdot \cdots \\
& \cdot \square^{2n-2}_{cs+} \cdot c_+(\square^{2n-1'}_{b+}, \square^{2n-1}_{cs-}) \cdot \square^{2n}_{cs+})
\end{aligned}
$$

FIGURE 46. Transformation rules for the trees of the bounded structures with non-self-connected separatrices between different boundary components in punctured surfaces.

5.7. **Correspondence between generic transitions of COT representations of Hamiltonian flows and those of Reeb graphs of Hamiltonians.** All transition rules of Hamiltonian flows can be interpreted into transition rules between Reeb graphs of Morse functions on surfaces. For instance, the rule $b_{\pm\pm(\mp)}$: $b_{++}\{\square^1_{b+}, b_{+-}(\square^2_{b+}, \square^3_{b-})\} \to b_{+-}(b_{++}\{\square^1_{b+}, \square^2_{b+}\}, \square^3_{b-})$ is shown in Figure 62.

5.8. **Complete generic transition rules between compact surfaces and unbounded punctured surfaces.** As mentioned above, since small perturbations are local operations, the existence of Hamiltonians implies that complete generic transition rules for Hamiltonian flows on compact surfaces (resp. unbounded punctured surface) are those on compact punctured spheres (resp. punctured planes).

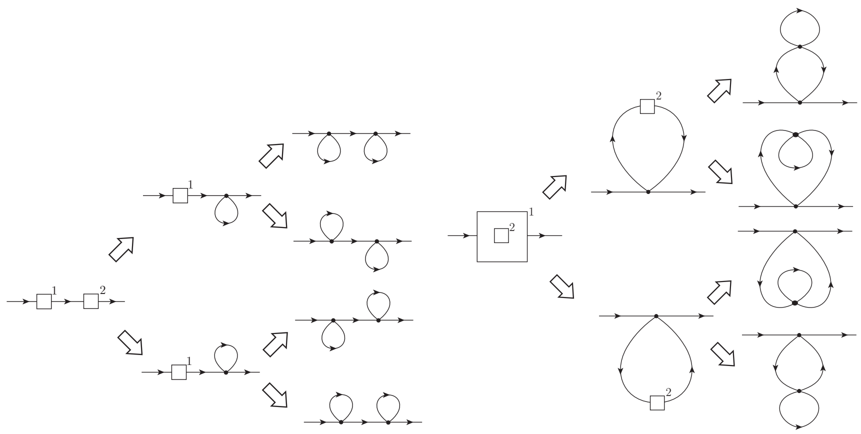

FIGURE 47. Complete list of eight unstable structures in a plane in addition to the ten unstable structures shown in Figure 33 and their inverses.

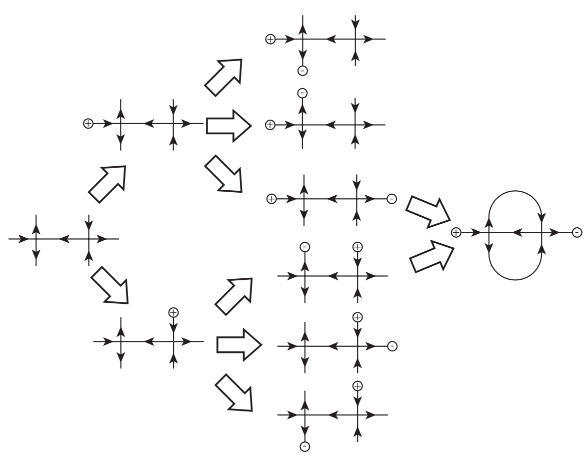

FIGURE 48. Complete list of one structurally unstable structures with a separatrix connecting saddles but without self-connected separatrices in punctured planes.

Corollary 28. *The complete generic transition rules of Hamiltonian flows on compact surfaces are shown after the Theorem 21.*

6. Applications to Reeb graphs of Morse functions on orientable compact surfaces

In this section, we interpret results for Hamiltonian flows on orientable compact surfaces to those for Morse functions.

6.1. **Notion of Morse functions.**

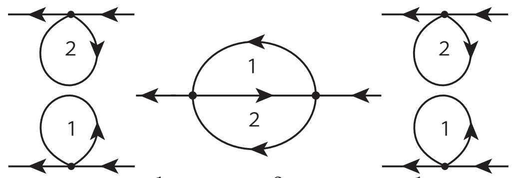

$$a_{(+-)}, a_{(-+)} : \ a_-(\square^1_{b-}) \cdot a_+(\square^2_{b+}) \to a_-(\square^1_{b-}) \cdot a_+(\square^2_{b+})$$

FIGURE 49. Transformation rules for the trees of unbounded structures without self-connected separatrices in planes.

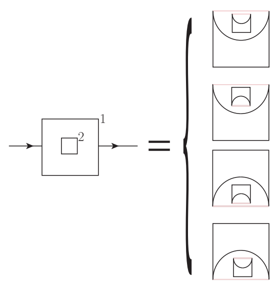

(a)

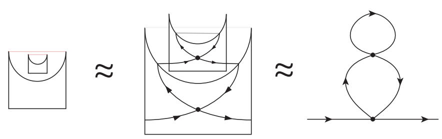

(b)

FIGURE 50. (a) Nested holes; (b) an example of nested holes.

6.1.1. *Reeb graph of a function.* For a function $f\colon X \to \mathbb{R}$ on a topological space X, the Reeb graph of f is the quotient space $X/\sim_f$, where the equivalence relation $\sim$ is defined by $x \sim_f y$ if there are a point $c \in \mathbb{R}$ and connected component of $f^{-1}(c)$ which contains x and y. The inverse image of $f^{-1}(c)$ is called the level set of level c.

6.1.2. *Hamiltonian flows on closed surfaces.* For a C^r $(r \geq 2)$ function $f\colon S \to \mathbb{R}$ on a surface S, denote by v_f the Hamiltonian flow defined by the Hamiltonian f.

6.1.3. *Morse function on a surface.* Recall that a C^r $(r \geq 2)$ function $f\colon S \to \mathbb{R}$ on a surface S is Morse if each critical point is non-degenerate (i.e., a saddle with index 0, 1, or 2). The union of connected components containing critical points of level sets of the function f is called the saddle connection diagram of f and is denoted by $D(f)$. Similarly, a connected component of the saddle connection diagram is called a saddle connection. An injective path in a saddle connection is separatrix if it connects critical points and contains no critical point in the interior of the path. The saddle connection diagram contains heteroclinic separatrices if there is a separatrix, called a heteroclinic separatrix, between distinct critical points in the diagram. For a Morse function $f\colon S \to \mathbb{R}$, we equip the Reeb graph $X/\sim_f$ with the

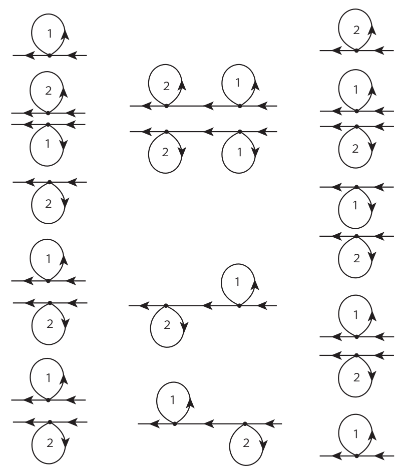

$$a_{\pm\pm}, a_{\pm\mp}: \ \square_a^1 \cdot \square_a^2 \ \to \ \square_a^2 \cdot \square_a^1$$

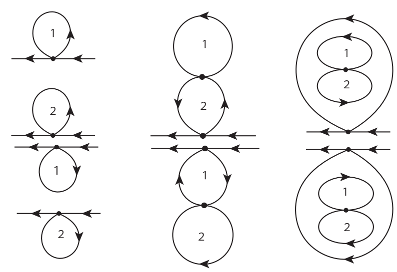

$$a_{\pm(\pm)}: \ a_\pm(\square_{b\pm}^1) \cdot a_\pm(\square_{b\pm}^2) \ \to \ a_\pm(b_{\pm\pm}\{\square_{b\pm}^1, \square_{b\pm}^2\})$$

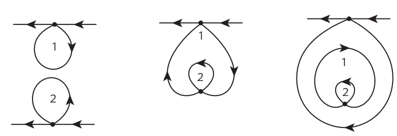

$$a_{-(+)}: \ a_-(\square_{b-}^1) \cdot a_+(\square_{b+}^2) \ \to \ a_-(b_{-+}(\square_{b-}^1, \square_{b+}^2))$$

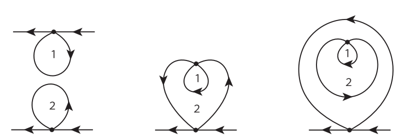

$$a_{+(-)}: \ a_-(\square_{b-}^1) \cdot a_+(\square_{b+}^2) \ \to \ a_+(b_{+-}(\square_{b+}^2, \square_{b-}^1))$$

FIGURE 51. Transformation rules for the trees of the outermost $a_\pm$ structures in planes.

directed graph structures induced by the direction of $\mathbb{R}$. In other words, the Reeb graph of a Morse function is a topological space and a directed graph. Reeb graphs are isomorphic if there is a homeomorphism preserving directed graph structures. A Morse function $f\colon S \to \mathbb{R}$ is simple if the inverse image $f^{-1}(c)$ for any $c \in \mathbb{R}$ contains at most one critical point. It should be noted that the Hamiltonian flow

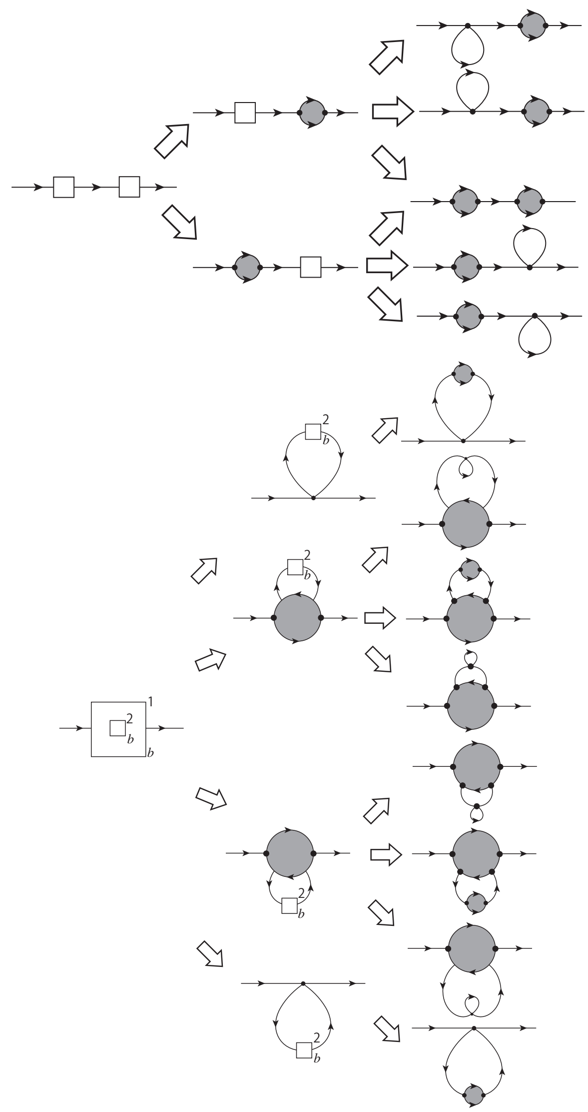

FIGURE 52. Complete list of fourteen structurally unstable structures with heteroclinic counter-clockwise orbits in punctured planes.

generated by a simple Morse function on an orientable closed surface is structurally stable in the set of Hamiltonian flow on the closed surface. Denote by $\mathcal{M}_g$ the set of C^r $(r \geq 2)$ Morse functions on a connected orientble closed surface of genus g equipped with the Whitney C^s topology for some integer $s \in [0, r]$. Denote by $\mathcal{M}$ the disjoint union $\bigsqcup_{g \in \mathbb{Z}_{\geq 0}} \mathcal{M}_g$. For any non-negative numbers $s_0, s_1, s_2 \in \mathbb{Z}_{\geq 0}$ with $s_0 - s_1 + s_2 = 2 - 2g$, denote by $\mathcal{M}(s_0, s_1, s_2)$ the connected component of $\mathcal{M}$ whose elements have s_i saddles with index i for any $i = 0, 1, 2$. Then $\mathcal{M} = \bigsqcup \mathcal{M}(s_0, s_1, s_2)$.

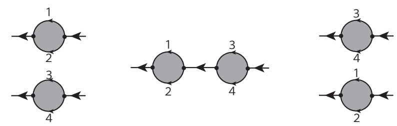

$$a_{22}:\ a_2(\square^1_{cs+},\square^2_{cs-})\cdot a_2(\square^3_{cs+},\square^4_{cs-})\to a_2(\square^3_{cs+},\square^4_{cs-})\cdot a_2(\square^1_{cs+},\square^2_{cs-})$$

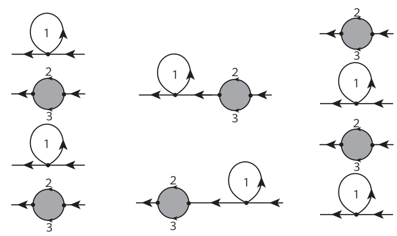

$$a_{+2},a_{2+}:a_+(\square^1_{b+})\cdot a_2(\square^2_{cs+},\square^3_{cs-})\to a_2(\square^2_{cs+},\square^3_{cs-})\cdot a_+(\square^1_{b+})$$

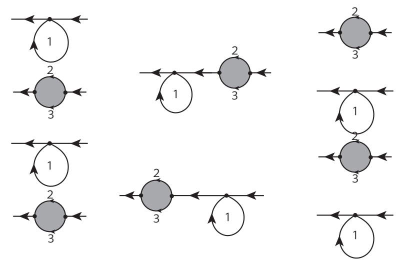

$$a_{-2},a_{2-}:a_-(\square^1_{b-})\cdot a_2(\square^2_{cs+},\square^3_{cs-})\to a_2(\square^2_{cs+},\square^3_{cs-})\cdot a_-(\square^1_{b-})$$

FIGURE 53. Transformation rules for the trees of the outermost a_2 structures in punctured planes ($\square^1_a\cdot\square^2_a \ \to\ \square^2_a\cdot\square^1_a$).

The Reeb graph of a function f is C^r ($r\geq 0$) structurally stable if there is a C^r-neighborhood $\mathcal{U}$ of f such that the Reeb graph of any function in $\mathcal{U}$ is isomorphic to the Reeb graph of f.

6.2. **Interpretations of 2D Hamiltonian flows into 2D Morse functions.** Non-degeneracy implies the following observation.

Lemma 29. *For a connected component $\mathcal{C}$ of $\mathcal{M}_g$, there are non-negative numbers $s_0,s_1,s_2\in\mathbb{Z}_{\geq 0}$ with $s_0-s_1+s_2=2-2g$ such that any function in $\mathcal{C}$ has s_i saddles with index i for any $i=0,1,2$. Moreover, any connected component of $\mathcal{M}$ is open.*

Proof. Let Σ_g be a closed surface of genus g. Since Euler characteristic of Σ_g is $2-2g$, the Morse theory states that $s_0,s_1,s_2\in\mathbb{Z}_{\geq 0}$. Non-degeneracy implies that each critical point is non-degenerate and is, therefore, preserved by any small perturbations. This means that the numbers of saddles with index i are constant on $\mathcal{C}$. Therefore any connected components of $\mathcal{M}_g$ are open and so are those of $\mathcal{M}$. $\square$

Morse theory and Lemma 6 imply the following observation.

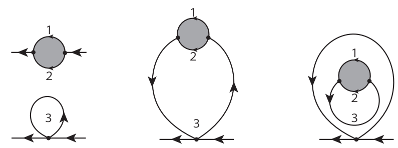

$$a_{+(2)}:\ a_2(\Box^1_{cs+}, \Box^2_{cs-}) \cdot a_+(\Box^3_{b+}) \to a_+(\beta_+\{\Box^1_{cs+} \cdot c_+(\Box^3_{b+}, \Box^2_{cs-})\})$$

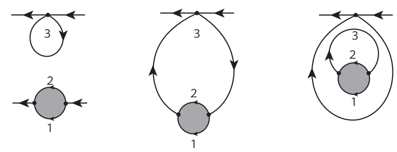

$$a_{-(2)}:\ a_-(\Box^1_{b-}) \cdot a_2(\Box^2_{cs+}, \Box^3_{cs-}) \to a_-(\beta_-\{c_-(\Box^1_{b-}, \Box^2_{cs+}) \cdot \Box^3_{cs-}\})$$

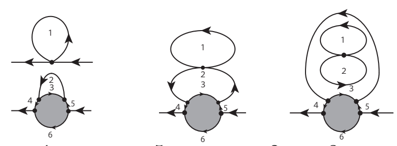

$$\begin{aligned} a_2(c_{+(+)}):\ & a_+(\Box^1_{b+}) \cdot a_2(\Box^5_{cs+} \cdot c_+(\Box^2_{b+}, \Box^3_{cs-}) \cdot \Box^4_{cs+}, \Box^6_{cs-}) \to \\ & a_2(\Box^5_{cs+} \cdot c_+(b_{++}\{\Box^1_{b+}, \Box^2_{b+}\}, \Box^3_{cs-}) \cdot \Box^4_{cs+}, \Box^6_{cs-}) \end{aligned}$$

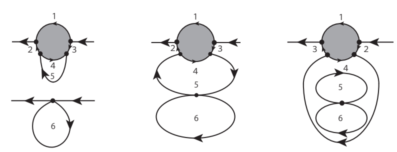

$$\begin{aligned} a_2(c_{-(-)}):\ & a_2(\Box^1_{cs+}, \Box^2_{cs-} \cdot c_-(\Box^5_{b-}, \Box^4_{cs+}) \cdot \Box^3_{cs-}) \cdot a_-(\Box^6_{b-}) \to \\ & a_2(\Box^1_{cs+}, \Box^2_{cs-} \cdot c_-(b_{--}\{\Box^5_{b-}, \Box^6_{b-}\}, \Box^4_{cs+}) \cdot \Box^3_{cs-}) \end{aligned}$$

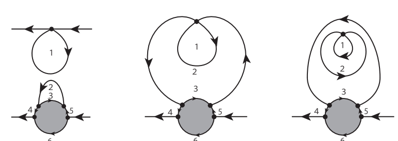

$$\begin{aligned} a_2(c_{+(-)}):\ & a_-(\Box^1_{b-}) \cdot a_2(\Box^5_{cs+} \cdot c_+(\Box^2_{b+}, \Box^3_{cs-}) \cdot \Box^4_{cs+}, \Box^6_{cs-}) \to \\ & a_2(\Box^5_{cs+} \cdot c_+(b_{+-}(\Box^2_{b+}, \Box^1_{b-}), \Box^3_{cs-}) \cdot \Box^4_{cs+}, \Box^6_{cs-}) \end{aligned}$$

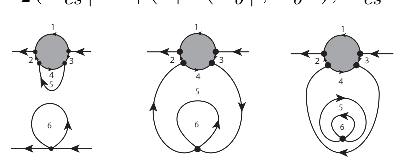

$$\begin{aligned} a_2(c_{-(+)}):\ & a_2(\Box^1_{cs+}, \Box^2_{cs-} \cdot c_-(\Box^5_{b-}, \Box^4_{cs+}) \cdot \Box^3_{cs-}) \cdot a_+(\Box^6_{b+}) \to \\ & a_2(\Box^1_{cs+}, \Box^2_{cs-} \cdot c_-(b_{-+}(\Box^5_{b-}, \Box^6_{b+}), \Box^4_{cs+}) \cdot \Box^3_{cs-}) \end{aligned}$$

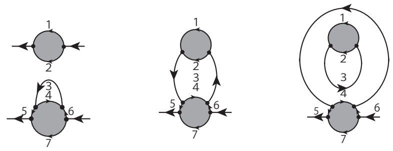

$$\begin{aligned} a_2(c_{+(2)}):\ & a_2(\Box^1_{cs+}, \Box^2_{cs-}) \cdot a_2(\Box^6_{cs+} \cdot c_+(\Box^3_{b+}, \Box^4_{cs-}) \cdot \Box^5_{cs+}, \Box^7_{cs-}) \to \\ & a_2(\Box^6_{cs+} \cdot c_+(\beta_+\{\Box^1_{cs+} \cdot c_+(\Box^3_{b+}, \Box^2_{cs-})\}, \Box^4_{cs-}) \cdot \Box^5_{cs+}, \Box^7_{cs-}) \end{aligned}$$

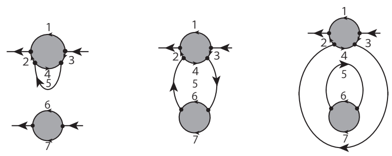

$$\begin{aligned} a_2(c_{-(2)}):\ & a_2(\Box^1_{cs+}, \Box^2_{cs-} \cdot c_-(\Box^5_{b-}, \Box^4_{cs-}) \cdot \Box^3_{cs-}) \cdot a_2(\Box^6_{cs+}, \Box^7_{cs-}) \to \\ & a_2(\Box^1_{cs+}, \Box^2_{cs-} \cdot c_-(\beta_-\{c_-(\Box^5_{b-}, \Box^6_{cs+}) \cdot \Box^7_{cs-}\}, \Box^4_{cs-}) \cdot \Box^3_{cs-}) \end{aligned}$$

Figure 54. Transformation rules for the trees of the outermost a_2 structures in punctured planes.

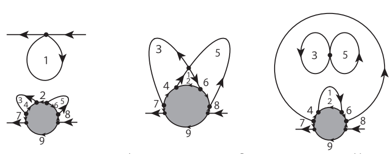

$$\begin{aligned} a_2(c_{(+-+)}):\ & a_-(\Box^1_{b-}) \cdot a_2(\Box^8_{cs+} \cdot c_+(\Box^5_{b+}, \Box^6_{cs-}) \\ & \cdot \Box^2_{cs+} \cdot c_+(\Box^3_{b+}, \Box^4_{cs-}) \cdot \Box^7_{cs+}, \Box^9_{cs-}) \to \\ & a_2(\Box^8_{cs+} \cdot c_+(b_{++}\{\Box^3_{b+}, \Box^5_{b+}\}, \Box^6_{cs-} \cdot \\ & c_-(\Box^1_{b-}, \Box^2_{cs+}) \cdot \Box^4_{cs-}) \cdot \Box^7_{cs+}, \Box^9_{cs-}) \end{aligned}$$

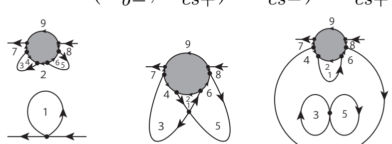

$$\begin{aligned} a_2(c_{(-+-)}):\ & a_2(\Box^9_{cs+}, \Box^7_{cs-} \cdot c_-(\Box^3_{b-}, \Box^4_{cs+}) \cdot \Box^2_{cs-} \\ & \cdot c_-(\Box^5_{b-}, \Box^6_{cs+}) \cdot \Box^8_{cs-}) \cdot a_+(\Box^1_{b+}) \to \\ & a_2(\Box^9_{cs+}, \Box^7_{cs-} \cdot c_-(b_{--}\{\Box^3_{b-}, \Box^5_{b-}\}, \\ & \Box^4_{cs+} \cdot c_+(\Box^1_{b+}, \Box^2_{cs-}) \cdot \Box^6_{cs+}) \cdot \Box^8_{cs-}) \end{aligned}$$

Figure 55. Transformation rules for the trees of the unbounded structures without self-connected separatrices but with exactly four separatrices each of which is between a saddle and ∂-saddle in punctured planes.

Lemma 30. *If the Hamiltonian flows of Hamiltonians f and h on an orientable compact surface S are topologically equivalent, then the Reeb graphs $S/\sim_f$ and $S/\sim_h$ are isomorphic.*

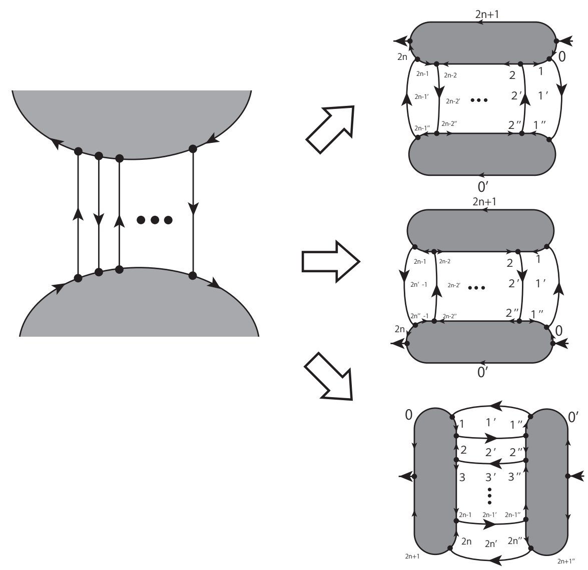

FIGURE 56. Complete list of fourteen structurally unstable structures with heteroclinic counter-clockwise orbits in punctured planes.

The converse does not hold because Reeb graphs entail no information on saddle connections. Moreover, Morse theory and Lemma 6 and Lemma 5 imply the following observation.

Lemma 31. *The following statements are equivalent for any functions $f, h \in \mathcal{M}_g$ whose Hamiltonian flows are structurally stable:*
(1) *The Reeb graphs $\Sigma_g/\sim_f$ and $\Sigma_g/\sim_h$ are isomorphic.*
(2) *The Hamiltonian flows v_f and v_h are topologically equivalent.*

The previous lemma implies the following statement.

Corollary 32. *The following statements are equivalent for any simple Morse functions f, h on an orientable closed surface Σ:*
(1) *The Reeb graphs $\Sigma/\sim_f$ and $\Sigma/\sim_h$ are isomorphic.*
(2) *The Hamiltonian flows v_f and v_h are topologically equivalent.*

Lemma 31 implies that following interpretation.

Lemma 33. *The following statements are equivalent for any function $f \in \mathcal{M}$:*
(1) $f \in \mathcal{M}(s_0, s_1, s_2)$.
(2) $v_f \in \mathcal{H}_{\mathrm{bd}}(s_0+s_2)$ *has exactly s_0 centers with counter-clockwise rotating direction and s_2 centers with clockwise rotating direction.*

Morse theory implies an analogy of Lemma 5 as follows.

Lemma 34. *The following statements are equivalent for any function $f \in \mathcal{M}_g$:*
(1) *The Reeb graph $\Sigma_g/\sim_f$ is C^0 structurally stable.*
(2) *The saddle connection diagram $D(f)$ contains no heteroclinic separatrices.*

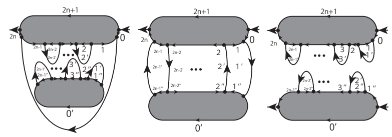

$$\begin{aligned}
a_2(c_{-(2n)}) : {} & a_2(\square^{2n+1}_{cs+}, \square^{2n}_{cs-} \cdot c_-(\beta_-\{\square^{0'}_{cs-} \cdot c_-(\square^{1'}_{b-}, \square^{1''}_{cs+}) \cdot \square^{2''}_{cs-} \\
& \cdot c_-(\square^{3'}_{b-}, \square^{3''}_{cs+}) \cdot \cdots \cdot c_-(\square^{2n-1'}_{b-}, \square^{2n-1''}_{cs+})\}, \square^{2n-1}_{cs+} \\
& \cdot c_+(\square^{2n-2'}_{b+}, \square^{2n-2}_{cs-}) \cdot \cdots \cdot c_+(\square^{2'}_{b+}, \square^{2}_{cs-}) \cdot \square^{1}_{cs+}) \cdot \square^{0}_{cs-}) \to \\
& a_2(\square^{2n+1}_{cs+}, \square^{2n}_{cs-} \cdot c_-(\square^{2n-1'}_{b-}, \square^{2n-1}_{cs+}) \cdot \cdots \cdot c_-(\square^{3'}_{b-}, \square^{3}_{cs+}) \cdot \square^{2}_{cs-} \\
& \cdot c_-(\square^{1'}_{b-}, \square^{1}_{cs+}) \cdot \square^{0}_{cs-}) \cdot a_2(\square^{1''}_{cs+} \cdot c_+(\square^{2'}_{b+}, \square^{2''}_{cs-}) \cdot \square^{3''}_{cs+} \cdot \cdots \\
& \cdot c_+(\square^{2n-2'}_{b+}, \square^{2n-2''}_{cs-}) \cdot \square^{2n-1''}_{cs+}, \square^{0'}_{cs-})
\end{aligned}$$

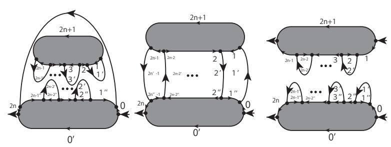

$$\begin{aligned}
a_2(c_{+(2n)}) : {} & a_2(\square^{0}_{cs+} \cdot c_+(\beta_+\{\square^{2n+1}_{cs+} \cdot c_+(\square^{2n-1'}_{b+}, \square^{2n-1}_{cs-}) \cdot \cdots \cdot c_+(\square^{3'}_{b+}, \square^{3}_{cs-}) \\
& \cdot \square^{2}_{cs+} \cdot c_+(\square^{1'}_{b+}, \square^{1}_{cs-})\}, \square^{1''}_{cs-} \cdot c_-(\square^{2'}_{b-}, \square^{2''}_{cs+}) \cdot \cdots \\
& \cdot c_-(\square^{2n-2'}_{b-}, \square^{2n-2''}_{cs+}) \cdot \square^{2n-1''}_{cs-}) \cdot \square^{2n}_{cs+}, \square^{0'}_{cs-}) \to \\
& a_2(\square^{2n+1}_{cs+}, \square^{2n-1}_{cs-} \cdot c_-(\square^{2n-2'}_{b-}, \square^{2n-2}_{cs+}) \cdot \cdots \cdot \square^{3}_{cs-} \cdot c_-(\square^{2'}_{b-}, \square^{2}_{cs+}) \cdot \square^{1}_{cs-}) \\
& \cdot a_2(\square^{0}_{cs+} \cdot c_+(\square^{1'}_{b+}, \square^{1''}_{cs-}) \cdot \square^{2''}_{cs+} \cdot c_+(\square^{3'}_{b+}, \square^{3''}_{cs-}) \cdot \cdots \cdot \square^{2n-2''}_{cs+} \cdot \\
& c_+(\square^{2n-1'}_{b+}, \square^{2n-1''}_{cs-}) \cdot \square^{2n''}_{cs+}, \square^{0'}_{cs-})
\end{aligned}$$

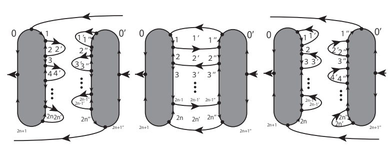

$$\begin{aligned}
a_{2n2} : {} & a_2(\square^{0}_{cs+}, \square^{2n+1}_{cs-} \cdot c_-(\square^{2n'}_{b-}, \square^{2n}_{cs+}) \cdot \cdots \cdot c_-(\square^{4'}_{b-}, \square^{4}_{cs+}) \cdot \square^{3}_{cs-} \\
& \cdot c_-(\square^{2'}_{b-}, \square^{2}_{cs+}) \cdot \square^{1}_{cs-}) \cdot a_2(\square^{0'}_{cs+} \cdot c_+(\square^{1'}_{b+}, \square^{1''}_{cs-}) \cdot \square^{2''}_{cs+} \cdot c_+(\square^{3'}_{b+}, \square^{3''}_{cs-}) \cdot \\
& \cdots \cdot c_+(\square^{2n-1'}_{b+}, \square^{2n-1''}_{cs-}) \cdot \square^{2n''}_{cs+}, \square^{2n+1''}_{cs-}) \to \\
& a_2(\square^{0'}_{cs+}, \square^{1''}_{cs-} \cdot c_-(\square^{2'}_{b-}, \square^{2''}_{cs+}) \cdot \square^{3''}_{cs-} \cdot c_-(\square^{4'}_{b-}, \square^{4''}_{cs+}) \cdot \cdots \\
& \cdot c_-(\square^{2n'}_{b-}, \square^{2n''}_{cs+}) \cdot \square^{2n+1''}_{cs-}) \cdot a_2(\square^{2n}_{cs+} \cdot c_+(\square^{2n-1'}_{b+}, \square^{2n-1}_{cs-}) \cdot \cdots \\
& \cdot c_+(\square^{3'}_{b+}, \square^{3}_{cs-}) \cdot \square^{2}_{cs+} \cdot c_+(\square^{1'}_{b+}, \square^{1}_{cs-}) \cdot \square^{0}_{cs+}, \square^{2n+1}_{cs-})
\end{aligned}$$

FIGURE 57. Complete list of three kinds of structurally unstable unbounded structures with heteroclinic orbits between different boundary components in punctured planes.

Proof. If $D(f)$ contains heteroclinic separatrices, then arbitrarily small perturbations can break heteroclinic separatrices by changing the critical values into different

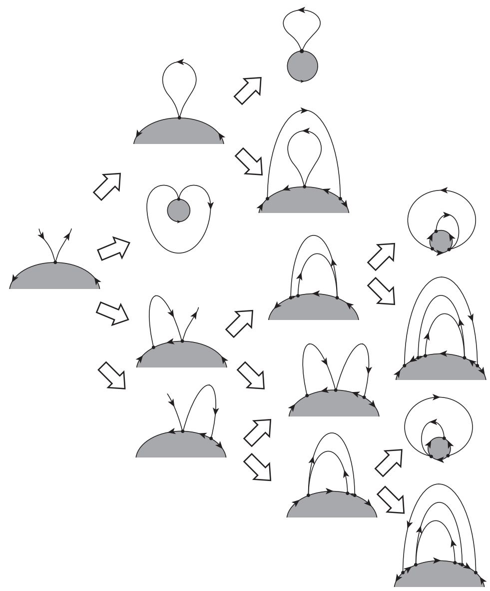

FIGURE 58. Complete list of sixteen structurally unstable structures with heteroclinic counter-clockwise orbits in compact punctured spheres.

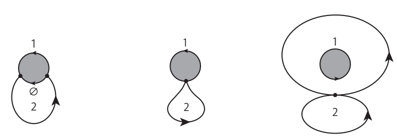

$$\beta_+(\Lambda_+): \ \beta_+\{\square^1_{cs+}\cdot c_+(\square^2_{b+},\lambda)\} \to b_{++}\{\beta_+\{\square^1_{cs+}\},\square^2_{b+}\}$$

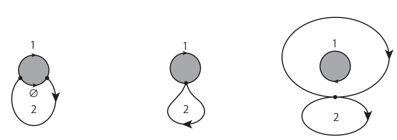

$$\beta_-(\Lambda_-): \ \beta_-\{\square^1_{cs-}\cdot c_-(\square^2_{b-},\lambda)\} \to b_{--}\{\beta_-\{\square^1_{cs+}\},\square^2_{b-}\}$$

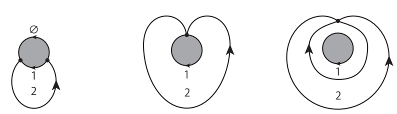

$$\beta_+(\Lambda_-): \ \beta_+\{c_+(\square^2_{b+},\square^1_{cs-})\} \to b_{+-}(\square^2_{b+},\square^1_{cs-})$$

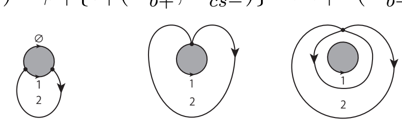

$$\beta_-(\Lambda_+): \ \beta_-\{c_-(\square^2_{b-},\square^1_{cs+})\} \to b_{-+}(\square^2_{b-},\square^1_{cs+})$$

values. This means that the assertion (1) implies the assertion (2). Suppose that

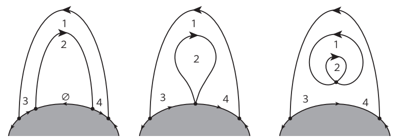

$$c_+(\Lambda_+):\ c_+(\square^1_{b+}, \square^4_{cs-}\cdot c_-(\square^2_{b-},\lambda)\cdot \square^3_{cs-}) \to c_+(b_{+-}(\square^1_{b+},\square^2_{b-}), \square^4_{cs-}\cdot\square^3_{cs-})$$

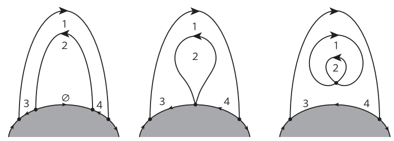

$$c_-(\Lambda_-):\ c_-(\square^1_{b-}, \square^4_{cs+}\cdot c_+(\square^2_{b+},\lambda)\cdot \square^3_{cs+}) \to c_-(b_{-+}(\square^1_{b-},\square^2_{b+}), \square^4_{cs+}\cdot\square^3_{cs+})$$

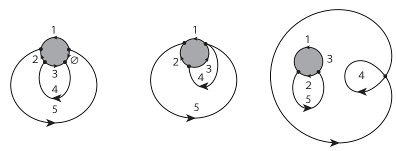

$$\begin{aligned}\beta_+(c_+(c^L_-)):\ &\beta_+\{\square^1_{cs+}\cdot c_+(\square^5_{b+},\square^2_{cs-}\cdot c_-(\square^4_{b-},\square^3_{cs+}))\} \to\\ &b_{+-}(\beta_+\{\square^1_{cs+}\cdot c_+(\square^5_{b+},\square^2_{cs-})\cdot\square^3_{cs+}\},\square^4_{b-})\end{aligned}$$

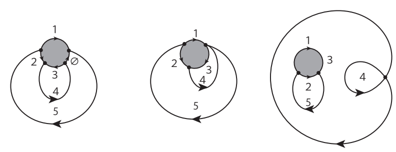

$$\begin{aligned}\beta_-(c_-(c^L_+)):\ &\beta_-\{\square^1_{cs-}\cdot c_-(\square^5_{b-},\square^2_{cs+}\cdot c_+(\square^4_{b+},\square^3_{cs-}))\} \to\\ &b_{-+}(\beta_-\{\square^1_{cs-}\cdot c_-(\square^5_{b-},\square^2_{cs+})\cdot\square^3_{cs-}\},\square^4_{b+})\end{aligned}$$

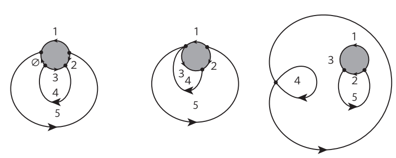

$$\begin{aligned}\beta_+(c_+(c^R_-)):\ &\beta_+\{\square^1_{cs+}\cdot c_+(\square^5_{b+},c_-(\square^4_{b-},\square^3_{cs+})\cdot\square^2_{cs-})\} \to\\ &b_{+-}(\beta_+\{\square^1_{cs+}\cdot\square^3_{cs+}\cdot c_+(\square^5_{b+},\square^2_{cs-})\},\square^4_{b-})\end{aligned}$$

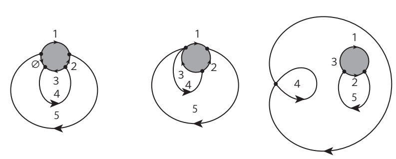

$$\begin{aligned}\beta_-(c_-(c^R_+)):\ &\beta_-\{\square^1_{cs-}\cdot c_-(\square^5_{b-},c_+(\square^4_{b+},\square^3_{cs-})\cdot\square^2_{cs+})\} \to\\ &b_{-+}(\beta_-\{\square^1_{cs-}\cdot\square^3_{cs-}\cdot c_-(\square^5_{b-},\square^2_{cs+})\},\square^4_{b+})\end{aligned}$$

$D(f)$ contains no heteroclinic separatrices. Because there are neither creations of critical points nor annihilations of critical points, the isomorphic classes of Reeb

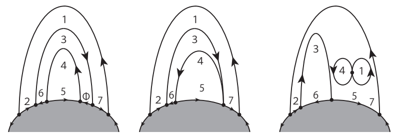

$$c_+(c_-(c_+^R)) : \; c_+(\square^1_{b+}, \square^7_{cs-} \cdot c_-(\square^3_{cs-}, c_+(\square^4_{b+}, \square^5_{cs-}) \cdot \square^6_{cs+}) \cdot \square^2_{cs-}) \to$$
$$c_+(b_{++}\{\square^1_{b+}, \square^4_{b+}\}, \square^7_{cs-} \cdot \square^5_{cs-} \cdot c_-(\square^3_{b-}, \square^6_{cs+}) \cdot \square^2_{cs-})$$

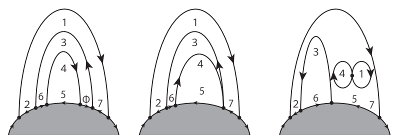

$$c_-(c_+(c_-^R)) : \; c_-(\square^1_{b-}, \square^7_{cs+} \cdot c_+(\square^3_{cs+}, c_-(\square^4_{b-}, \square^5_{cs+}) \cdot \square^6_{cs-}) \cdot \square^2_{cs+}) \to$$
$$c_-(b_{--}\{\square^1_{b-}, \square^4_{b-}\}, \square^7_{cs+} \cdot \square^5_{cs+} \cdot c_+(\square^3_{b+}, \square^6_{cs-}) \cdot \square^2_{cs+})$$

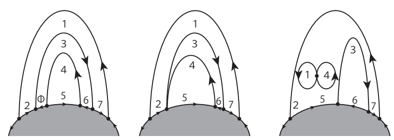

$$c_+(c_-(c_+^L)) : \; c_+(\square^1_{b+}, \square^7_{cs-} \cdot c_-(\square^3_{cs-}, \square^6_{cs+} \cdot c_+(\square^4_{b+}, \square^5_{cs-})) \cdot \square^2_{cs-}) \to$$
$$c_+(b_{++}\{\square^4_{b+}, \square^1_{b+}\}, \square^7_{cs-} \cdot c_-(\square^3_{b-}, \square^6_{cs+}) \cdot \square^5_{cs-} \cdot \square^2_{cs-})$$

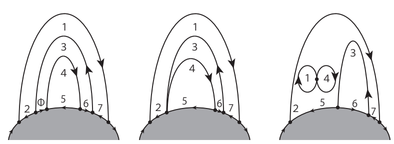

$$c_-(c_+(c_-^L)) : \; c_-(\square^1_{b-}, \square^7_{cs+} \cdot c_+(\square^3_{cs+}, \square^6_{cs-} \cdot c_-(\square^4_{b-}, \square^5_{cs+})) \cdot \square^2_{cs+}) \to$$
$$c_-(b_{--}\{\square^4_{b-}, \square^1_{b-}\}, \square^7_{cs+} \cdot c_+(\square^3_{b+}, \square^6_{cs-}) \cdot \square^5_{cs+} \cdot \square^2_{cs+})$$

graphs of Morse functions can be transformed by h-unstable transitions. The complement of the union of connected components containing critical values of level sets are the finite union of annuli $\mathbb{A}_i$ consisting of circles, each of which is a connected component of a level set. Then consider circle γ_i in such annuli $\mathbb{A}_i$ whose values of the Hamiltonian are the means $V_i/2 = (\max\{H(x) \mid x \in \partial\mathbb{A}_i\} + \min\{H(x) \mid x \in \partial\mathbb{A}_i\})/2$ of the two values on the boundary $\partial\mathbb{A}_i$. By construction, each connected component of $S - \bigsqcup \gamma_i$ contains exactly one critical point. The existence of minimal value $\min_i V_i$ of differences of the values on the boundary components $\partial\mathbb{A}_i$ implies that arbitrarily small perturbations cannot create heteroclinic separatrices. This means that arbitrarily small perturbations do not transform the isomorphic structure of the Reeb graph $\Sigma_g/\sim_f$. $\square$

The set of functions in $\mathcal{M}(s_0, s_1, s_2)$ which are C^0 structurally stable is denote by $\mathcal{M}_{\mathrm{str}}(s_0, s_1, s_2)$. We describe the complete generic transition rules of Morse functions on orientable compact surfaces. Precisely, Morse theory implies analogies of Lemma 8 and Lemma 24 as follows.

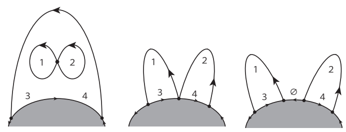

$$c_{++}: \ c_+(b_{++}\{\square^2_{b+}, \square^1_{b+}\}, \square^4_{cs-} \cdot \square^3_{cs-}) \to c_+(\square^2_{b+}, \square^4_{cs-}) \cdot c_+(\square^1_{b+}, \square^3_{cs-})$$

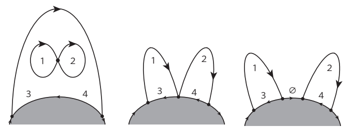

$$c_{--}: \ c_-(b_{--}\{\square^2_{b-}, \square^1_{b-}\}, \square^4_{cs+} \cdot \square^3_{cs+}) \to c_-(\square^2_{b-}, \square^4_{cs+}) \cdot c_-(\square^1_{b-}, \square^3_{cs+})$$

FIGURE 59. Complete list of sixteen bounded pinching structures in punctured spheres.

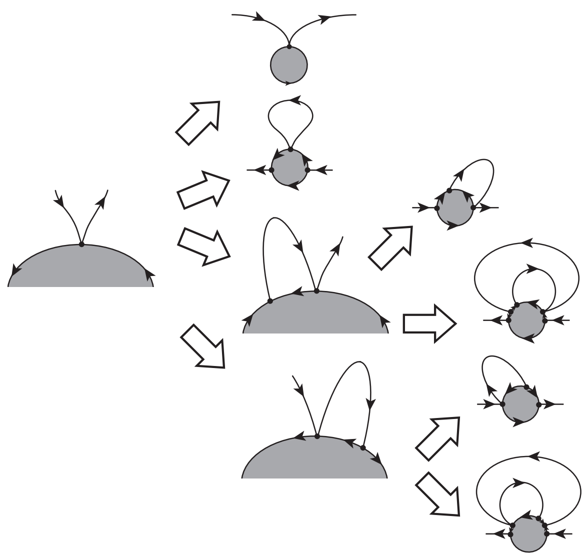

FIGURE 60. Complete list of fourteen structurally unstable structures with heteroclinic counter-clockwise orbits in punctured planes.

Proposition 35. *The set of functions in $\mathcal{M}(s_0, s_1, s_2)$ whose Hamiltonian flows are h-unstable is open in $\mathcal{M} - \mathcal{M}_{\mathrm{str}}(s_0, s_1, s_2)$ and is a dense subset of the difference $\mathcal{M}(s_0, s_1, s_2) - \mathcal{M}_{\mathrm{str}}(s_0, s_1, s_2)$. Such functions are the intermediate states of transitions in Figure 63–64. Moreover, they correspond to the rules $(b_{\pm\pm\pm})$, $(b_{\pm\pm(\mp)})$, $(b_{\pm\{\mp\mp\}})$, $(b_{\pm(\mp(\mp))})$, $(b_{\pm(\mp(\pm))})$, and $(b_{\pm\mp\pm})$, as shown in Figures 35–37 for structurally stable Hamiltonian flows on closed surfaces.*

Proof. First, we fix a function $f \in \mathcal{M}(s_0, s_1, s_2) - \mathcal{M}_{\mathrm{str}}(s_0, s_1, s_2)$. Then there is a critical value $c \in \mathbb{R}$ such that there is a heteroclinic separatrix γ with critical value c that connects two critical points x and y. By preserving a neighborhood of $\gamma \sqcup \{x, y\}$

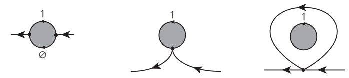

$$a_{\emptyset}(\Lambda_+):\ a_2(\square^1_{cs+},\lambda)\to a_+(\beta_+\{\square^1_{cs+}\})$$

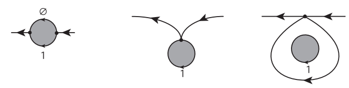

$$a_{\emptyset}(\Lambda_-):\ a_2(\lambda,\square^1_{cs-})\to a_-(\beta_-\{\square^1_{cs-}\})$$

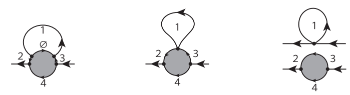

$$a_2(\Lambda_+):\ a_2(\square^3_{cs+}\cdot c_+(\square^1_{b+},\lambda)\cdot\square^2_{cs+},\square^4_{cs-})\to a_+(\square^1_{b+})\cdot a_2(\square^3_{cs+}\cdot\square^2_{cs+},\square^4_{cs-})$$

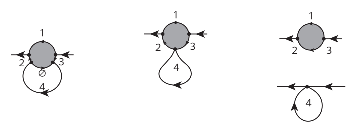

$$a_2(\Lambda_-):\ a_2(\square^1_{cs+},\square^2_{cs-}\cdot c_-(\square^4_{b-},\lambda)\cdot\square^3_{cs-})\to a_2(\square^1_{cs+},\square^2_{cs-}\cdot\square^3_{cs-})\cdot a_-(\square^4_{b-})$$

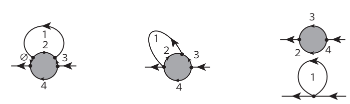

$$a_2(c^L_+):\ a_2(\square^3_{cs+}\cdot c_+(\square^1_{b+},\square^2_{cs-}),\square^4_{cs-})\to a_2(\square^3_{cs+},\square^2_{cs-}\cdot\square^4_{cs-})\cdot a_+(\square^1_{b+})$$

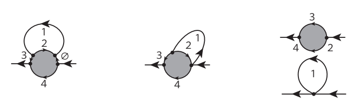

$$a_2(c^R_+):\ a_2(c_+(\square^1_{b+},\square^2_{cs-})\cdot\square^3_{cs+},\square^4_{cs-})\to a_2(\square^3_{cs+},\square^4_{cs-}\cdot\square^2_{cs-})\cdot a_+(\square^1_{b+})$$

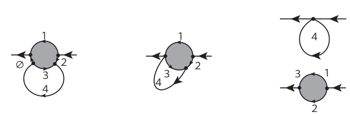

$$a_2(c^R_-):\ a_2(\square^1_{cs+},c_-(\square^4_{b-},\square^3_{cs+})\cdot\square^2_{cs-})\to a_-(\square^4_{b-})\cdot a_2(\square^1_{cs+}\cdot\square^3_{cs+},\square^2_{cs-})$$

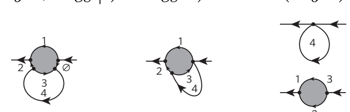

$$a_2(c^L_-):\ a_2(\square^1_{cs+},\square^2_{cs-}\cdot c_-(\square^4_{b-},\square^3_{cs+}))\to a_-(\square^4_{b-})\cdot a_2(\square^3_{cs+}\cdot\square^1_{cs+},\square^2_{cs-})$$

through arbitrarily small perturbation, we can obtain the resulting function g, whose saddle connection diagram contains no heteroclinic separatrices (excluding those connecting x and y), such that each level set excluding c contains at most one critical point. This means that the Hamiltonian flow of g is h-unstable. Therefore the set of functions in $\mathcal{M}(s_0,s_1,s_2)$ whose Hamiltonian flows are h-unstable is dense in $\mathcal{M}(s_0,s_1,s_2)-\mathcal{M}_{\mathrm{str}}(s_0,s_1,s_2)$.

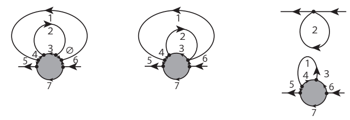

$$a_2(c_+(c_-^R)):\ a_2(\square^6_{cs+}\cdot c_+(\square^1_{b+}, c_-(\square^2_{b-}, \square^3_{cs+})\cdot\square^4_{cs-})\cdot\square^5_{cs+}, \square^7_{cs-}) \to$$
$$a_-(\square^2_{b-})\cdot a_2(\square^6_{cs+}\cdot\square^3_{cs+}\cdot c_+(\square^1_{b+}, \square^4_{cs-})\cdot\square^5_{cs+}, \square^7_{cs-})$$

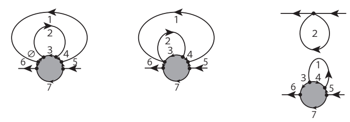

$$a_2(c_+(c_-^L)):\ a_2(\square^5_{cs+}\cdot c_+(\square^1_{b+}, \square^4_{cs-}\cdot c_-(\square^2_{b-}, \square^3_{cs+}))\cdot\square^6_{cs+}, \square^7_{cs-}) \to$$
$$a_-(\square^2_{b-})\cdot a_2(\square^5_{cs+}\cdot c_+(\square^1_{b+}, \square^4_{cs-})\cdot\square^3_{cs+}\cdot\square^6_{cs+}, \square^7_{cs-})$$

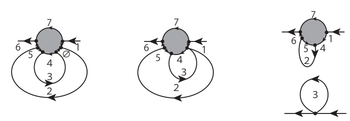

$$a_2(c_-(c_+^R)):\ a_2(\square^7_{cs+}, \square^6_{cs-}\cdot c_-(\square^2_{b-}, \square^5_{cs+}\cdot c_+(\square^3_{b+}, \square^4_{cs-}))\cdot\square^1_{cs-}) \to$$
$$a_2(\square^7_{cs+}, \square^6_{cs-}\cdot c_-(\square^2_{b-}, \square^5_{cs+})\cdot\square^4_{cs-}\cdot\square^1_{cs-})\cdot a_+(\square^3_{b+})$$

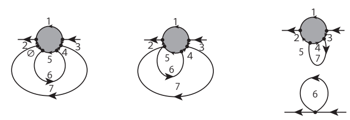

$$a_2(c_-(c_+^L)):\ a_2(\square^1_{cs+}, \square^2_{cs-}\cdot c_-(\square^7_{b-}, c_+(\square^6_{b+}, \square^5_{cs-})\cdot\square^4_{cs+})\cdot\square^3_{cs-}) \to$$
$$a_2(\square^1_{cs+}, \square^2_{cs-}\cdot\square^5_{cs-}\cdot c_-(\square^7_{b-}, \square^4_{cs+})\cdot\square^3_{cs-})\cdot a_+(\square^6_{b+})$$

FIGURE 61. Complete list of twelve unbounded pinching structures in punctured planes.

We fix a function $f \in \mathcal{M}_{\mathrm{str}}(s_0, s_1, s_2)$, whose Hamiltonian flows are h-unstable. Then, we determine a critical value $c \in \mathbb{R}$, such that there exists a heteroclinic separatrix γ_c with critical value c that connects two critical points x and y. If μ_c is the saddle connection containing x, any saddle connection except for μ_c contains no heteroclinic separatrices. The finiteness of separatrices of f implies that any saddle connection μ has a neighborhood U_μ such that $U_\mu - \mu$ is a finite disjoint union of open annuli consisting of circles, which are connected components of a level set. Any small perturbation in $\mathcal{M}$ on U_μ for any saddle connection μ except μ_c contains no heteroclinic separatrices and preserves the non-existence of heteroclinic separatrices on the saddle connection. Any small perturbation in $\mathcal{M}$ on U_{μ_c} contains at most one saddle connection with heteroclinic separatrices. Finally, any small perturbation in $\mathcal{M}(s_0, s_1, s_2) - \mathcal{M}_{\mathrm{str}}(s_0, s_1, s_2)$ on U_{μ_c} preserves μ_c. This means that the set of functions in $\mathcal{M}(s_0, s_1, s_2)$ whose Hamiltonian flows are h-unstable is open in $\mathcal{M}(s_0, s_1, s_2) - \mathcal{M}_{\mathrm{str}}(s_0, s_1, s_2)$ on U_{μ_c} and so in $\mathcal{M} - \mathcal{M}_{\mathrm{str}}(s_0, s_1, s_2)$. $\square$

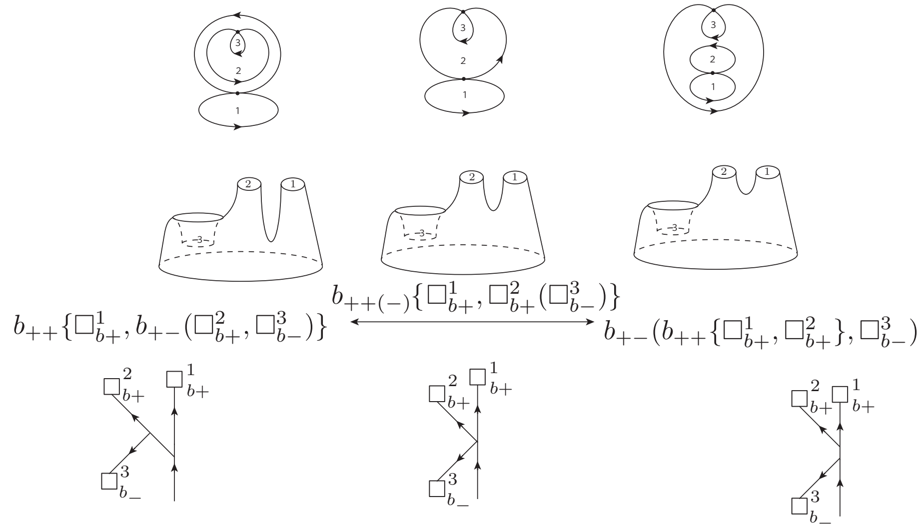

FIGURE 62. Transition rule $b_{++(-)}$.

6.3. **Morse functions with horizontal boundary on compact surfaces.** The invariance of the boundary of a surface for a Hamiltonian flow corresponds to the condition that each boundary component has a single value of the Hamiltonian. Therefore we call that a function is a function with horizontal boundary if each boundary component has a single value of it. As the closed surface case, notice that one can interpret results for Hamiltonian flows on compact surfaces into those for Morse functions with horizontal boundary on orientable compact surfaces.

7. FINAL REMARKS

In this paper, we explored the creations of genus elements. The annihilation of a boundary component is not merely the inverse operation of creation incremented by one but rather of creation incremented by positive integers. Therefore, the annihilation of one genus element is more complicated than creation incremented by one. Nevertheless, we intend to report on the complete rules of annihilation of genus elements in future research.

Roughly speaking, a Hamiltonian flow without heteroclinic separatrices and degenerate singular points, except for one k-saddle (resp. ∂-$k/2$-saddle), constitutes a "codimension $2k$" (resp. "codimension $(k-1)$") transition. In fact, k-saddles (resp. ∂-$k/2$-saddles, non-self-connected separatrices) correspond to "codimension $2k$" (resp. "codimension $(k-1)$", "codimension one") structures; hence, the "codimensions" of flows can be defined as the sum of "codimensions" of such elements. Therefore a stratification of the set of Hamiltonian flows with finitely many singular points into the subset of "higher codimensional transitions" can be constructed. This will also be undertaken as a future research direction. Each critical point of a function C^r $(r \geq 2)$ function with finitely many critical points on an orientable compact surface corresponds to either a topological center or a multi-saddle of its Hamiltonian flow with Hamiltonian f because of the finite existence of singular

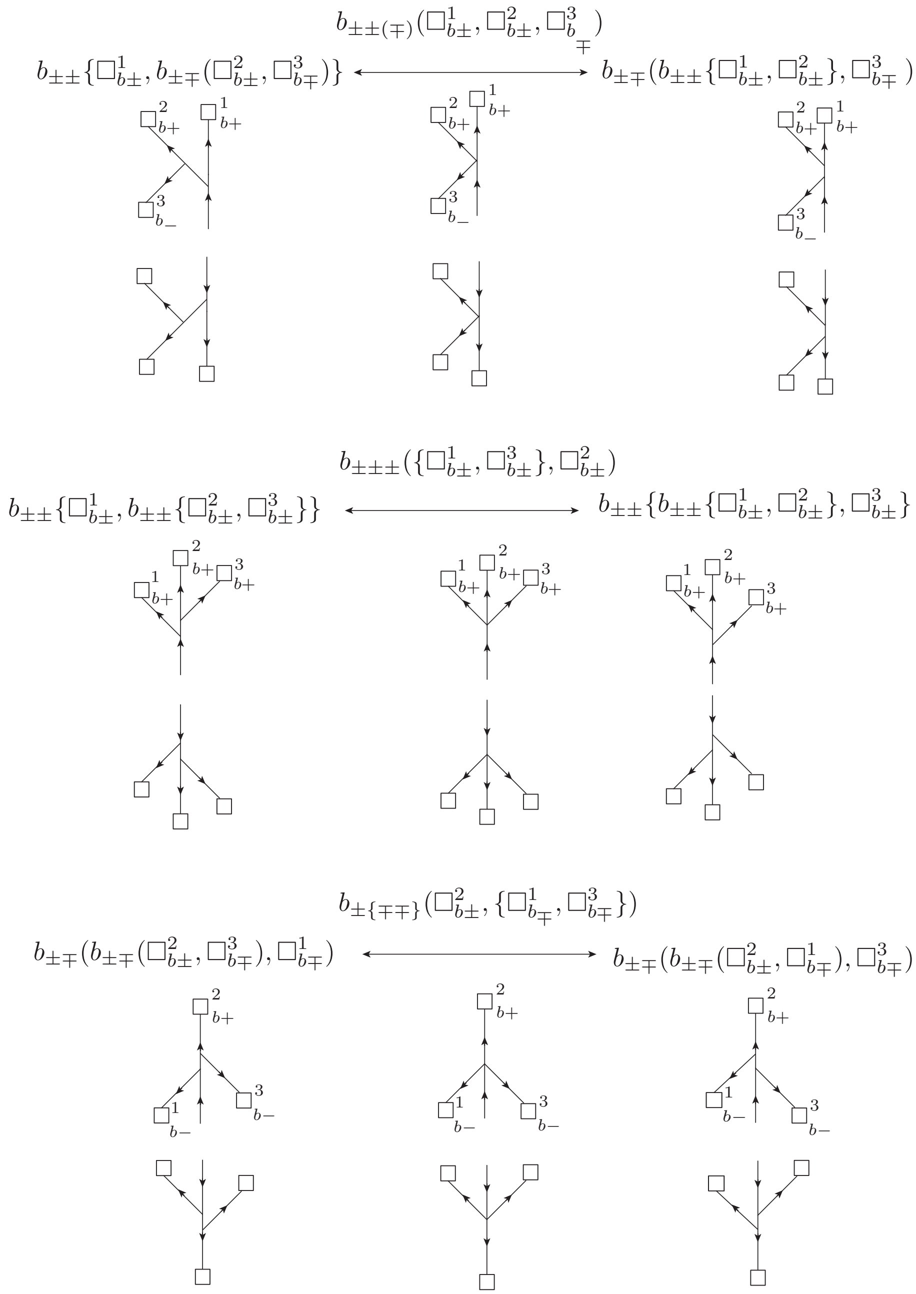

FIGURE 63. The first half of complete generic transition rules of Morse functions on orientable compact surfaces.

points. This means that a function on an orientable compact surface whose Hamiltonian flow without heteroclinic separatrices and without degenerate singular points except for one 2-saddle, corresponds to a non-generic transition with "codimension two". A stratification of the set of "higher codimensional transitions" will also be investigated in a future work.

In this paper, we deal with only topological centers, multi-saddles, and a 1-source–sink point. On the other hand, we can discuss other degenerate singular points. In particular, since finitely sectored singular point (see details [15]) with not only hyperbolic sectors and elliptic sectors but also parabolic sectors are appear as the points at infinities of in Hamiltonian flows on planes and punctured surfaces, results for Hamiltonian flow with finitely sectored singular points also will be reported in near future.

References

[1] S. K. Aranson, G. R. Belitsky, and E. V. Zhuzhoma. *Introduction to the qualitative theory of dynamical systems on surfaces*. American Mathematical Society, 1996.

[2] H. Aref and M. Brøns. On stagnation points and streamline topology in vortex flows. *Journal of Fluid Mechanics*, 370:1–27, 1998.

[3] V. I. Arnold, V. Afrajmovich, Y. S. Il'yashenko, and L. Shil'nikov. *Dynamical systems V: bifurcation theory and catastrophe theory*, volume 5. Springer Science & Business Media, 2013.

[4] M. Cobo, C. Gutierrez, and J. Llibre. Flows without wandering points on compact connected surfaces. *Transactions of the American Mathematical Society*, 362(9):4569–4580, 2010.

[5] H. Comon, M. Dauchet, R. Gilleron, C. Löding, F. Jacquemard, D. Lugiez, S. Tison, and M. Tommasi. Tree automata techniques and applications. Available on: `http://www.grappa.univ-lille3.fr/tata`, 2007. release October, 12th 2007.

[6] A. T. Fomenko and H. Zieschang. A topological invariant and a criterion for the equivalence of integrable hamiltonian systems with two degrees of freedom. *Izvestiya Rossiiskoi Akademii Nauk. Seriya Matematicheskaya*, 54(3):546–575, 1990.

[7] C. Gutiérrez. Smoothing continuous flows on two-manifolds and recurrences. *Ergodic Theory and dynamical systems*, 6(1):17–44, 1986.

[8] R. Kidambi and P. K. Newton. Streamline topologies for integrable vortex motion on a sphere. *Physica D: Nonlinear Phenomena*, 140(1-2):95–125, 2000.

[9] T. Ma and S. Wang. *Geometric theory of incompressible flows with applications to fluid dynamics*. Number 119. American Mathematical Soc., 2005.

[10] A. Mayer. Trajectories on the closed orientable surfaces. *Rec. Math.[Mat. Sbornik] NS*, 12(54):71–84, 1943.

[11] H. Moffatt. The topology of scalar fields in 2d and 3d turbulence. In *IUTAM symposium on geometry and statistics of turbulence*, pages 13–22. Springer, 2001.

[12] T. Sakajo and T. Yokoyama. Transitions between streamline topologies of structurally stable hamiltonian flows in multiply connected domains. *Physica D: Nonlinear Phenomena*, 307:22–41, 2015.

[13] T. Sakajo and T. Yokoyama. Tree representations of streamline topologies of structurally stable 2d incompressible flows. *IMA Journal of Applied Mathematics*, 83(3):380–411, 2018.

[14] T. Yokoyama. A topological characterization for non-wandering surface flows. *Proceedings of the American Mathematical Society*, 144(1):315–323, 2016.

[15] T. Yokoyama. Decompositions of surface flows. *arXiv preprint arXiv:1703.05501*, 2017.

[16] T. Yokoyama and T. Sakajo. Word representation of streamline topologies for structurally stable vortex flows in multiply connected domains. *Proceedings of the Royal Society A: Mathematical, Physical and Engineering Sciences*, 469(2150):20120558, 2013.

Department of Software Engineering, Nanzan University, Yamazato-cho 18, Showa-ku, Nagoya, Aichi 466-8673, Japan
Email address: `tyokoyama@acm.org`

Department of Mathematics, Kyoto University of Education, 1 Fujinomori, Fukakusa, Fushimi-ku, Kyoto 612-8522, Japan
Email address: `tomoo@kyokyo-u.ac.jp`

$$b_{\pm(\mp(\pm))}(\square^3_{b\pm}, \square^2_{b\mp}, \square^1_{b\pm})$$

$$b_{\pm\mp}(\square^3_{b\pm}, b_{\mp\pm}(\square^2_{b\mp}, \square^1_{b\pm})) \longleftrightarrow b_{\pm\mp}(b_{\pm\pm}\{\square^1_{b\pm}, \square^3_{b\pm}\}, \square^2_{b\mp})$$

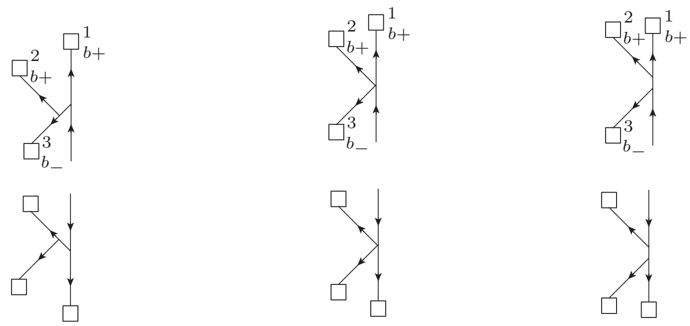

$$b_{\pm(\mp(\mp))}(\square^3_{b\pm}, b_{\mp\mp}\{\square^1_{b\mp}, \square^2_{b\mp})$$

$$b_{\pm\mp}(b_{\pm\mp}(\square^3_{b\pm}, \square^2_{b\mp}), \square^1_{b\mp}) \longleftrightarrow b_{\pm\mp}(\square^3_{b\pm}, b_{\mp\mp}\{\square^1_{b\mp}, \square^2_{b\mp}\})$$

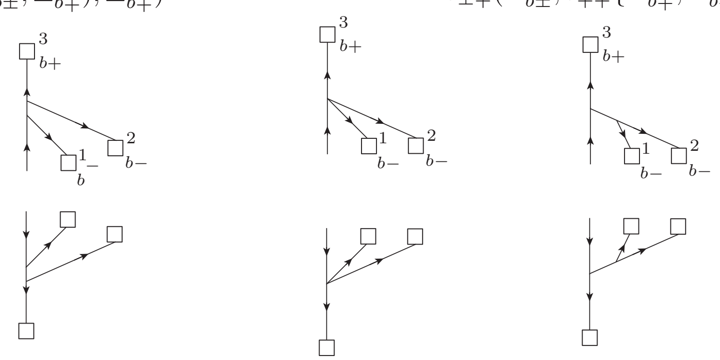

$$b_{\pm\mp}(b_{\pm\pm}\{\square^1_{\pm}, \square^3_{\pm}\}, \square^2_{\mp}) \xleftrightarrow{b_{(\pm\mp\pm)}} b_{\pm\mp}(b_{\pm\pm}\{\square^1_{\pm}, \square^3_{\pm}\}, \square^2_{\mp})$$

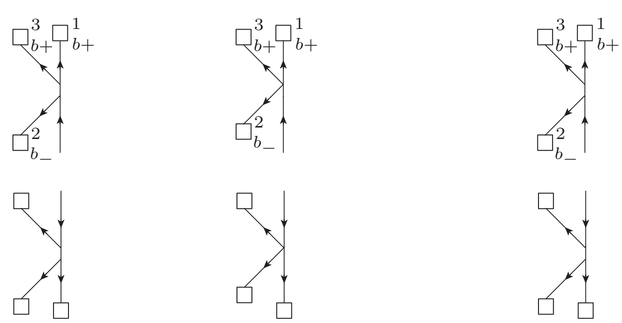

FIGURE 64. The second half of the complete generic transition rules of Morse functions on orientable compact surfaces.